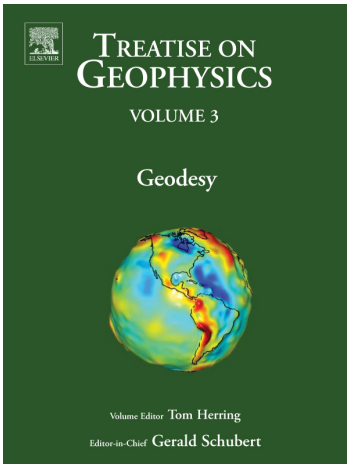

3.09 Earth Rotation Variations – Long Period

R. S. Gross, Jet Propulsion Laboratory, California Institute of Technology, Pasadena, CA, USA

Nomenclature

a	radius of a sphere having the same volume as the Earth (m)
$\mathbf{h}$	angular momentum vector due to motion relative to the rotating, body-fixed terrestrial reference frame ($\mathrm{kg\,m^2\,s^{-1}}$)
h_x	x-component of the angular momentum due to motion relative to the rotating, body-fixed terrestrial reference frame ($\mathrm{kg\,m^2\,s^{-1}}$)
h_y	y-component of the angular momentum due to motion relative to the rotating, body-fixed terrestrial reference frame ($\mathrm{kg\,m^2\,s^{-1}}$)
h_z	z-component of the angular momentum due to motion relative to the rotating, body-fixed terrestrial reference frame ($\mathrm{kg\,m^2\,s^{-1}}$)
i	$\sqrt{-1}$
k_2	degree-2 body tide Love number of the Earth (dimensionless)
k'_2	degree-2 load Love number of the Earth (dimensionless)
k_r	parameter accounting for the effects of rotational deformation on the length-of-day (dimensionless)

Treatise on Geophysics, vol. 3, pp. 239-294

$\mathbf{m}$	complex-valued position of the rotation pole within the terrestrial reference frame (arcseconds)
m	amplitude of the free wobble of a rigid axisymmetric body (arcseconds)
m_x	x-component of the position of the rotation pole within the terrestrial reference frame (arcseconds)
m_y	y-component of the position of the rotation pole within the terrestrial reference frame (arcseconds)
m_z	time rate-of-change of (UT1–TAI) (seconds/day)
$\mathbf{n}$	complex-valued correction to the nutations in longitude and obliquity (arcseconds); also unit vector normal to a plane
$\dot{n}$	tidal acceleration of the Moon (arcseconds/century^2)
n_o	parameter related to the change in the mean moment of inertia of the Earth caused by the purely radial component of the rotational potential (dimensionless)
$\mathbf{p}$	complex-valued position of the Celestial Intermediate Pole within the terrestrial reference frame (arcseconds)
p_x	x-component of the position of the Celestial Intermediate Pole within the terrestrial reference frame (arcseconds)
p_y	y-component of the position of the Celestial Intermediate Pole within the terrestrial reference frame (arcseconds)
p_z	time rate-of-change of (UT1–TAI) (seconds/day)
$\mathbf{r}$	position vector (m)
r	position in radial direction (m)
$\mathbf{r}_c$	vector of the coordinates of an observing station given in the celestial reference frame (m)
$\mathbf{r}_i$	vector of the coordinates of an observing station given in the intermediate reference frame (m)
$\mathbf{r}_t$	vector of the coordinates of an observing station given in the terrestrial reference frame (m)
t	time (s)
t_o	reference time (s)
$\mathbf{u}$	velocity vector (m s^{-1})
u	eastward velocity (m s^{-1})
v	northward velocity (m s^{-1})
$\hat{\mathbf{x}}$	unit vector in direction of the x-coordinate axis of the terrestrial reference frame
$\hat{\mathbf{y}}$	unit vector in direction of the y-coordinate axis of the terrestrial reference frame
$\hat{\mathbf{z}}$	unit vector in direction of the z-coordinate axis of the terrestrial reference frame
A	least principal moment of inertia of the Earth (kg m^2) area of ring laser gyroscope (m^2) amplitude of periodic motion (s or arcseconds)
$\mathbf{A}$	transformation matrix that transforms coordinates from the terrestrial to the intermediate reference frames (dimensionless)
A'	average of the least and intermediate principal moments of inertia of the Earth (kg m^2)
A_c	least principal moment of inertia of the core (kg m^2)
A_m	least principal moment of inertia of the crust and mantle (kg m^2)
A'_m	average of the least and intermediate principal moments of inertia of the crust and mantle (kg m^2)
A_p	amplitude of prograde component of periodic polar motion (arcseconds)
A_r	amplitude of retrograde component of periodic polar motion (arcseconds)
B	intermediate principal moment of inertia of the Earth (kg m^2)
C	greatest principal moment of inertia of the Earth (kg m^2)
C_c	greatest principal moment of inertia of the core (kg m^2)
C_m	greatest principal moment of inertia of the crust and mantle (kg m^2)
D	coefficient relating changes in the inertia tensor of the Earth to changes in the wobble of the crust and mantle (kg m^2)
D	Delaunay argument for the mean elongation of the Moon from the Sun (deg)
$\tilde{D}$	coefficient relating changes in the inertia tensor of the Earth to changes in the length-of-day (kg m^2)

$\boldsymbol{E}$	coefficient relating changes in the relative angular momentum of the core to changes in the wobble of the crust and mantle ($\mathrm{kg\,m^2\,s^{-1}}$)
$\boldsymbol{E}'$	coefficient relating changes in the relative angular momentum of the core to changes in the wobble of the crust and mantle ($\mathrm{kg\,m^2\,s^{-1}}$)
$\tilde{\boldsymbol{E}}$	coefficient relating changes in the relative angular momentum of the core to changes in the length-of-day ($\mathrm{kg\,m^2\,s^{-1}}$)
$\boldsymbol{F}$	Delaunay argument for L–Ω, where L is the mean longitude of the Moon (deg)
$\boldsymbol{G}$	Newtonian gravitational constant ($\mathrm{m^3\,kg^{-1}\,s^{-2}}$)
$\boldsymbol{H}$	hour angle of the true equinox of date (s)
$\mathbf{I}$	inertia tensor ($\mathrm{kg\,m^2}$)
$\boldsymbol{I}$	Delaunay argument for the mean anomaly of the Moon (deg)
$\boldsymbol{I}'$	Delaunay argument for the mean anomaly of the Sun (deg)
$\mathbf{I}_o$	initial inertia tensor ($\mathrm{kg\,m^2}$)
$\mathbf{L}$	angular momentum vector ($\mathrm{kg\,m^2\,s^{-1}}$)
$\boldsymbol{M}$	mass of the Earth (kg)
$\boldsymbol{M}_{\mathbf{atm}}$	mass of the atmosphere (kg)
$\boldsymbol{M}_{\mathbf{c}}$	mass of the core (kg)
$\boldsymbol{M}_{\mathbf{m}}$	mass of the crust and mantle (kg)
$\boldsymbol{M}_{\mathbf{ocn}}$	mass of the oceans (kg)
$\mathbf{N}$	nutation coordinate transformation matrix (dimensionless)
$\mathbf{P}$	precession coordinate transformation matrix (dimensionless)
$\boldsymbol{P}$	optical path length of ring laser gyroscope (m)
$\boldsymbol{Q}$	quality factor of periodic motion (dimensionless)
$\mathbf{S}$	spin coordinate transformation matrix (dimensionless)
$\boldsymbol{T}$	period of periodic motion (s)
TAI	Temps Atomique International (International Atomic Time) (s)
UT0	Universal Time (s)
UT1	Universal Time corrected for the effects of polar motion (s)
$\boldsymbol{V}$	volume ($\mathrm{m^3}$)
$\mathbf{W}$	antisymmetric rotation matrix ($\mathrm{rad\,s^{-1}}$)
$\mathbf{X}$	x-component of wobble coordinate transformation matrix (dimensionless)
$\mathbf{Y}$	y-component of wobble coordinate transformation matrix (dimensionless)
α	phase of periodic motion (deg)
$\alpha_{\mathbf{p}}$	phase of prograde component of periodic polar motion (deg)
$\alpha_{\mathbf{r}}$	phase of retrograde component of periodic polar motion (deg)
$\alpha_{\mathbf{3}}$	factor modifying the degree-2 load Love number of the Earth because of core decoupling (dimensionless)
γ	Greenwich mean sidereal time reckoned from the lower culmination of the vernal equinox (GMST$+\pi$) (deg)
$\delta\boldsymbol{D}$	coefficient relating changes in the inertia tensor of the Earth to changes in the wobble of the crust and mantle ($\mathrm{kg\,m^2}$)
$\delta\boldsymbol{D}_{\mathbf{12}}$	coefficient relating changes in the inertia tensor of the Earth to changes in the wobble of the crust and mantle ($\mathrm{kg\,m^2}$)
$\delta\boldsymbol{D}_{\mathbf{13}}$	coefficient relating changes in the inertia tensor of the Earth to changes in the Earth's rotation ($\mathrm{kg\,m^2}$)
$\delta\boldsymbol{D}_{\mathbf{23}}$	coefficient relating changes in the inertia tensor of the Earth to changes in the Earth's rotation ($\mathrm{kg\,m^2}$)
$\delta\boldsymbol{f}$	Sagnac frequency, ($\mathrm{rad\,s^{-1}}$)
$\delta\boldsymbol{h}_{\boldsymbol{x}}$	x-component of the change in relative angular momentum due to motion in the core caused by a rigid rotation of the crust and mantle ($\mathrm{kg\,m^2\,s^{-1}}$)
$\delta\boldsymbol{h}_{\boldsymbol{y}}$	y-component of the change in relative angular momentum due to motion in the core caused by a rigid rotation of the crust and mantle ($\mathrm{kg\,m^2\,s^{-1}}$)
$\delta\boldsymbol{h}_{\boldsymbol{z}}$	z-component of the change in relative angular momentum due to motion in the core caused by a rigid rotation of the crust and mantle ($\mathrm{kg\,m^2\,s^{-1}}$)
$\delta\boldsymbol{I}_{\boldsymbol{xz}}$	change in the (x,z)-element of the inertia tensor of the Earth due to changes in the rotation of the Earth ($\mathrm{kg\,m^2}$)
$\delta\boldsymbol{I}_{\boldsymbol{yz}}$	change in the (y,z)-element of the inertia tensor of the Earth due to changes in the rotation of the Earth ($\mathrm{kg\,m^2}$)

$\delta \boldsymbol{I}_{zz}$	change in the (z,z)-element of the inertia tensor of the Earth due to changes in the rotation of the Earth (kg m^2)
$\delta\varepsilon$	correction to the nutation in obliquity (arcseconds)
$\delta\psi$	correction to the nutation in longitude (arcseconds)
ε_a	ellipticity of the surface of the Earth (dimensionless)
ε_c	ellipticity of the surface of the core (dimensionless)
ε_o	mean obliquity of the ecliptic (degrees)
λ	East longitude (deg); also wavelength of laser beam used in ring laser gyroscope (m)
ρ	density (kg m^{-3})
σ	frequency (rad s^{-1})
$\sigma_{\mathbf{c}}$	frequency given in the celestial reference frame (rad s^{-1})
$\sigma_{\mathbf{t}}$	frequency given in the terrestrial reference frame (rad s^{-1})
$\sigma_{\mathbf{r}}$	frequency of the free wobble of a rigid triaxial Earth (rad s^{-1})
$\sigma_{\mathbf{ra}}$	frequency of the free wobble of a rigid axisymmetric Earth (rad s^{-1})
$\sigma_{\mathbf{cw}}$	frequency of the free wobble of a deformable Earth with fluid core (rad s^{-1})
σ_o	observed complex-valued frequency of the Chandler wobble (rad s^{-1})
$\boldsymbol{\tau}$	torque vector (kg m^2 s^{-2})
τ	amplitude decay time constant (s)
ϕ	North latitude (deg)
$\phi_{\mathbf{r},x}$	x-component of the excitation function of a rigid triaxial Earth (arcseconds)
$\phi_{\mathbf{r},y}$	y-component of the excitation function of a rigid triaxial Earth (arcseconds)
$\phi_{\mathbf{r},z}$	z-component of the excitation function of a rigid triaxial Earth (seconds/day)
$\phi_{\mathbf{ra},x}$	x-component of the excitation function of a rigid axisymmetric Earth (arcseconds)
$\phi_{\mathbf{ra},y}$	y-component of the excitation function of a rigid axisymmetric Earth (arcseconds)
χ	complex-valued excitation function of a deformable Earth with fluid core (arcseconds)
χ_x	x-component of the excitation function of a deformable Earth with fluid core (arcseconds)
χ_y	y-component of the excitation function of a deformable Earth with fluid core (arcseconds)
χ_z	z-component of the excitation function of a deformable Earth with fluid core (arcseconds)
$\boldsymbol{\omega}$	angular velocity vector (rad s^{-1})
$\boldsymbol{\omega}_{\mathbf{o}}$	initial angular velocity vector (rad s^{-1})
ω_x	x-component of the angular velocity (rad s^{-1})
ω_y	y-component of the angular velocity (rad s^{-1})
ω_z	z-component of the angular velocity (rad s^{-1})
$\Lambda_{\mathbf{o}}$	nominal length-of-day (s)
$\Delta\phi$	variation of latitude (arcseconds)
$\Delta \boldsymbol{k}'_{\mathbf{an}}$	modification of the degree-2 load Love number of the Earth due to mantle anelasticity (dimensionless)
$\Delta \boldsymbol{k}_{\mathbf{ocn,s}}$	oceanic Love number for the spin of the Earth (dimensionless)
$\Delta \boldsymbol{k}_{\mathbf{ocn,w}}$	oceanic Love number for the wobble of the Earth (dimensionless)
$\Delta \mathbf{I}$	perturbation to the initial inertia tensor (kg m^2)
$\Delta \boldsymbol{I}_{xx}$	(x,x)-element of the perturbation to the initial inertia tensor (kg m^2)
$\Delta \boldsymbol{I}_{xy}$	(x,y)-element of the perturbation to the initial inertia tensor (kg m^2)
$\Delta \boldsymbol{I}_{xz}$	(x,z)-element of the perturbation to the initial inertia tensor (kg m^2)
$\Delta \boldsymbol{I}_{yy}$	(y,y)-element of the perturbation to the initial inertia tensor (kg m^2)
$\Delta \boldsymbol{I}_{yz}$	(y,z)-element of the perturbation to the initial inertia tensor (kg m^2)
$\Delta \boldsymbol{I}_{zz}$	(z,z)-element of the perturbation to the initial inertia tensor (kg m^2)
$\Delta\omega_z$	z-component of the perturbation to the initial angular velocity (rad s^{-1})
$\Delta\Lambda$	change in the length-of-day (s)
$\Delta\boldsymbol{\omega}$	perturbation to the initial angular velocity vector (rad s^{-1})
Ω	mean angular velocity of Earth (rad s^{-1})
Ω	Delaunay argument for the mean longitude of the ascending node of the Moon (deg)

3.09.1 Introduction

The Earth is a dynamic system – it has a fluid, mobile atmosphere and oceans, a continually changing global distribution of ice, snow, and water, a fluid core that is undergoing some type of hydromagnetic motion, a mantle both thermally convecting and rebounding from the glacial loading of the last ice age, and mobile tectonic plates. In addition, external forces due to the gravitational attraction of the Sun, Moon, and planets also act upon the Earth. These internal dynamical processes and external gravitational forces exert torques on the solid Earth, or displace its mass, thereby causing the Earth's rotation to change.

Changes in the rotation of the solid Earth are studied by applying the principle of conservation of angular momentum to the Earth system. Under this principle, the rotation of the solid Earth changes as a result of (1) applied external torques, (2) internal mass redistribution, and (3) the transfer of angular momentum between the solid Earth and the fluid regions with which it is in contact; concomitant torques are due to hydrodynamic or magnetohydrodynamic stresses acting at the fluid/solid Earth interfaces (*see* Chapter 9.10).

Here, changes in the Earth's rotation that occur on timescales greater than a day are discussed. Using the principle of conservation of angular momentum, the equations governing small variations in both the rate of rotation and in the position of the rotation vector with respect to the Earth's crust are first derived. These equations are then rewritten in terms of the Earth rotation parameters that are actually reported by Earth rotation measurement services. The techniques that are used to monitor the Earth's rotation by the measurement services are then reviewed, a description of the variations that are observed by these techniques is given, and possible causes of the observed variations are discussed.

3.09.2 Theory of Earth Rotation Variations at Long Periods

3.09.2.1 Instantaneous Rotation Vector

In a rotating reference frame that has been attached in some manner to the solid body of the Earth, the Eulerian equation of motion that relates changes in the angular momentum $\mathbf{L}(t)$ of the Earth to the external torques $\boldsymbol{\tau}(t)$ acting on it is (Munk and MacDonald, 1960; Lambeck, 1980, 1988; Moritz and Mueller, 1988; Eubanks, 1993)

$$\frac{\partial \mathbf{L}(t)}{\partial t} + \boldsymbol{\omega}(t) \times \mathbf{L}(t) = \boldsymbol{\tau}(t) \qquad [1]$$

where, strictly speaking, $\boldsymbol{\omega}(t)$ is the angular velocity of the rotating frame with respect to inertial space. But since the rotating frame has been attached to the solid body of the Earth, it is also interpreted as being the angular velocity of the Earth with respect to inertial space. In general, the angular momentum $\mathbf{L}(t)$ can be written as the sum of two terms: (1) that part $\mathbf{h}(t)$ due to motion relative to the rotating reference frame, and (2) that part due to the changing inertia tensor $I(t)$ of the Earth which is changing because the distribution of the Earth's mass is changing:

$$\mathbf{L}(t) = \mathbf{h}(t) + I(t) \cdot \boldsymbol{\omega}(t) \qquad [2]$$

Combining eqns [1] and [2] yields the Liouville equation

$$\frac{\partial}{\partial t}\left[\mathbf{h}(t) + I(t) \cdot \boldsymbol{\omega}(t)\right] + \boldsymbol{\omega}(t) \times \left[\mathbf{h}(t) + I(t) \cdot \boldsymbol{\omega}(t)\right] = \boldsymbol{\tau}(t) \qquad [3]$$

The external torques acting on the Earth due to the gravitational attraction of the Sun, Moon, and planets cause the Earth to nutate and precess. Since the nutations and precession of the Earth are discussed in Chapter 3.10 of this volume, the external torques $\boldsymbol{\tau}(t)$ in eqn [3] will be set to zero. Note, however, that tidal effects on the Earth's rotation, which are also caused by the gravitational attraction of the Sun, Moon, and planets, are discussed here in Sections 3.09.4.1.3 and 3.09.4.2.3

The Earth's rotation deviates only slightly from a state of uniform rotation, the deviation being a few parts in 10^8 in speed, corresponding to changes of a few milliseconds (ms) in the length of the day, and about a part in 10^6 in the position of the rotation axis with respect to the crust of the Earth, corresponding to a variation of several hundred milliarcseconds (mas) in polar motion. Such small deviations in rotation can be studied by linearizing eqn [3]. Let the Earth initially be uniformly rotating at the constant rate Ω about the z-coordinate axis of the body-fixed reference frame and orient the frame within the

Earth in such a manner that the inertia tensor of the Earth is diagonal in this frame:

$$\boldsymbol{\omega}_o = \Omega\hat{\mathbf{z}} \qquad [4]$$

$$I_o = \begin{pmatrix} A & 0 & 0 \\ 0 & B & 0 \\ 0 & 0 & C \end{pmatrix} \qquad [5]$$

where the hat denotes a vector of unit length, Ω is the mean angular velocity of the Earth, and A, B, and C are the mean principal moments of inertia of the Earth ordered such that $A < B < C$. In this initial state, in which all time-dependent quantities vanish, the Earth is rotating at a constant rate about its figure axis, there are no mass displacements, and there is no relative angular momentum. So, for example, the atmosphere, oceans, and core are at rest with respect to the solid Earth and merely corotate with it.

Now let this initial state be perturbed by the appearance of mass displacements and relative angular momentum. In general, since the crust and mantle of the Earth can deform, they can undergo motion relative to the rotating reference frame and hence can contribute to the relative angular momentum. However, let the body-fixed reference frame in the perturbed state be oriented in such a manner that the relative angular momentum due to motion of the crust and mantle vanishes. In this frame, which is known as the Tisserand mean-mantle frame of the Earth (Tisserand, 1891), the motion of the atmosphere, oceans, and core have relative angular momentum, but the motion of the crust and mantle does not.

In the Tisserand mean-mantle frame, the perturbed instantaneous rotation vector and inertia tensor of the Earth can be written without loss of generality as

$$\begin{aligned} \boldsymbol{\omega}(t) &= \boldsymbol{\omega}_o + \Delta\boldsymbol{\omega}(t) \\ &= \Omega\hat{\mathbf{z}} + \Omega[m_x(t)\,\hat{\mathbf{x}} + m_y(t)\,\hat{\mathbf{y}} + m_z(t)\,\hat{\mathbf{z}}] \end{aligned} \qquad [6]$$

$$\begin{aligned} I(t) &= I_o + \Delta I(t) \\ &= \begin{pmatrix} A & 0 & 0 \\ 0 & B & 0 \\ 0 & 0 & C \end{pmatrix} + \begin{pmatrix} \Delta I_{xx}(t) & \Delta I_{xy}(t) & \Delta I_{xz}(t) \\ \Delta I_{xy}(t) & \Delta I_{yy}(t) & \Delta I_{yz}(t) \\ \Delta I_{xz}(t) & \Delta I_{yz}(t) & \Delta I_{zz}(t) \end{pmatrix} \end{aligned} \qquad [7]$$

where the terms with the subscript 'o' denote the initial values given by eqns [4] and [5], $\Omega m_i(t)$ are the elements of the time-dependent perturbation $\Delta\boldsymbol{\omega}(t)$ to the rotation vector, and the $\Delta I_{ij}(t)$ are the elements of the time-dependent perturbation $\Delta I(t)$ to the inertia tensor.

The equation that relates small changes in the Earth's rotation to the mass displacements and relative angular momenta that are causing the rotation to change can be derived by substituting eqns [6] and [7] into eqn [3] and then linearizing the resulting expression by assuming that $h_i(t) << \Omega C$, $m_i(t) << 1$, and $\Delta I_{ij}(t) << C$. By keeping terms to first order in these small quantities, the equatorial and axial components of eqn [3] can be written as

$$\begin{aligned} &\frac{1}{\sigma_r}\frac{\partial m_x(t)}{\partial t} + \left[\frac{B(C-B)}{A(C-A)}\right]^{1/2} m_y(t) \\ &\quad = -\left(\frac{B}{A}\right)^{1/2}\left[\frac{1}{\Omega}\frac{\partial \phi_{r,x}(t)}{\partial t} - \phi_{r,y}(t)\right] \end{aligned} \qquad [8]$$

$$\begin{aligned} &\frac{1}{\sigma_r}\frac{\partial m_y(t)}{\partial t} - \left[\frac{A(C-A)}{B(C-B)}\right]^{1/2} m_x(t) \\ &\quad = -\left(\frac{A}{B}\right)^{1/2}\left[\frac{1}{\Omega}\frac{\partial \phi_{r,y}(t)}{\partial t} + \phi_{r,x}(t)\right] \end{aligned} \qquad [9]$$

$$\frac{1}{\Omega}\frac{\partial m_z(t)}{\partial t} = -\frac{1}{\Omega}\frac{\partial \phi_{r,z}(t)}{\partial t} \qquad [10]$$

where the external torques have been set to zero,

$$\sigma_r^2 = \left(\frac{C-A}{A}\right)\left(\frac{C-B}{B}\right)\Omega^2 \qquad [11]$$

and the $\phi_{r,i}(t)$, known as excitation functions, are

$$\phi_{r,x}(t) = \frac{h_x(t) + \Omega\,\Delta I_{xz}(t)}{\Omega\sqrt{(C-A)(C-B)}} \qquad [12]$$

$$\phi_{r,y}(t) = \frac{h_y(t) + \Omega\,\Delta I_{yz}(t)}{\Omega\sqrt{(C-A)(C-B)}} \qquad [13]$$

$$\phi_{r,z}(t) = \frac{1}{C\Omega}\left[h_z(t) + \Omega\,\Delta I_{zz}(t)\right] \qquad [14]$$

Equations [8] and [9] are coupled, first-order differential equations that describe the motion of the rotation pole in the rotating, body-fixed reference frame as it responds to the applied excitation. In the absence of excitation, the solution of these equations, which describes the natural or free motion of the rotation pole, can be written as

$$m_x(t) = m\cos(\sigma_r t + \alpha) \qquad [15]$$

$$m_y(t) = \left[\frac{A(C-A)}{B(C-B)}\right]^{1/2} m\sin(\sigma_r t + \alpha) \qquad [16]$$

where m is the amplitude of the motion along the x-axis and α is the phase of the motion. The natural motion described by eqns [15] and [16] is prograde undamped elliptical motion of frequency σ_r. Using

Table 1 Geodetic parameters of the Earth

Parameter	Value	Source
G	$6.67259 \times 10^{-11}\,m^3\,kg^{-1}\,s^{-2}$	(a)
M_{atm}	$5.1441 \times 10^{18}\,kg$	(b)
M_{ocn}	$1.4 \times 10^{21}\,kg$	(c)
Whole Earth (observed)		
Ω	$7.292115 \times 10^{-5}\,rad\,s^{-1}$	(a)
M	$5.9737 \times 10^{24}\,kg$	(a)
C	$8.0365 \times 10^{37}\,kg\,m^2$	(a)
B	$8.0103 \times 10^{37}\,kg\,m^2$	(a)
A	$8.0101 \times 10^{37}\,kg\,m^2$	(a)
$C-A$	$2.6398 \times 10^{35}\,kg\,m^2$	(a)
$C-B$	$2.6221 \times 10^{35}\,kg\,m^2$	(a)
$B-A$	$1.765 \times 10^{33}\,kg\,m^2$	(a)
Whole Earth (modeled)		
a	6371.0 km	(d)
n_o	0.15505	(e)
k_2	0.298	(f)
$\Delta k_{ocn,w}$	0.047715	(g)
$\Delta k_{ocn,s}$	0.043228	(g)
k_r	0.997191	(g)
k_2'	−0.305	(f)
$\Delta k_{an}'$	$-0.011 + i0.003$	(f)
α_3	0.792	(h)
Crust and mantle (PREM)		
ε_a	3.334×10^{-3}	(d)
M_m	$4.0337 \times 10^{24}\,kg$	(d)
C_m	$7.1236 \times 10^{37}\,kg\,m^2$	(d)
A_m	$7.0999 \times 10^{37}\,kg\,m^2$	(d)
Core (PREM)		
ε_c	2.546×10^{-3}	(d)
M_c	$1.9395 \times 10^{24}\,kg$	(d)
C_c	$9.1401 \times 10^{36}\,kg\,m^2$	(d)
A_c	$9.1168 \times 10^{36}\,kg\,m^2$	(d)

PREM, preliminary reference Earth model (Dziewonski and Anderson, 1981).
Sources: (a) Groten (2004), (b) Trenberth and Guillemot (1994), (c) Yoder (1995), (d) Mathews *et al*. (1991), (e) Dahlen (1976), (f) Wahr (2005), (g) this paper, (h) Wahr (1983).

the values in **Table 1** for A, B, and C of the whole Earth, the period of the natural frequency, given by $2\pi/\sigma_r$, is found to be 304.46 sidereal days.

Euler (1765) first predicted that the Earth should freely wobble as it rotates, and that the period of this free wobble, assuming that the Earth is rigid, would be about 10 months. However, it was not until 1891 that the free wobble of the Earth was first detected in astronomical observations by Seth Carlo Chandler, Jr. (Chandler, 1891), albeit at a period of 14 months. The free wobble of the Earth is now known as the Chandler wobble in his honor.

Equations [8]–[14] describe changes in the rotation of a rigid body of arbitrary shape that is subject to small perturbing excitation. By recognizing that $(B-A)/A = 2.2 \times 10^{-5} << 1$ for the Earth (see **Table 1**), so that dynamically the Earth is nearly axisymmetric, eqns [8] and [9] can be simplified by replacing A and B in them with the average $A' = (A+B)/2$ of the equatorial principal moments of inertia of the Earth:

$$\frac{1}{\sigma_{ra}}\frac{\partial m_x(t)}{\partial t} + m_y(t) = \phi_{ra,\,y}(t) - \frac{1}{\Omega}\frac{\partial \phi_{ra,\,x}(t)}{\partial t} \qquad [17]$$

$$\frac{1}{\sigma_{ra}}\frac{\partial m_y(t)}{\partial t} - m_x(t) = -\phi_{ra,\,x}(t) - \frac{1}{\Omega}\frac{\partial \phi_{ra,\,y}(t)}{\partial t} \qquad [18]$$

where the excitation functions $\phi_{ra,\,i}(t)$ of a rigid axisymmetric body are

$$\phi_{ra,\,x}(t) = \frac{h_x(t) + \Omega\,\Delta I_{xz}(t)}{(C-A')\,\Omega} \qquad [19]$$

$$\phi_{ra,\,y}(t) = \frac{h_y(t) + \Omega\,\Delta I_{yz}(t)}{(C-A')\,\Omega} \qquad [20]$$

In the absence of excitation, the free motion of a rigid axisymmetric body is prograde undamped circular motion of natural frequency

$$\sigma_{\mathrm{ra}} = \left(\frac{C-A'}{A'}\right)\Omega \qquad [21]$$

Note that eqns [10] and [14], which describe changes in the rate of rotation of a rigid body, are the same whether the body is dynamically axisymmetric or triaxial.

Equations [10], [14], and [17]–[21] describe changes in the rotation of a rigid axisymmetric body that is subject to small perturbing excitation. But the Earth is not rigid – it has an atmosphere and oceans, a fluid core, and a solid crust and mantle that can deform in response not only to the applied excitation but also to changes in rotation that are caused by the excitation. In general, changes in rotation can be expected to cause changes in both the Earth's inertia tensor and in relative angular momentum. However, by definition of the Tisserand mean-mantle frame, there are no changes in relative angular momentum caused by motion of the crust and mantle. Furthermore, if it is assumed that the oceans stay in equilibrium as the rotation of the solid Earth changes so that no oceanic currents are generated by the changes in rotation, then there are also no changes in relative angular momentum due to motion of the oceans. And effects of the atmosphere can be ignored here because of its relatively small mass (see **Table 1**). Thus, only the core will contribute to changes in relative angular momentum caused by changes in rotation.

Smith and Dahlen (1981) used the results of Hough (1895) to show that the change $\delta h_i(\sigma)$ in relative angular momentum due to core motion caused by a rigid rotation of an axisymmetric crust and mantle is

$$\begin{pmatrix}\delta h_x(\sigma)\\ \delta h_y(\sigma)\\ \delta h_z(\sigma)\end{pmatrix} = \begin{pmatrix} E & iE' & 0\\ -iE' & E & 0\\ 0 & 0 & \tilde{E}\end{pmatrix}\begin{pmatrix} m_x(\sigma)\\ m_y(\sigma)\\ m_z(\sigma)\end{pmatrix} \qquad [22]$$

where to first order in the ellipticity ε_{c} of the surface of the core and at frequencies $\sigma << \Omega$

$$E = \left(\sigma^2/\Omega\right) A_{\mathrm{c}} \qquad [23]$$

$$E' = -\sigma\left(1-\varepsilon_{\mathrm{c}}\right) A_{\mathrm{c}} \qquad [24]$$

$$\tilde{E} = -\Omega\, C_{\mathrm{c}} \qquad [25]$$

where A_{c} and C_{c} are the equatorial and axial principal moments of inertia of the core and eqn [25] for $\tilde{E}$ has been inferred here by realizing that the core cannot respond to axial changes in the rotation of the mantle if the core–mantle boundary is axisymmetric and if there is no coupling between the core and the mantle (Merriam, 1980; Wahr *et al.*, 1981; Yoder *et al.*, 1981). Note that because of the assumption of dynamical axisymmetry, the equatorial components of eqn [22] are uncoupled from the axial, so that no spin–wobble coupling is introduced by the response of the core to changes in rotation.

Dahlen (1976) studied the passive influence of the oceans on the Earth's rotation, including the changes δI_{ij} in the Earth's inertia tensor that are caused by changes in the rotation of the Earth. In the absence of oceans, and assuming that the Earth responds to the centripetal potential associated with changes in rotation in exactly the same manner that a nonrotating Earth would respond to a static potential of the same amplitude and type, Dahlen (1976) found

$$\begin{pmatrix}\delta I_{xz}\\ \delta I_{yz}\\ \delta I_{zz}\end{pmatrix} = \frac{a^5\Omega^2}{3G}\begin{pmatrix} k_2 & 0 & 0\\ 0 & k_2 & 0\\ 0 & 0 & n_0+\frac{4}{3}k_2\end{pmatrix}\begin{pmatrix} m_x\\ m_y\\ m_z\end{pmatrix} \qquad [26]$$

where k_2 is the second-degree body tide Love number of the whole Earth (not of just the mantle (see Smith and Dahlen, 1981, p. 239), although for a different opinion see Dickman (2005)), n_{o} arises from the change in the mean moment of inertia of the Earth caused by the term in the centripetal potential that gives rise to a purely radial deformation of the Earth, G is the Newtonian gravitational constant, and a is the mean radius of the Earth (that is, the radius of a sphere having the same volume as that of the Earth).

When equilibrium oceans are present, Dahlen (1976) found that eqn [26] for the changes in the inertia tensor caused by changes in rotation is modified to

$$\begin{pmatrix}\delta I_{xz}\\ \delta I_{yz}\\ \delta I_{zz}\end{pmatrix} = \begin{pmatrix} D+\delta D & \delta D_{12} & \delta D_{13}\\ \delta D_{12} & D-\delta D & \delta D_{23}\\ \delta D_{13} & \delta D_{23} & \tilde{D}\end{pmatrix}\begin{pmatrix} m_x\\ m_y\\ m_z\end{pmatrix} \qquad [27]$$

where

$$D = \left(k_2 + \Delta k_{\mathrm{ocn,w}}\right)\frac{a^5\,\Omega^2}{3G} \qquad [28]$$

$$\tilde{D} = \left[n_{\mathrm{o}} + \frac{4}{3}\left(k_2 + \Delta k_{\mathrm{ocn,s}}\right)\right]\frac{a^5\,\Omega^2}{3G} \qquad [29]$$

where the influence of equilibrium oceans has been written in terms of an 'oceanic Love number' Δk_{ocn}

which modifies the second-degree body tide Love number k_2. Dahlen (1976) found that because of the nonuniform distribution of the oceans, the oceanic Love number is different for each component. However, the average of the equatorial components has been taken here to define a mean oceanic Love number $\Delta k_{\mathrm{ocn,w}}$ for the wobble. From eqn [27], it is seen that the nonuniform distribution of the oceans has also coupled the equatorial components to the axial via the off-diagonal elements δD_{13} and δD_{23}. However, the numerical results of Dahlen (1976) for Earth model 1066A (Gilbert and Dziewonski, 1975) show that this coupling is very weak, with $\delta D_{13}/D = 2.17 \times 10^{-3}$ and $-\delta D_{23}/D = 0.55 \times 10^{-3}$. The coupling between the equatorial components is also very weak, with $-\delta D_{12}/D = 3.15 \times 10^{-3}$.

Using eqns [22]–[25] to account for the relative angular momentum of the core caused by changes in rotation, eqns [27]–[29] to account for both the rotational deformation of the Earth and the passive response of equilibrium oceans to changes in rotation, and keeping terms to first order in small quantities, the linearized Liouville equation becomes

$$\frac{1}{\sigma_{\mathrm{cw}}}\frac{\partial m_x(t)}{\partial t} + m_y(t) = \chi_y(t) - \frac{1}{\Omega}\frac{\partial \chi_x(t)}{\partial t} \qquad [30]$$

$$\frac{1}{\sigma_{\mathrm{cw}}}\frac{\partial m_y(t)}{\partial t} - m_x(t) = -\chi_x(t) - \frac{1}{\Omega}\frac{\partial \chi_y(t)}{\partial t} \qquad [31]$$

$$\frac{1}{\Omega}\frac{\partial m_z(t)}{\partial t} = -\frac{1}{\Omega}\frac{\partial \chi_z(t)}{\partial t} \qquad [32]$$

where the theoretical frequency of the Chandler wobble is

$$\sigma_{\mathrm{cw}} = \left(\frac{C - A' - D}{A'_{\mathrm{m}} + \varepsilon_{\mathrm{c}} A_{\mathrm{c}} + D}\right)\Omega \qquad [33]$$

where $A'_{\mathrm{m}} = A' - A_{\mathrm{c}}$ is the equatorial principal moment of inertia of the crust and mantle, and the excitation functions $\chi_i(t)$ are

$$\chi_x(t) = \frac{h_x(t) + \Omega\,(1 + k'_2)\,\Delta I_{xz}(t)}{(C - A' - D)\,\Omega} \qquad [34]$$

$$\chi_y(t) = \frac{h_y(t) + \Omega\,(1 + k'_2)\,\Delta I_{yz}(t)}{(C - A' - D)\,\Omega} \qquad [35]$$

$$\chi_z(t) = k_{\mathrm{r}}\,\frac{h_z(t) + \Omega\,(1 + \alpha_3 k'_2)\,\Delta I_{zz}(t)}{C_{\mathrm{m}}\,\Omega} \qquad [36]$$

where C_{m} is the axial principal moment of inertia of the crust and mantle and k_{r} is a factor, whose value is near unity (see **Table 1**), that accounts for the effects of rotational deformation on the axial component:

$$k_{\mathrm{r}} = \left\{1 + \left[n_{\mathrm{o}} + \frac{4}{3}\left(k_2 + \Delta k_{\mathrm{ocn,s}}\right)\right]\frac{a^5\Omega^2}{3G}\frac{1}{C_{\mathrm{m}}}\right\}^{-1} \qquad [37]$$

The deformation of the Earth associated with surficial excitation processes that load the solid Earth has been taken into account in eqns [34]–[36] by including the second-degree load Love number k'_2 where, because of core decoupling, the load Love number in the axial component is modified by a factor of α_3 (Merriam, 1980; Wahr, 1983; Nam and Dickman, 1990; Dickman 2003). Expressions for the excitation functions for processes that do not load the solid Earth can be recovered from eqns [34]–[36] by setting the load Love number k'_2 to zero.

Equations [30]–[36] describe changes in the rotation of an elastic axisymmetric body having a fluid core and equilibrium oceans that is subject to small perturbing excitation. Equation [33] for the theoretical Chandler frequency of such a body was first derived by Smith and Dahlen (1981). Applying this result to the Earth, they found that elasticity of the solid Earth lengthens the period of the Chandler wobble from the rigid Earth value by 143.0 sidereal days, deformation of the oceans lengthens it a further 29.8 sidereal days, and the presence of a fluid core decreases it by 50.5 sidereal days. Using the values in **Table 1** for the Earth, the theoretical period of the Chandler wobble is found to be 426.8 sidereal days, or about 7.4 sidereal days shorter than the observed period of 434.2 ± 1.1 (1σ) sidereal days (Wilson and Vicente, 1990). This discrepancy between the theoretical and observed periods of the Chandler wobble is probably mainly due to the effects of mantle anelasticity, since departures of the oceans from equilibrium as large as 1% increase the Chandler period by only 0.3 sidereal days (Smith and Dahlen, 1981).

Mantle anelasticity modifies the body tide Love number k_2 and hence, via D, the frequency of the Chandler wobble and the equatorial excitation functions. It also modifies the load Love number k'_2. In the absence of accurate models of mantle anelasticity at the frequencies of interest here, namely, at frequencies $\sigma < \Omega$, a hybrid approach is taken to include its effects. The observed complex-valued frequency σ_0 of the Chandler wobble is substituted for its theoretical value in eqns [30] and [31]. It is also substituted for its theoretical value in the excitation

functions after rewriting them in terms of the theoretical value by using eqn [33] to eliminate D. The results are

$$\frac{1}{\sigma_o}\frac{\partial m_x(t)}{\partial t} + m_y(t) = \chi_y(t) - \frac{1}{\Omega}\frac{\partial \chi_x(t)}{\partial t} \quad [38]$$

$$\frac{1}{\sigma_o}\frac{\partial m_y(t)}{\partial t} - m_x(t) = -\chi_x(t) - \frac{1}{\Omega}\frac{\partial \chi_y(t)}{\partial t} \quad [39]$$

$$m_z(t) = -\chi_z(t) \quad [40]$$

where the excitation functions become

$$\chi_x(t) = \frac{h_x(t) + \Omega\,[1 + (k_2' + \Delta k_{an}')]\,\Delta I_{xz}(t)}{[C - A' + A_m' + \varepsilon_c A_c]\,\sigma_o} \quad [41]$$

$$\chi_y(t) = \frac{h_y(t) + \Omega\,[1 + (k_2' + \Delta k_{an}')]\,\Delta I_{yz}(t)}{[C - A' + A_m' + \varepsilon_c A_c]\,\sigma_o} \quad [42]$$

$$\chi_z(t) = k_r \frac{h_z(t) + \Omega\,[1 + \alpha_3(k_2' + \Delta k_{an}')]\,\Delta I_{zz}(t)}{C_m\,\Omega} \quad [43]$$

where $\Delta k_{an}'$ accounts for the effects of mantle anelasticity on the load Love number. Eqns [38]–[43] are the final expressions for the changes $m_i(t)$ in the rotation of the Earth caused by small excitation $\chi_i(t)$. Numerically, using 434.2 sidereal days (Wilson and Vicente, 1990) for the observed period of the Chandler wobble and the values in **Table 1** for the other constants, the real parts of the excitation functions can be written as

$$\chi_x(t) = \frac{1.608\,[h_x(t) + 0.684\,\Omega\,\Delta I_{xz}(t)]}{(C - A')\,\Omega} \quad [44]$$

$$\chi_y(t) = \frac{1.608\,[h_y(t) + 0.684\,\Omega\,\Delta I_{yz}(t)]}{(C - A')\,\Omega} \quad [45]$$

$$\chi_z(t) = \frac{0.997}{C_m\,\Omega}[h_z(t) + 0.750\,\Omega\,\Delta I_{zz}(t)] \quad [46]$$

These results agree with those of Wahr (1982, 1983, 2005) to within 2%, with most of the disagreement being due to differences in the values of the numerical constants.

The approach used here to derive linearized Liouville equations that can be used to study small changes in the Earth's rotation follows the approach of Smith and Dahlen (1981) and Wahr (1982, 1983, 2005). Other approaches have been given by Barnes *et al.* (1983), Eubanks (1993; also see Aoyama and Naito, 2000), and Dickman (1993, 2003). Dickman (2003) compares these different approaches and discusses the implications of nonzero coupling between the core and mantle; Wahr (2005) discusses the implications of mantle anelasticity. The influence of triaxiality on oceanless elastic bodies with a fluid core, with application to the rotation of Mars, has been studied by Yoder and Standish (1997) and Van Hoolst and Dehant (2002).

3.09.2.2 Celestial Intermediate Pole

Small changes in the Earth's rotation caused by small changes in relative angular momentum or small changes in the Earth's inertia tensor can be studied using eqns [38]–[43], where the $\Omega m_i(t)$ are the elements of the change $\Delta\boldsymbol{\omega}(t)$ to the Earth's rotation vector, so that $m_x(t)$, $m_y(t)$, and $1 + m_z(t)$ are the direction cosines of the rotation vector with respect to the coordinate axes of the rotating, body-fixed terrestrial reference frame. Alternatively, $m_x(t)$ and $m_y(t)$ can be interpreted as being the angular offsets of the rotation vector from the $\hat{\mathbf{z}}$-axis of the rotating reference frame in the $\hat{\mathbf{x}}$ and $\hat{\mathbf{y}}$ directions. That is, $m_x(t)$ and $m_y(t)$ specify the location of the rotation pole within the rotating, body-fixed terrestrial reference frame, where the rotation pole is that point defined by the intersection of the rotation axis with the surface of the Earth near the North Pole. But Earth rotation measurement services do not report the location of the rotation pole within the rotating, body-fixed terrestrial reference frame. Instead, they report the location of the celestial intermediate pole (CIP).

Just three time-dependent angles, the Euler angles, are required to directly transform the coordinates of some station from the terrestrial frame to the celestial frame. These angles are time dependent, of course, because the Earth, and hence the body-fixed terrestrial reference frame, is rotating. But, by tradition, an intermediate reference frame is used with the result that five angles are required to completely transform station coordinates from the terrestrial to the celestial reference frames (e.g., Sovers *et al.*, 1998):

$$\mathbf{r}_c(t) = \mathsf{PNSXY}\,\mathbf{r}_t(t) \quad [47]$$

where $\mathbf{r}_t(t)$ are, in general, the time-dependent coordinates of the station in the rotating, body-fixed terrestrial frame, $\mathbf{r}_c(t)$ are the coordinates of the station in the celestial frame, and P, N, S, X, and Y are the classical transformation matrices with P accounting for the precession of the Earth, N accounting for nutation, S accounting for spin, and X and Y accounting for the x- and y-components of polar motion. By first applying X and Y, the terrestrial coordinates of the station are transformed to an intermediate frame whose reference pole is the CIP; S represents a spin through a large angle about the $\hat{\mathbf{z}}$-axis

of the intermediate frame; P and N finally transform the intermediate frame to the celestial frame. This approach of using an intermediate frame and five angles (two polar motion parameters, two nutation parameters, and a spin parameter) to transform station coordinates between the terrestrial and celestial reference frames has been traditionally followed in order to separate polar motion from precession–nutation. This separation is done in such a manner that the precessional and nutational motion of the Earth is long period when observed in the celestial reference frame, and polar motion is long period when observed in the terrestrial reference frame.

Earth rotation measurement services report the parameters that are needed to carry out the transformation given by eqn [47], namely, the polar motion parameters $p_x(t)$ and $p_y(t)$ that are required in X and Y and that give the location of the CIP in the rotating, body-fixed terrestrial reference frame, the nutation parameters $\delta\psi(t)$ and $\delta\varepsilon(t)$ that are required in N and that are corrections in longitude and obliquity to the adopted nutation model that are needed to give the location of the CIP in the celestial reference frame, and a spin parameter UT1(t) that is required in S and that represents the angle through which the Earth has rotated. The precession transformation matrix P depends on the lunisolar and planetary precession constants.

The relationship between the polar motion parameters $p_x(t)$ and $p_y(t)$ that are reported by Earth rotation measurement services and the elements $\Omega m_x(t)$ and $\Omega m_y(t)$ of the Earth's rotation vector that are needed in eqns [38] and [39] can be derived by considering the properties of transformation matrices (Goldstein, 1950). The transformation of station coordinates between two frames having a common origin implies a rotation. Applying the transformation matrix to the position vector of some station to get its coordinates in a new frame is equivalent to a rotation of the coordinate axes. If the initial reference frame is the terrestrial reference frame of the Earth and the final frame is the celestial reference frame, and because the terrestrial reference frame has been fixed to the body of the Earth, then the equivalent rotation of the coordinate axes is simply the rotation of the Earth. Because an intermediate frame has been used to separate polar motion from precession–nutation, in order to derive the relationship between the polar motion parameters $p_x(t)$ and $p_y(t)$ and the elements $\Omega m_x(t)$ and $\Omega m_y(t)$ of the Earth's rotation vector, it is sufficient to consider the transformation matrix $\mathsf{A}^{\mathsf{T}} = \mathsf{S}\,\mathsf{X}\,\mathsf{Y}$ that transforms station coordinates between the terrestrial and intermediate reference frames:

$$\mathbf{r}_{\mathrm{i}}(t) = \mathsf{A}^{\mathsf{T}}(t)\,\mathbf{r}_{\mathrm{t}}(t) \qquad [48]$$

where the superscript 'T' denotes the transpose and $\mathbf{r}_{\mathrm{i}}(t)$ are the coordinates of the station in the intermediate frame. The elements ω_i of the rotation vector that is associated with this transformation matrix, that is, of the rotation vector of the Earth, are the three independent elements of the antisymmetric matrix $\mathsf{W}(t)$ (Kinoshita *et al.*, 1979; Gross, 1992):

$$\mathsf{W}(t) = \frac{\partial \mathsf{A}(t)}{\partial t}\mathsf{A}^{\mathsf{T}}(t) = \begin{pmatrix} 0 & \omega_z & -\omega_y \\ -\omega_z & 0 & \omega_x \\ \omega_y & -\omega_x & 0 \end{pmatrix} \qquad [49]$$

From Sovers *et al.* (1998), the classical X, Y, and S transformation matrices are

$$\mathsf{X}(t) = \begin{pmatrix} \cos p_x(t) & 0 & -\sin p_x(t) \\ 0 & 1 & 0 \\ \sin p_x(t) & 0 & \cos p_x(t) \end{pmatrix} \qquad [50]$$

$$\mathsf{Y}(t) = \begin{pmatrix} 1 & 0 & 0 \\ 0 & \cos p_y(t) & \sin p_y(t) \\ 0 & -\sin p_y(t) & \cos p_y(t) \end{pmatrix} \qquad [51]$$

$$\mathsf{S}(t) = \begin{pmatrix} \cos H(t) & -\sin H(t) & 0 \\ \sin H(t) & \cos H(t) & 0 \\ 0 & 0 & 1 \end{pmatrix} \qquad [52]$$

where by tradition the positive direction of $p_y(t)$ is taken to be toward 90° W longitude, and H is the hour angle of the true equinox of date which is related to UT1 and the hour angle of the mean equinox of date by the equation of the equinoxes. By forming $\mathsf{A}^{\mathsf{T}} = \mathsf{S}\,\mathsf{X}\,\mathsf{Y}$, using eqn [49], and keeping terms to first order in small quantities, the desired elements of the rotation vector of the terrestrial frame with respect to the intermediate frame is obtained (Brzezinski, 1992; Gross, 1992; Brzezinski and Capitaine, 1993):

$$\omega_x(t) = \Omega\, p_x(t) - \frac{\partial p_y(t)}{\partial t} \qquad [53]$$

$$\omega_y(t) = -\Omega\, p_y(t) - \frac{\partial p_x(t)}{\partial t} \qquad [54]$$

$$\omega_z(t) = [1 + p_z(t)]\,\Omega \qquad [55]$$

where the time rate-of-change of H has been set equal to $(1+p_z)\Omega$ where $p_z(t)=m_z(t)$ represents small departures from uniform spin at the mean sidereal rotation rate Ω of the Earth.

In complex notation, with $\mathbf{m}(t)=m_x(t)+im_y(t)$ and $\mathbf{p}(t)=p_x(t)-ip_y(t)$, where the negative sign accounts for $p_y(t)$ being positive toward 90° W longitude, eqns [53] and [54] can be written as

$$\mathbf{m}(t) = \mathbf{p}(t) - \frac{i}{\Omega}\frac{\partial \mathbf{p}(t)}{\partial t} \qquad [56]$$

For frequencies of motion $\sigma << \Omega$, the second term on the right-hand side of eqn [56] becomes much smaller than the first and the motion of the rotation pole becomes the same as the motion of the CIP. But for frequencies of motion $|\sigma| \approx \Omega$, the motions of the rotation and celestial intermediate poles are very different. This difference becomes important when studying rapid motions such as those caused by the diurnal and semidiurnal ocean tides (see Section 3.09.4.2.3). For example, the amplitude of the prograde diurnal tide-induced motion of the rotation pole is about twice as large as that of the CIP.

Using eqns [53] and [54] for the relationship between the reported polar motion parameters $p_x(t)$ and $p_y(t)$ and the elements $\omega_x(t)$ and $\omega_y(t)$ of the Earth's rotation vector, eqns [38] and [39] can be written in complex notation as (Brzezinski, 1992; Gross, 1992)

$$\mathbf{p}(t) + \frac{i}{\sigma_o}\frac{\partial \mathbf{p}(t)}{\partial t} = \boldsymbol{\chi}(\boldsymbol{\tau}) \qquad [57]$$

where $\boldsymbol{\chi}(t) = \chi_x(t) + i\chi_y(t)$. The axial component, eqn [40], is usually written in terms of changes $\Delta\Lambda(t)$ of the length of the day as

$$\frac{\Delta\Lambda(t)}{\Lambda_O} = \chi_z(t) \qquad [58]$$

where Λ_O is the nominal length-of-day (LOD) of 86 400 s. Equations [57] and [58] are the final expressions, written in terms of the parameters actually reported by Earth rotation measurement services, for the changes in the rotation of the Earth caused by small excitation $\chi_i(t)$, where the excitation functions are given by eqns [41]–[43].

Since five angles are traditionally used to transform station coordinates between the terrestrial and celestial reference frames when only three are required, the five traditional Earth orientation parameters (EOPs) are not independent of each other. Because the frequency σ_c of some motion as observed in the celestial reference frame is related to the frequency σ_t of that same motion as observed in the terrestrial reference frame by

$$\sigma_c = \sigma_t + \Omega \qquad [59]$$

then motion having a retrograde nearly diurnal frequency in the terrestrial reference frame ($\sigma_t \approx -\Omega$) will be of low frequency (long period) when observed in the celestial reference frame. That is, retrograde, nearly diurnal polar motions are equivalent to nutations. In particular, the two polar motion parameters are related to the two nutation parameters by (Brzezinski, 1992; Brzezinski and Capitaine, 1993)

$$\mathbf{p}(t) = -\mathbf{n}(t)\,e^{-i\Omega t} \qquad [60]$$

where Greenwich mean sidereal time (GMST) has been approximated by Ωt in the exponent and $\mathbf{n}(t)=\delta\psi(t)\ \sin\varepsilon_o + i\delta\varepsilon(t)$ with ε_o being the mean obliquity of the ecliptic.

A degeneracy also exists between the EOPs and different realizations of the terrestrial reference frame. Since by eqn [49] the Earth's rotation vector can be determined from the transformation matrix that transforms station coordinates between the terrestrial and celestial reference frames, if the realization of the terrestrial reference frame changes, then the elements of the rotation vector will change. In particular, a positive change in the x-component of polar motion is equivalent to a left-handed (clockwise) rotation of the terrestrial reference frame about the $\hat{\mathbf{y}}$-axis; a positive change in the y-component of polar motion, remembering that $p_y(t)$ is defined to be positive toward 90° W longitude, is equivalent to a left-handed rotation of the terrestrial reference frame about the $\hat{\mathbf{x}}$-axis; and a positive change in UT1 is equivalent to a right-handed (counter-clockwise) rotation of the terrestrial reference frame about the $\hat{\mathbf{z}}$-axis.

The polar motion parameters $p_x(t)$ and $p_y(t)$ give the location in the terrestrial frame of the reference pole of the intermediate frame, whatever that intermediate frame may be. The 1980 International Astronomical Union (IAU) theory of nutation adopted the celestial ephemeris pole (CEP) as the reference pole of the intermediate frame (Seidelmann, 1982), defining it to be a pole that exhibits no nearly diurnal motions in either the body-fixed terrestrial frame or in the celestial frame. The CEP was chosen (Seidelmann, 1982) to be the B-axis of Wahr (1981), which is the axis of figure for the Tisserand mean outer surface of the Earth, where the averaging procedure is such that the

resulting *B*-axis does not move in response to body tides. Since observing stations are attached to the outer surface of the Earth, their measurements are sensitive to the motion of the Earth's surface in space. Wahr (1981) thus generalized the concept of the Tisserand mean-mantle frame to that of the Tisserand mean-surface frame, with his *B*-axis being the reference axis of the Tisserand mean-surface frame that moves in space with the mean motion of the observing stations.

In 2000, the IAU adopted the CIP as the reference pole of the intermediate frame (McCarthy and Petit, 2004, chapter 5). The definition of the CIP extends that of the CEP by clarifying the definition of polar motion and precession–nutation. The CEP was defined in such a manner that it exhibits no nearly diurnal motion in either the terrestrial or celestial reference frames. That is, precession–nutation was considered to be motion of the CEP as viewed in the celestial reference frame with the frequency of motion ranging between −0.5 and +0.5 cycles per sidereal day (cpsd), and polar motion was considered to be motion of the CEP as viewed in the terrestrial reference frame with the frequency of motion in that frame ranging between −0.5 and +0.5 cpsd (Capitaine, 2000). Since frequencies of motion in the two frames are related by eqn [59], in the celestial reference frame polar motion was motion of the CEP with frequencies ranging between +0.5 and +1.5 cpsd. Thus, motion of the CEP in the celestial frame was defined for frequencies between −0.5 and +1.5 cpsd, with the division between polar motion and precession–nutation being at a frequency of +0.5 cpsd. Motion of the CEP outside this celestial frequency band was undefined. Similarly, motion of the CEP in the terrestrial reference frame was defined for frequencies between −1.5 and +0.5 cpsd with the division between polar motion and precession–nutation being at a frequency of −0.5 cpsd. Motion of the CEP outside this terrestrial frequency band was also undefined (see **Figure 1**).

Since 1980, when the CEP was adopted as the reference pole of the intermediate frame, models of polar motion with frequencies outside the terrestrial frequency band within which the motion of the CEP was defined became available. These polar motions were due to the effects of diurnal and semidiurnal ocean tides. Models of nutations having frequencies outside the celestial frequency band within which the CEP was defined also became available, as did space-geodetic measurements

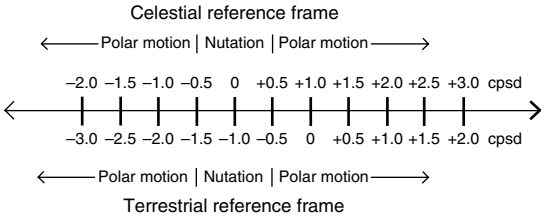

Figure 1 Schematic illustration of the relationship between the frequency of some motion as viewed in the celestial (top half of figure) and terrestrial (bottom half of figure) reference frames (see eqn [59]). By convention, nutation is motion of the CIP having frequencies in the range [−0.5, +0.5] cpsd as viewed in the celestial frame. As viewed in the terrestrial frame, this same nutational motion of the Earth has frequencies in the range [−1.5, −0.5] cpsd. Motion at all other frequencies is considered to be polar motion.

having subdaily temporal resolution. With these improvements in models and measurements came the need to extend the definition of the CEP to all possible frequencies of motion, not just those between −0.5 and +1.5 cpsd in the celestial frame, or −1.5 to +0.5 cpsd in the terrestrial frame. At the time that the definition of the intermediate pole was extended, its name was changed to the CIP. When defining the CIP, the concept used in defining the CEP of a pole having no nearly diurnal motions in either the terrestrial or celestial reference frames had to be abandoned because ocean tides can cause polar motions having frequencies near +1 cpsd as viewed in the terrestrial reference frame.

The CIP is still chosen to be the axis of figure for the Tisserand mean outer surface of the Earth, as it was for the CEP. And the CIP is defined in such a manner that precession–nutation is still considered to be motion of the CIP as viewed in the celestial reference frame with the frequency of motion ranging between −0.5 and +0.5 cpsd (Capitaine, 2000). But now polar motion is considered to be motion of the CIP in the celestial frame at all other frequencies, or motion of the CIP in the terrestrial frame at all frequencies except those between −1.5 and −0.5 cpsd (see **Figure 1**). This has the effect of including in nutation those ocean tidal terms having retrograde nearly diurnal frequencies as viewed in the terrestrial reference frame, and of including in polar motion those nutation terms having frequencies less than −0.5 cpsd or greater than +0.5 cpsd as viewed in the celestial reference frame (see **Table 2**).

Table 2 Coefficients of those nutation terms that are included in polar motion by definition of the CIP

Degree of potential	Fundamental argument						Period (solar days)	$p_x(t)$, (μas)		$p_y(t)$, (μas)	
	γ	l	l′	F	D	Ω		sin	cos	sin	cos
2	1	1	0	0	0	0	0.96244	0.76	−0.43	0.43	0.76
2	1	0	0	0	0	−1	0.99712	1.93	−1.11	1.11	1.93
2	1	0	0	0	0	0	0.99727	14.27	−8.19	8.19	14.27
2	1	0	0	−2	2	−2	1.00275	−4.76	2.73	−2.73	−4.76
2	1	−1	0	0	0	0	1.03472	0.84	−0.48	0.48	0.84
2	1	0	0	−2	0	−2	1.07581	−11.36	6.52	−6.52	−11.36
2	1	0	0	−2	0	−1	1.07598	−2.14	1.23	−1.23	−2.14
2	1	1	0	−2	−2	−2	1.22346	−0.44	0.25	−0.25	−0.44
2	1	−1	0	−2	0	−2	1.11951	−2.31	1.32	−1.32	−2.31
2	1	−1	0	−2	0	−1	1.11970	−0.44	0.25	−0.25	−0.44
3	0	1	0	1	0	1	13.719	1.28	0.16	−0.16	1.28
3	0	0	0	1	0	0	27.212	2.62	0.32	−0.32	2.62
3	0	0	0	1	0	1	27.322	16.64	2.04	−2.04	16.64
3	0	0	0	1	0	2	27.432	−0.87	−0.11	0.11	−0.87
3	0	1	0	1	−2	1	193.560	2.10	0.27	−0.27	2.10
3	0	0	0	1	−1	1	365.242	1.31	0.20	−0.20	1.31
3	0	1	1	−1	0	−1	411.807	1.05	0.27	−0.27	1.05
3	0	1	1	−1	0	0	438.360	−0.63	0.12	−0.12	−0.63
3	0	−1	0	1	0	0	2190.35	−2.78	−0.31	0.31	−2.78
3	0	−1	0	1	0	1	3231.50	−16.16	−1.83	1.83	−16.16
3	0	−1	0	1	0	2	6159.14	0.78	0.09	−0.09	0.78
3	0	1	0	−1	0	−2	−6159.14	−0.68	−0.09	0.09	−0.68
3	0	1	0	−1	0	−1	−3231.50	12.32	1.59	−1.59	12.32
3	0	1	0	−1	0	0	−2190.35	1.86	0.24	−0.24	1.86
3	0	−1	0	−1	2	−1	−193.560	0.81	0.10	−0.10	0.81
3	0	0	0	−1	0	−2	−27.432	−0.82	−0.10	0.10	−0.82
3	0	0	0	−1	0	−1	−27.322	15.75	1.93	−1.93	15.75
3	0	0	0	−1	0	0	−27.212	2.48	0.30	−0.30	2.48
3	0	−1	0	−1	0	−1	−13.719	1.39	0.17	−0.17	1.39
Rate of secular polar motion (μas/yr) due to the zero-frequency tide											
4	0	0	0	0	0	0			−3.80		−4.31

Terms with amplitudes less than 0.5 microarcsecond (μas) are not tabulated. γ is GMST reckoned from the lower culmination of the vernal equinox (GMST + π). l, l', F, D, and Ω are the Delaunay arguments, expressions for which are given in Simon *et al*. (1994). The period, given in solar days, is the approximate period of the term as viewed in the terrestrial reference frame. Terms having positive (negative) periods indicate prograde (retrograde) circular motion. Summing prograde and retrograde circular motions having the same period yields elliptical motion. The nearly diurnal terms, like the nearly diurnal and nearly semidiurnal ocean tidal terms, are not included in the polar motion parameters reported by Earth rotation measurement services. However, the secular rate and the long-period terms, like the long-period ocean tidal terms, are included in the reported polar motion parameters. Also see McCarthy and Petit (2004, table 5.1).
Reproduced from Mathews PM and Bretagnon P (2003) Polar motions equivalent to high frequency nutations for a nonrigid Earth with anelastic mantle. *Astronomy and Astrophysics* 400: 1113–1128, with permission from Springer.

3.09.3 Earth Rotation Measurement Techniques

Changes in the Earth's rate of rotation become apparent when comparing time kept by the rotating Earth, known as Universal Time (UT), to uniform timescales based either upon atomic clocks or upon the motion of the Sun and other celestial bodies. Prior to the development of atomic clocks, the most accurate measurements of changes in the Earth's rate of rotation were obtained by timing the occultations of stars by the Moon. With the advent of atomic clocks in 1955, a uniform atomic timescale became available that could be used as a reference when measuring the transit times of stars as they pass through the local meridian. Changes in the Earth's rate of rotation could then be determined more accurately from optical astrometric measurements of star transits than they could from measurements of lunar occultations. And prior to the development of space-geodetic techniques, optical astrometric measurements of changes in the apparent latitudes of observing

stations yielded the most accurate estimates of polar motion. The space-geodetic techniques of very long baseline interferometry (VLBI), global navigation satellite systems (GNSSs) like the global positioning system (GPS), and satellite and lunar laser ranging (LLR) are now the most accurate techniques available for measuring changes in both the Earth's rate of rotation and in polar motion.

3.09.3.1 Lunar Occultation

The most recent re-reduction of lunar occultation measurements for Universal Time and Length-of-day changes is that of Jordi *et al.* (1994) who analyzed about 53 000 observations of lunar occultations spanning 1830.0–1955.5. They used a reference frame defined by the FK5 star catalog, the LE200 lunar ephemeris, and corrections for the limb profile of the Moon. The Universal Time series they obtained consists of values and 1σ uncertainties for the difference between Terrestrial Time (TT) and Universal Time (TT–UT1) spanning 1830.0–1955.5 at 4-month intervals. Terrestrial Time is a dynamical timescale that can be related to International Atomic Time (TAI) by adding 32.184 s to TAI (Seidelmann *et al.*, 1992).

Jordi *et al.* (1994) extended their (TT–UT1) series to 1992 by using values of (UT1–TAI) obtained from the Bureau International de l'Heure (BIH) and the International Earth Rotation and Reference Systems Service (IERS). They then derived a LOD series spanning 1830–1987 at 4-month intervals by finite differencing and smoothing the extended UT1 series. Gross (2001) combined the lunar occultation measurements of Jordi *et al.* (1994) with optical astrometric and space-geodetic measurements to produce a smoothed LOD series spanning 1832.5–1997.5 at yearly intervals. Other UT1 and LOD series based upon lunar occultation measurements are those of Morrison (1979), Stephenson and Morrison (1984), McCarthy and Babcock (1986), and Liao and Greiner-Mai (1999).

3.09.3.2 Optical Astrometric

The International Latitude Service (ILS) was established by the International Association of Geodesy (IAG) in 1895 for the purpose of monitoring the wobbling motion of the Earth that had been detected by Seth Carlo Chandler, Jr., in 1891. As the Earth wobbles, the apparent latitude of an astronomical observing station will vary. To measure this variation of latitude and infer the underlying polar motion that is causing it, the ILS established six observing stations that were well distributed in longitude and that were all located at nearly the same latitude of 39° 8′ N. A seventh station, Kitab, was added in 1930 to replace the station at Tschardjui that ceased operations in 1919 due to a nearby river changing its course and adversely affecting the seeing conditions at Tschardjui. Locating all the ILS stations at nearly the same latitude allowed common star pairs to be observed by the same Horrebow–Talcott method (Munk and MacDonald, 1960, chapter 7), thereby allowing the polar motion to be determined from the latitude observations free of first-order errors in the reference star catalog.

The use of different star catalogs, standards, and data reduction procedures during the history of the ILS observing program can introduce discontinuities in the polar motion series derived from the ILS observations. In order to produce a homogeneous polar motion series unaffected by these sources of error, Yumi and Yokoyama (1980) re-reduced 772 395 latitude observations taken at the seven ILS observing stations using the Melchior and Dejaiffe (1969) star catalog and the 1964 IAU System of Astronomical Constants. The resulting polar motion series, known as the homogeneous ILS series, spans October 1899 to December 1978 at monthly intervals.

During the 20th century, numerous other optical astrometric measurements of latitude and longitude were taken at other stations and by other methods besides those of the ILS. At the BIH, Li (1985) and Li and Feissel (1986) re-reduced 240 140 optical astrometric measurements of longitude and 259 159 measurements of latitude taken at 136 observing stations. In order to produce an Earth orientation series independent of the ILS series, no measurements taken at the ILS stations were used. The resulting UT1 and polar motion series, which is known as the BIH series, spans January 5.0, 1962, to December 31.0, 1981, at 5-day intervals.

The High Precision Parallax Collecting Satellite (HIPPARCOS) star catalog, being constructed from observations taken above the Earth's atmosphere, is substantially more accurate than earlier ground-based catalogs such as the Melchior and Dejaiffe (1969) catalog used by Yumi and Yokoyama (1980). The improved accuracy of the HIPPARCOS star catalog motivated Vondrák (1991, 1999) and Vondrák *et al.* (1992, 1995, 1997, 1998) to once again re-reduce optical astrometric measurements for EOPs. All available optical astrometric measurements, numbering 4 315 628 from 48 instruments including those taken at

the ILS stations, were collected and corrected for instrumental errors and such systematic effects as plate tectonic motion, ocean loading, and tidal variations. The corrected measurements were then used to estimate nutation, polar motion, and Universal Time. The resulting Earth orientation series, known as the HIPPARCOS series, consists of values and uncertainties for polar motion and nutation spanning 1899.7–1992.0 at quasi-5-day intervals, with UT1 estimates starting in 1956 shortly after atomic clocks first became available.

3.09.3.3 Space Geodetic

An integral part of geodesy has always been the definition and realization of a terrestrial, body-fixed reference frame, a celestial, space-fixed reference frame, and the determination of the EOPs (precession, nutation, spin, and polar motion) that link these two reference frames together. But with the advent of space geodesy – with the placement of laser retroreflectors on the Moon by Apollo astronauts and Soviet landers, the launch of the LAser GEOdynamics Satellite (LAGEOS), the development of VLBI, and the development of GNSSs like the GPS – a quantum leap has been taken in our ability to realize the terrestrial and celestial reference frames and to determine the EOPs.

The only space-geodetic measurement technique capable of independently determining all of the EOPs is multibaseline VLBI (*see* Chapter 3.11). All of the other techniques need to either apply external constraints to the determined EOPs or can determine only subsets of the EOPs, only linear combinations of the EOPs, or only their time rates-of-change.

3.09.3.3.1 Very long baseline interferometry

Radio interferometry is routinely used to make highly accurate measurements of UT1 and polar motion with observing sessions lasting from about an hour to a day. The VLBI technique measures the difference in the arrival time of a radio signal at two or more radio telescopes that are simultaneously observing the same distant extragalactic radio source (Lambeck, 1988, chapter 8; Robertson, 1991; Sovers *et al.*, 1998). This technique is therefore sensitive to processes that change the relative position of the radio telescopes with respect to the source, such as a change in the orientation of the Earth in space or a change in the position of the telescopes due to, for example, tidal displacements or tectonic motions. If just two telescopes are observing the same source, then only two components of the Earth's orientation can be determined. A rotation of the Earth about an axis parallel to the baseline connecting the two radio telescopes does not change the relative position of the telescopes with respect to the source, and hence this component of the Earth's orientation is not determinable from VLBI observations taken on that single baseline. Multibaseline VLBI observations with satisfactory geometry can determine all of the components of the Earth's orientation including their time rates-of-change.

The International VLBI Service for Geodesy and Astrometry (IVS; Schlüter *et al.*, 2002), a service of both the IAG and the IAU, was established on 11 February 1999 to support research in geodesy, geophysics, and astrometry. As part of its activities, it coordinates the acquisition and reduction of VLBI observations for the purpose, in part, of monitoring changes in the Earth's rotation and defining and maintaining the international terrestrial and celestial reference frames. VLBI data products, including EOPs determined from both single and multibaseline observations, are available through the IVS website (see **Table 3**).

3.09.3.3.2 Global navigation satellite system

GNSSs consist of two major elements: (1) a space-based element consisting of a constellation of transmitting satellites, and (2) a ground-based element consisting of a network of receivers. In the GPS of the United States, the satellites, including spares, are at altitudes of 20 200 km in orbits with periods of 11 h 58 min located in six orbital planes, each inclined at 55° to the Earth's equator with four or more satellites in each plane. In the GLObal NAvigation Satellite System (GLONASS) of Russia, the satellites are at altitudes of 19 100 km in circular orbits with periods of 11 h 15 min located in three orbital planes, each inclined at 64.8° to the Earth's equator with eight satellites in each plane. In the future Galileo system of Europe, which is expected to be fully operational in 2008, the satellites will be at altitudes of 23 222 km in circular orbits with periods of 14 h 22 min located in three orbital planes, each inclined at 56° to the Earth's equator with nine satellites and one spare in each plane.

In GNSSs, the navigation signals are broadcast by the satellites at more than one frequency, thereby enabling first-order corrections to be made for ionospheric refraction effects. The ground-based multichannel receivers detect the navigation signals being broadcast by those satellites that are above the

Table 3 Sources of Earth orientation data

Data type	URL
Very long baseline interferometry	
IVS	http://ivscc.gsfc.nasa.gov/
Global navigation satellite system	
IGS	http://igscb.jpl.nasa.gov/
Satellite and lunar laser ranging	
ILRS	http://ilrs.gsfc.nasa.gov/
DORIS	
IDS	http://ids.cls.fr/
Intertechnique combinations	
IERS	http://www.iers.org/
JPL	ftp://euler.jpl.nasa.gov/keof/

URL, Uniform Resource Locator, IVS, International VLBI Service for Geodesy and Astrometry; VLBI, very long baseline interferometry; IGS, International GNSS Service; GNSS, global navigation satellite system; ILRS, International Laser Ranging Service; DORIS, Doppler orbitography and radio positioning integtrated by satellite; IDS International DORIS Service; IERS, International Earth Rotation and Reference Systems Service; JPL, Jet Propulsion Laboratory.

horizon (up to the number of channels in the receiver). In principle, trilateration can then be used to determine the position of each receiver, and by extension the orientation of the network of receivers as a whole. In practice, in order to achieve higher accuracy, more sophisticated analysis techniques are employed to determine the EOPs and other quantities such as orbital parameters of the satellites, positions of the stations, and atmospheric parameters such as the zenith path delay (Bock and Leppard, 1990; Blewitt, 1993; Beutler *et al.*, 1996; Hofmann-Wellenhof *et al.*, 1997; Leick, 2003).

Only polar motion and its time rate-of-change can be independently determined from GNSS measurements. UT1 cannot be separated from the orbital elements of the satellites and hence cannot be determined from GNSS data. The time rate-of-change of UT1, which is related to the length of the day, can be determined from GNSS measurements. But because of the corrupting influence of orbit error, VLBI measurements are usually used to constrain the GNSS-derived LOD estimates.

The International GNSS Service (IGS; Beutler *et al.*, 1999), a service of the IAG, was established on 1 January 1994 under its former name of the International GPS Service to support Earth science research. As part of its activities, it coordinates the acquisition and reduction of GNSS observations for the purpose, in part, of maintaining the ITRF and monitoring changes in the Earth's rotation and geocenter. GNSS data products, including EOPs, are available through the IGS website (see **Table 3**).

3.09.3.3.3 Satellite and lunar laser ranging

In the technique of satellite laser ranging (SLR), the round trip time-of-flight of laser light pulses are accurately measured as they are emitted from a laser system located at some ground-based observing station, travel through the Earth's atmosphere to some artificial satellite orbiting the Earth, are reflected by retroreflectors carried onboard that satellite, and return to the same observing station from which they were emitted (Lambeck, 1988, chapter 6). This time-of-flight range measurement is converted into a distance measurement by using the speed of light and correcting for a variety of known or modeled effects such as atmospheric path delay and satellite center-of-mass offset. Although a number of satellites carry retroreflectors for tracking and navigation purposes, the LAGEOS I and II satellites were specifically designed and launched to study geodetic properties of the Earth including its rotation and are the satellites most commonly used to determine EOPs. Including range measurements to the Etalon I and II satellites has been found to strengthen the solution for the EOPs, so these satellites are now often included when determining EOPs.

The EOPs are recovered from the basic range measurements in the course of determining the satellite's orbit. The basic range measurement is sensitive to any geophysical process that changes the distance between the satellite and the observing station, such as displacements of the satellite due to perturbations of the Earth's gravitational field, motions of the observing station due to tidal displacements or plate

tectonics, or a change in the orientation of the Earth (which changes the location of the observing station with respect to the satellite). These and other geophysical processes must be modeled when fitting the satellite's orbit to the range measurements as obtained at a number of globally distributed tracking stations. Adjustments to the *a priori* models used for these effects can then be obtained during the orbit determination procedure, thereby enabling, for example, the determination of station positions and EOPs (Smith *et al.*, 1985, 1990, 1994; Tapley *et al.*, 1985, 1993). However, because variations in UT1 cannot be separated from variations in the orbital node of the satellite, which are caused by the effects of unmodeled forces acting on the satellite, it is not possible to independently determine UT1 from SLR measurements. But independent estimates of the time rate-of-change of UT1, or equivalently, of LOD, can be determined from SLR measurements, as can polar motion and its time rate-of-change.

The technique of LLR is similar to that of SLR except that the laser retroreflector is located on the Moon instead of on an artificial satellite (Mulholland, 1980; Lambeck, 1988, chapter 7; Williams *et al.*, 1993; Dickey *et al.*, 1994a; Shelus, 2001). LLR is technically more challenging than SLR because of the need to detect the much weaker signal that is returned from the Moon. Larger, more powerful laser systems with more sophisticated signal detection systems need to be employed in LLR; consequently, there are far fewer stations that range to the Moon than to artificial satellites. In fact, there are currently only two stations that regularly range to the Moon: the McDonald Observatory in Texas and the Observatoire de la Côte d'Azur in the south of France.

The EOPs are typically determined from LLR data by analyzing the residuals at each station after the lunar orbit and other parameters such as station and reflector locations have been fit to the range measurements (Stolz *et al.*, 1976; Langley *et al.*, 1981a; Dickey *et al.*, 1985). From this single-station technique, two linear combinations of UT1 and the polar motion parameters $p_x(t)$ and $p_y(t)$ can be determined, namely, UT0 and the variation of latitude $\Delta\phi_i(t)$ at that station:

$$\Delta\phi_i(t) = p_x(t)\cos\lambda_i - p_y(t)\sin\lambda_i \quad [61]$$

$$\mathrm{UT0}(t) - \mathrm{TAI}(t) = \mathrm{UT1}(t) - \mathrm{TAI}(t) + [p_x(t)\sin\lambda_i + p_y(t)\cos\lambda_i]\tan\phi_i \quad [62]$$

where ϕ_i and λ_i are the nominal latitude and longitude of station i. A rotation of the Earth about an axis connecting the station with the origin of the terrestrial reference frame does not change the distance between the station and the Moon, and hence this component of the Earth's orientation cannot be determined from single-station LLR observations.

The International Laser Ranging Service (ILRS; Pearlman *et al.*, 2002, 2005) is a service of the IAG that was established on 22 September 1998 to support research in geodesy, geophysics, and lunar science. As part of its activities, the ILRS coordinates the acquisition and reduction of SLR and LLR observations for the purpose, in part, of maintaining the ITRF and monitoring the Earth's rotation and geocenter motion. SLR and LLR data products, including EOPs, are available through the ILRS website (see **Table 3**).

3.09.3.3.4 Doppler orbitography and radio positioning integrated by satellite

Like GNSSs, the French Doppler orbitography and radio positioning integrated by satellite (DORIS) system also consists of space-based and ground-based elements (Tavernier *et al.*, 2005; Willis *et al.*, 2006). But in the DORIS system, the transmitting beacons are located on the ground and the receivers are located on the satellites. Currently, there are 56 globally distributed beacons broadcasting to receivers onboard five satellites (SPOT-2, SPOT-4, SPOT-5, Jason-1, and the Environmental Satellite (ENVISAT)). The ocean topography experiment (TOPEX)/positioning ocean solid earth ice dynamics orbiting/orbital navigator (POSEIDON) (TOPEX/POSEIDON) and decommissioned SPOT-3 satellites also carried DORIS receivers and the future Jason-2 satellite will carry a DORIS receiver.

In the DORIS system, the Doppler shift of two transmitted frequencies is accurately measured. The use of two frequencies allows corrections to be made for ionospheric effects. Processing these Doppler measurements, usually as range-rate (Tapley *et al.*, 2004), allows the orbit of the satellite to be determined along with other quantities such as station positions and EOPs. As with other satellite techniques, UT1 cannot be determined from DORIS measurements, but its time rate-of-change can be determined, as can polar motion and its rate-of-change (Willis *et al.*, 2006).

The International DORIS Service (IDS; Tavernier *et al.*, 2005) is a service of the IAG that was established on 1 July 2003 to support research in geodesy and geophysics. As part of its activities, the

IDS coordinates the acquisition and reduction of DORIS observations for the purpose, in part, of maintaining the ITRF and monitoring the Earth's rotation and geocenter motion. DORIS data products, including EOPs, are available through the IDS website (see **Table 3**).

3.09.3.4 Ring Laser Gyroscope

Ring laser gyroscopes are a promising emerging technology for determining the Earth's rotation. In a ring laser gyroscope, two laser beams propagate in opposite directions around a ring. Since the ring laser gyroscope is rotating with the Earth, the effective path length of the beam that is corotating with the Earth is slightly longer than the path that is counterrotating with it. Because the effective path lengths of the two beams differ, their frequencies differ, so they interfere with each other to produce a beat pattern (Stedman, 1997). The beat frequency $\delta f(t)$, which can be measured and is known as the Sagnac frequency, is proportional to the instantaneous angular velocity $\boldsymbol{\omega}(t)$ of the Earth:

$$\delta f(t) = \frac{4A}{\lambda P}\,\mathbf{n}\cdot\boldsymbol{\omega}(t) \qquad [63]$$

where A is the area of the ring, P is the optical path length, λ is the wavelength of the laser beam in the absence of rotation, and $\mathbf{n}$ is the unit vector normal to the plane of the ring. By making the instrument rigid and the laser stable so that A, P, and λ are constants, the component of the Earth's instantaneous rotation vector that is parallel to the normal of the plane of the ring can be determined from measurements of the Sagnac frequency. All three components of the Earth's rotation vector are determinable from three mutually orthogonal colocated ring laser gyroscopes, or from a globally distributed network of gyroscopes.

Ring laser gyroscopes measure the absolute rotation of the Earth in the sense that, in principle, just a single measurement of the Sagnac frequency is required to determine $\mathbf{n}\cdot\boldsymbol{\omega}$. All of the other techniques discussed above are relative sensors because they infer the Earth's rotation from the change in the orientation of the Earth that takes place between at least two measurements that are separated in time. Thus, ring laser gyroscopes are fundamentally different from the space-geodetic techniques that are currently used to regularly monitor the Earth's rotation. Measurements taken by ring laser gyroscopes can therefore be expected to contribute to our understanding of the Earth's changing rotation, particularly of changes that occur on subdaily to daily timescales (Schreiber *et al.*, 2004).

3.09.3.5 Intertechnique Combinations

EOPs can be determined from measurements taken by each of the techniques discussed above. But each technique has its own unique strengths and weaknesses in this regard. Not only is each technique sensitive to a different subset and/or linear combination of the EOPs, but the averaging time for their determination is different, as is the interval between observations, the precision with which they can be determined, and the duration of the resulting EOP series. By combining the individual series determined by each technique, a series of the Earth's orientation can be obtained that is based upon independent measurements and that spans the greatest possible time interval. Such a combined Earth orientation series is useful for a number of purposes, including a variety of scientific studies and as an *a priori* series for use in data reduction procedures. However, care must be taken in generating such a combined series in order to account for differences in the underlying reference frames within which each individual series is determined, which can lead to differences in the bias and rate of the Earth orientation series, as well as to properly assign weights to the observations prior to combination.

The IERS, a service of both the IAG and the IAU, was established on 1 January 1988 under its former name of the International Earth Rotation Service to serve the astronomical, geophysical, and geodetic communities by, in part, providing the International Celestial Reference Frame (ICRF), the ITRF, and the EOPs that are needed to transform station coordinates between these two frames (Feissel and Gambis, 1993; Vondrák and Richter, 2004). As part of its activities, the IERS combines and predicts EOPs determined by the space-geodetic techniques using a weighted-average approach (Luzum *et al.*, 2001; Gambis, 2004; Johnson *et al.*, 2005). The EOPs produced by the IERS are available through its website (see **Table 3**).

Since the 1980s, a Kalman filter has been used at the Jet Propulsion Laboratory (JPL) to combine and predict EOPs in support of interplanetary spacecraft tracking and navigation (Freedman *et al.*, 1994a; Gross *et al.*, 1998). A Kalman filter has many properties that make it an attractive method of combining Earth orientation series. It allows the full accuracy of the measurements to be used, whether they are degenerate or full rank, are irregularly or regularly spaced in time, or are corrupted by systematic or

other errors that can be described by stochastic models. And by using a stochastic model for the process, a Kalman filter can objectively account for the growth in the uncertainty of the EOPs between measurements. The combined and predicted Earth orientation series produced at JPL using a Kalman filter can be obtained by anonymous ftp from the address given in **Table 3**.

3.09.4 Observed and Modeled Earth Rotation Variations

The Earth's rotation changes on all observable timescales, from subdaily to decadal and longer. The wide range of timescales on which the Earth's rotation changes reflects the wide variety of processes that are causing it to change, including external tidal forces, surficial fluid processes involving the atmosphere, oceans, and hydrosphere, and internal processes acting both within the solid Earth itself and between the fluid core and solid Earth. The changes in the Earth's rotation that are observed and the models that have been developed to explain them are reviewed here.

3.09.4.1 UT1 and LOD Variations

LOD observations (**Figure 2**) show that it consists mainly of (1) a linear trend of rate +1.8 ms/cy, (2) decadal variations having an amplitude of a few milliseconds, (3) tidal variations having an amplitude of about 1ms, (4) seasonal variations having an amplitude of about 0.5 ms, and (5) smaller amplitude variations occurring on all measurable timescales. Here, the length-of-day variations that are observed and the models that have been developed to explain them are reviewed (*see* Chapter 3.10).

The length of the day is the rotational period of the Earth. Changes $\Delta\Lambda(t)$ in the length of the day are related to changes in Universal Time and to changes $\Delta\omega_z(t) = \Omega m_z(t)$ in the axial component of the Earth's angular velocity by

$$\frac{\Delta\Lambda(t)}{\Lambda_o} = -m_z(t) = -\frac{\partial(\mathrm{UT1}-\mathrm{TAI})}{\partial t} \qquad [64]$$

By eqns [43] and [58], the LOD will change as a result of changes in the axial component $h_z(t)$ of relative angular momentum and of changes in the axial component $\Omega\,\Delta I_{zz}(t)$ of angular momentum due to changes in the mass distribution of the Earth. Modeling the observed changes in the LOD therefore requires computing both types of changes in angular momentum for the different components of the Earth system. By definition, the angular momentum vector $\mathbf{L}(t)$ of some component of the Earth system such as the atmosphere or oceans is given by

$$\mathbf{L}(t) = \int_{V(t)} \rho(\mathbf{r},t)\,\mathbf{r} \times [\boldsymbol{\omega} \times \mathbf{r} + \mathbf{u}(\mathbf{r},t)]\,\mathrm{d}V \qquad [65]$$

where the integral is taken over the, in general, time-dependent volume $V(t)$ of that component of the Earth system under consideration, the first term in the square brackets represents changes in the angular momentum due to changes in mass distribution, the second term represents changes due to relative motion, and $\mathbf{r}$ is the position vector of some mass element of density $\rho(\mathbf{r},t)$ that is moving with Eulerian velocity $\mathbf{u}(\mathbf{r},t)$ with respect to a terrestrial reference frame that (1) is fixed to the solid Earth, (2) is oriented such that its x- and y-coordinate axes are along the Greenwich and 90° E meridians, respectively, with both axes lying in the equatorial plane, (3) has an origin located at the center of the Earth, and (4) is rotating with angular velocity $\boldsymbol{\omega}$ with respect to an inertial reference frame. In general, $\boldsymbol{\omega}$ is not constant in time but exhibits variations in both magnitude (related to changes in the LOD) and direction (related to polar motion). However, these changes are small, and for the purpose of deriving expressions for the angular momentum of different components of

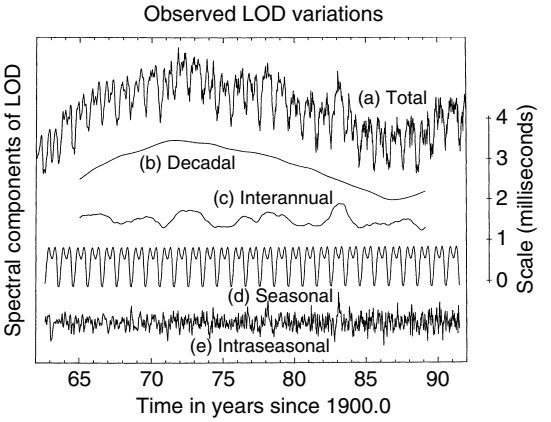

Figure 2 (a) Observed LOD variations during 1962–91 from the COMB91 combined optical astrometric and space-geodetic Earth orientation series and its decomposition into variations on (b) decadal, (c) interannual, (d) seasonal, and (e) intraseasonal timescales. Tidal variations are not shown. From Dickey JO, Marcus SL, Hide R, Eubanks TM, and Boggs DH (1994b) Angular momentum exchange among the soild Earth, atmosphere and oceans: A case study of the 1982–83. El Niño event. *Journal of Geophysical Research* 99(B12): 23921–23937.

the Earth system it can be assumed that the terrestrial reference frame is uniformly rotating at the rate Ω about the z-coordinate axis: $\boldsymbol{\omega} = \Omega\,\hat{\mathbf{z}}$. In this case, the axial component of the mass term of the angular momentum can be written as

$$\Omega\,\Delta I_{zz}(t) = \Omega \int_{V(t)} \rho(\mathbf{r},\, t)\, r^2 \cos^2\phi \,\mathrm{d}V \qquad [66]$$

where ϕ is north latitude. Similarly, the axial component of the motion term of the angular momentum can be written as

$$h_z(t) = \int_{V(t)} \rho(\mathbf{r},\, t)\, r \cos\phi\, u(\mathbf{r},\, t)\,\mathrm{d}V \qquad [67]$$

where $u(\mathbf{r}, t)$ is the eastward component of the velocity.

3.09.4.1.1 Secular trend, tidal dissipation, and glacial isostatic adjustment

Tidal dissipation causes the Earth's angular velocity and hence rotational angular momentum to decrease (*see* Chapter 3.07). Since the angular momentum of the Earth–Moon system is conserved, the orbital angular momentum of the Moon must increase to balance the decrease in the Earth's rotational angular momentum. The increase in the orbital angular momentum of the Moon is accomplished by an increase in the radius of the Moon's orbit and a decrease in the Moon's orbital angular velocity. But early observations of the Moon's position showed that it was apparently accelerating, not decelerating, in its orbit. This apparent acceleration of the Moon was a result of assuming that the Earth is rotating with a constant, rather than decreasing, angular velocity when predicting the Moon's position. If the Earth's angular velocity is actually decreasing but is assumed to be constant when predicting the position of the Moon, then the observed position of the Moon will appear to be ahead of its predicted position, that is, the Moon will appear to be accelerating in its orbit. That the Moon is apparently accelerating in its orbit was first noted by Halley (1695). But it was not until 1939 that Spencer Jones (1939) was able to conclusively demonstrate that the angular velocity of the Earth is actually decreasing and that the apparent acceleration of the Moon in its orbit was an artifact of assuming that the angular velocity of the Earth was constant.

Halley (1695) also seems to have been the first to appreciate the importance of ancient and medieval records of lunar and solar eclipses for determining the apparent acceleration of the Moon and the corresponding decrease in the angular velocity of the Earth over the past few thousand years. The change in the Earth's rate of rotation can be deduced from the discrepancy between when and where eclipses should have been observed if the angular velocity of the Earth were constant to when and where they were actually observed as recorded in Babylonian clay tablets and Chinese, European, and Arabic books and manuscripts (Stephenson, 1997).

When using eclipse observations to deduce the secular change in the length of the day over the past few thousand years, the positions of the Sun and Moon must be accurately known. Of primary importance in this regard is the value for the tidal acceleration $\dot{n}$ of the Moon since it controls the long-term behavior of the Moon's motion. The tidal acceleration of the Moon can be determined from observations of the timings of transits of Mercury (e.g., Spencer Jones, 1939; Morrison and Ward, 1975) as well as from satellite and lunar laser ranging measurements. Tidal forces distort the figure of the Earth and hence its gravitational field which in turn perturbs the orbits of artificial satellites. SLR measurements can detect these tidal perturbations in the satellites' orbits and can therefore be used to construct tide models and hence determine the tidal acceleration of the Moon. Using this approach, Christodoulidis *et al.* (1988) report a value of -25.27 ± 0.61 arcseconds per century^2 ($''$/cy^2) for the tidal acceleration $\dot{n}$ of the Moon due to dissipation by solid Earth and ocean tides. Other SLR-derived values for $\dot{n}$ have been reported by Cheng *et al.* (1990, 1992), Marsh *et al.* (1990, 1991), Dickman (1994), Lerch *et al.* (1994), and Ray (1994).

Like the orbits of artificial satellites, the orbit of the Moon is also perturbed by tidal forces. Since LLR measurements can detect tidal perturbations in the Moon's orbit, they can be used to determine the tidal acceleration of the Moon. In addition to being sensitive to orbital perturbations caused by tides on the Earth, LLR measurements, unlike SLR measurements, are also sensitive to orbital perturbations caused by tides on the Moon. Using LLR measurements, Williams *et al.* (2001) report a value of $-25.73 \pm 0.5''$/cy^2 for the tidal acceleration of the Moon, which by Kepler's law corresponds to an increase of 3.79 ± 0.07 cm yr^{-1} in the semimajor axis of the Moon's orbit, and which includes a contribution of $+0.29\ ''$/cy^2 from dissipation within the Moon itself. Only about half of the discrepancy between the SLR- and LLR-derived values for $\dot{n}$ due to dissipation by just tides on the Earth is currently understood (Williams *et al.*, 2001). Other

LLR-derived values for $\dot{n}$ have been reported by Newhall *et al.* (1988), Dickey *et al.* (1994a), and Chapront *et al.*, (2002).

By *a priori* adopting a value for the tidal acceleration $\dot{n}$ of the Moon, lunar and solar eclipse observations can be used to determine the secular increase in the length of the day over the past few thousand years. The most recent re-reductions of lunar and solar eclipse observations for LOD changes are those of Stephenson and Morrison (1995) and Morrison and Stephenson (2001). Besides using eclipse observations spanning 700 BC to AD 1600, they also used lunar occultation observations spanning 1600–1955.5 and optical astrometric and space-geodetic measurements spanning 1955.5–1990. Adopting a value of $-26.0''/\text{cy}^2$ for $\dot{n}$, Morrison and Stephenson (2001) found that the LOD has increased at a rate of $+1.80 \pm 0.1$ ms/cy on average during the past 2700 years (see **Figure 3**). In addition to a secular trend, Stephenson and Morrison (1995) and Morrison and Stephenson (2001) also found evidence for a fluctuation in the LOD that has a peak-to-peak amplitude of about 8 ms and a period of about 1500 years (**Figure 3**).

By conservation of angular momentum, a tidal acceleration of the Moon of $-26.0''/\text{cy}^2$ should be accompanied by a $+2.3$ ms/cy increase in the length of the day (Stephenson and Morrison, 1995). Since the observed increase in the length of the day is only $+1.8$ ms/cy (Morrison and Stephenson, 2001), some other mechanism or combination of mechanisms must be acting to change the length of the day by -0.5 ms/cy. By eqns [43] and [58], changes in both the axial component of relative angular momentum and in the polar moment of inertia of the Earth can cause the LOD to change. A secular trend in the general circulation of fluids like the atmosphere and oceans, and hence in atmospheric and oceanic angular momentum, is unlikely to be sustained over the course of a few thousand years. In fact, using results from a 100-year run of the Hadley Centre general circulation model of the atmosphere, de Viron *et al.* (2004) found that the modeled secular trend in atmospheric angular momentum (AAM) during 1870–1997 causes a secular trend in LOD of only $+0.08$ ms/cy.

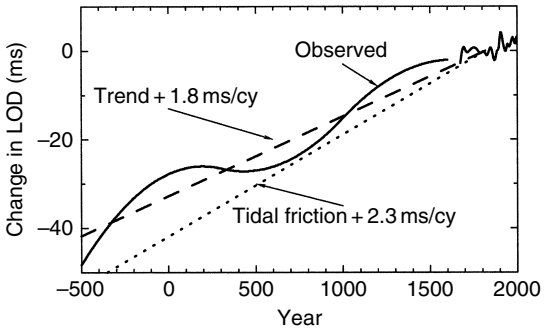

Figure 3 Secular change in the LOD during the past 2500 years estimated from lunar and solar eclipse, lunar occultation, optical astrometric, and space-geodetic observations. The difference between the observed secular trend and that caused by tidal friction is due to the effects of glacial isostatic adjustment and other processes such as ice sheet mass change and the accompanying nonsteric change in sea level. From Morrison LV and Stephenson FR (2001) Historical eclipses and the variability of the Earth's rotation. *Journal of Geodynamics* 32: 247–265.

One of the most important mechanisms acting to cause a secular trend in the LOD on timescales of a few thousand years is glacial isostatic adjustment (GIA). The isostatic adjustment of the solid Earth in response to the decreasing load on it following the last deglaciation causes the figure of the Earth to change, and hence the LOD to change. Since the solid Earth is rebounding in the regions at high latitude where the ice load was formerly located, the figure of the Earth is becoming less oblate, the Earth's rotation is accelerating, and the LOD is decreasing. Models of GIA show that its effect on the LOD is very sensitive to the assumed value of lower-mantle viscosity (e.g., Wu and Peltier, 1984; Peltier and Jiang, 1996; Vermeersen *et al.*, 1997; Mitrovica and Milne, 1998; Johnston and Lambeck, 1999; Tamisea *et al.*, 2002; Sabadini and Vermeersen, 2004). But by deriving a model for the radial viscosity profile of the Earth that fits both postglacial decay times and free-air gravity anomalies associated with mantle convection, Mitrovica and Forte (1997) found that GIA should cause a secular trend in the LOD amounting to -0.5 ms/cy, a value in remarkable agreement with that needed to explain the difference between the observed secular trend in the length of the day and that caused by tidal dissipation.

However, GIA is not the only mechanism that will cause a secular trend in the length of the day. The present-day change in glacier and ice sheet mass and the accompanying change in nonsteric sea level will also cause a secular trend in LOD (e.g., Peltier, 1988; Trupin *et al.*, 1992; Mitrovica and Peltier, 1993; Trupin, 1993; James and Ivins, 1995, 1997; Nakada and Okuno, 2003; Tosi *et al.*, 2005). But the effect of this mechanism on LOD is very sensitive to the still-unknown present-day

mass change of glaciers and ice sheets, particularly of the Antarctic ice sheet. By adopting various scenarios for the mass change of Antarctica, models predict that its mass change alone should cause a secular trend in the LOD ranging anywhere from −0.72 to +0.31 ms/cy (James and Ivins, 1997). Other mechanisms that may cause a secular trend in LOD include tectonic processes taking place under nonisostatic conditions (Vermeersen and Vlaar, 1993; Vermeersen *et al.*, 1994; Sabadini and Vermeersen, 2004), plate subduction (Alfonsi and Spada, 1998), earthquakes (Chao and Gross, 1987), and deformation of the mantle caused by pressure variations acting at the core–mantle boundary that are associated with motion of the fluid core (Fang *et al.*, 1996; Dumberry and Bloxham, 2004; Greff-Lefftz *et al.*, 2004).

The fluctuation in the LOD of 1500-year period found by Stephenson and Morrison (1995) and Morrison and Stephenson (2001) is currently of unknown origin. However, given its large amplitude, which is too large to be caused by atmospheric and oceanic processes but which is comparable in size to the amplitude of the decadal variations, it is probably caused (Dumberry and Bloxham, 2006) by the same core–mantle interactions (*see* Chapter 8.12), such as gravitational coupling (Rubincam, 2003), that are known to cause decadal variations in the LOD.

3.09.4.1.2 Decadal variations and core–mantle interactions

While lunar and solar eclipse observations are valuable for studying the secular trend in the LOD, they are too sparse and inaccurate to reveal decadal variations (*see* Chapter 5.05). Instead, lunar occultation observations, which are available since the early 1600s (Martin, 1969; Morrison *et al.*, 1981), are used to study decadal variations in the length of the day. **Figure 4** compares three different LOD series derived from lunar occultation observations. Gross (2001; black curve) derived a LOD series spanning 1832.5–1997.5 at yearly intervals by analyzing UT1 measurements obtained from lunar occultation observations by Jordi *et al.* (1994), from the HIPPARCOS optical astrometric series of Vondrák (1991, 1999) and Vondrák *et al.* (1992, 1995, 1997, 1998), and from the COMB97 combined optical astrometric and space-geodetic series of Gross (2000a). McCarthy and Babcock (1986; red curve) derived a LOD series spanning 1657.0–1984.5 at half-yearly intervals by analyzing UT1 measurements obtained from lunar occultation observations by Martin (1969) and Morrison (1979), from the optical astrometric series of McCarthy (1976), and from a series obtained from the BIH. Stephenson and Morrison (1984; green curve) obtained a LOD series spanning 1630–1980 at 5-year intervals before 1780 and at yearly intervals afterward by analyzing the lunar occultation and solar

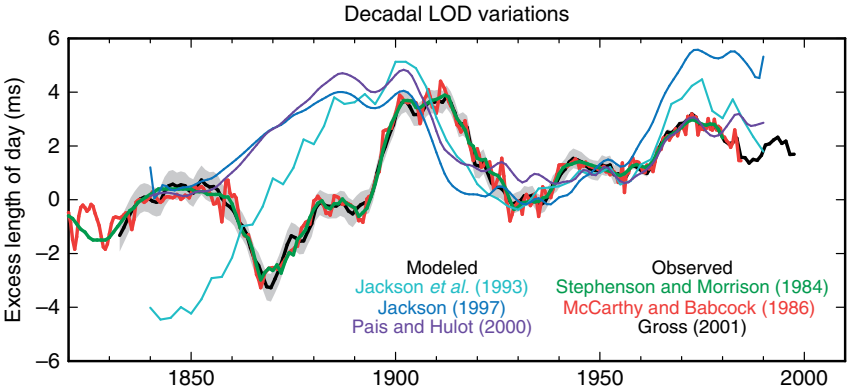

Figure 4 Plots of observed and modeled LOD variations on decadal timescales. The observed LOD series are those of Gross (2001; black curve with gray shading representing $\pm 1\sigma$ standard error), McCarthy and Babcock (1986; red curve), and Stephenson and Morrison (1984; green curve). Note that after about 1955 the uncertainties of the Gross (2001) LOD values are less than the width of the black line. The modeled CAM series are those of Jackson *et al*. (1993; teal curve), the *uvm-s* model of Jackson (1997; light blue curve), and the PH-inversion model of Pais and Hulot (2000; purple curve). A secular trend of +1.8 ms/cy has been added to the modeled CAM series to match the observed secular trend (see Section 3.09.4.1.1). An arbitrary bias has also been added to the modeled series in order to facilitate their comparison with the observed series. Adapted from Gross RS (2001) A combined length-of-day series spanning 1832–1997: LUNAR97. *Physics of the Earth and Planetary Interiors* 123: 65–76.

eclipse observations cataloged by Morrison (1978) and Morrison *et al.* (1981), combining them with an LOD series derived from optical astrometric measurements of UT1 obtained from the BIH. As can be seen from **Figure 4**, during their common time span, these three different LOD series are consistent with each other to within the 1σ standard error of the Gross (2001) series. Other LOD series that have been derived from lunar occultation observations are those of Morrison (1979), Jordi *et al.* (1994), and Liao and Greiner-Mai (1999).

The peak-to-peak variation in the LOD seen in **Figure 4** is about 7 ms, a variation far too large to be caused by atmospheric and oceanic processes (Gross *et al.*, 2005). That atmospheric processes cannot cause such large decadal-scale LOD variations can be easily demonstrated by considering the change in the LOD that would be caused if the motion of the atmosphere were to stop entirely. Because of the pole-to-equator temperature gradient, the atmosphere superrotates with respect to the solid Earth at an average rate of about 7 m s^{-1} (*see* Chapter 8.07). If the superrotation of the atmosphere were to stop so that the atmosphere just passively corotates with the solid Earth, then by conservation of angular momentum the LOD would decrease by about 3 ms (Hide *et al.*, 1980). Since stopping the atmospheric motion entirely does not cause a LOD change as large as that observed in **Figure 4**, some other mechanism or combination of mechanisms must be acting to cause the large decadal-scale LOD variations that are observed.

The most important mechanism acting to cause decadal variations in the length of the day is core–mantle coupling. While it has been recognized for quite some time that the core is the only viable source of the large decadal LOD variations that are observed (e.g., Munk and MacDonald, 1960; Lambeck, 1980), it was not until 1988 that Jault *et al.* (1988) were able to model the core angular momentum (CAM) and show that it causes decadal LOD variations that agree reasonably well with those observed.

The flow of the fluid at the top of the core can be inferred from surface observations of the secular variation of the magnetic field by assuming that (1) the mantle is a perfect insulator so that the magnetic field can be expressed as the gradient of a potential, which facilitates the downward continuation of the magnetic field to the top of the core; (2) the core is a perfect conductor so that the magnetic field is 'frozen' into the core fluid and is thus advected by the horizontal flow at the top of the core; (3) the flow at the top of the core is tangentially geostrophic so that it is governed by the balance between the horizontal components of just the pressure gradient and the coriolis force at the top of the core (Bloxham and Jackson, 1991; Whaler and Davis, 1997); and (4) the flow is large scale. The last two assumptions are required in order to reduce the inherent nonuniqueness of core surface flow determinations. Other assumptions about the core surface flow fields that have been made are that the flow is purely toroidal so that it has no radial component (Whaler, 1980; Bloxham, 1990), that the flow is steady in time (Gubbins, 1982; Voorhies and Backus, 1985), that the flow is steady within a drifting reference frame (Davis and Whaler, 1996; Holme and Whaler, 2001), or that the flow includes a helical component (Amit and Olson, 2006).

While surface magnetic field observations can be used to infer the flow at the top of the core, the flow everywhere within the core must be known in order to compute the angular momentum of the core and hence the effect of core motion on the length of the day. Jault *et al.* (1988) realized from dynamical considerations that for geostrophic flows on decadal timescales, the axisymmetric, or zonal, component of the core flow can be described by relative motion of nested cylinders that are coaxial with the rotation axis. This model for the motion of the core at depth allows the axial angular momentum of the core, and hence the effect of core motion on the LOD, to be computed from the flow fields at the top of the core that are inferred from surface magnetic field observations (Jault *et al.*, 1988; Jackson *et al.*, 1993; Jackson, 1997; Hide *et al.*, 2000; Pais and Hulot, 2000; Holme and Whaler, 2001; Pais *et al.*, 2004; Amit and Olson, 2006). Models of the CAM that have been computed in this manner are available through the IERS Special Bureau for the Core (SBC) website (see **Table 4**). **Figure 4** compares the observed decadal LOD variations with the modeled results obtained by Jackson *et al.* (1993), Jackson (1997), and Pais and Hulot (2000). As can be seen, while the agreement is not perfect, CAM models produce decadal LOD variations that have about the same amplitude and phase as those observed.

In the coaxial nested cylinder model of the zonal core flow, the rotation of adjacent cylinders are coupled because of the magnetic field lines that thread through them. If for some reason the rotation of the cylinders is disturbed, then the magnetic field provides a restoring force that will cause the cylinders to oscillate. As first proposed by Braginsky (1970), it is the exchange with the mantle of the angular momentum associated with these torsional

Table 4 Sources of angular momentum models

Model type	URL
Global geophysical fluids	
IERS GGFC	http://www.ecgs.lu/ggfc/
Atmospheric	
IERS SBA	http://www.aer.com/scienceResearch/diag/sb.html
Oceanic	
IERS SBO	http://euler.jpl.nasa.gov/sbo/
Hydrologic	
IERS SBH	http://www.csr.utexas.edu/research/ggfc/
Mantle	
IERS SBM	http://bowie.gsfc.nasa.gov/ggfc/mantle.htm
Core	
IERS SBC	http://www.astro.oma.be/SBC/main.html
Tides	
IERS SBT	http://bowie.gsfc.nasa.gov/ggfc/tides/

URL, Uniform Resource Locator; IERS, International Earth Rotation and Reference Systems Service; GGFC, Global Geophysical Fluids Center; SBA, Special Bureau for the Atmosphere; SBO, Special Bureau for the Oceans; SBH, Special Bureau for Hydrology; SBM, Special Bureau for the Mantle; SBC, Special Bureau for the Core; SBT, Special Bureau for Tides.

oscillations of the fluid core that causes the LOD to change (Zatman and Bloxham, 1997, 1998, 1999; Buffett, 1998; Hide *et al.*, 2000; Pais and Hulot, 2000; Buffett and Mound, 2005; Mound and Buffett, 2005).

While the exchange of CAM with the solid Earth can clearly cause decadal LOD variations of approximately the right amplitude and phase, the mechanism or mechanisms by which the angular momentum is exchanged between the core and solid Earth is less certain. Possible core–mantle coupling mechanisms are viscous torques, topographic torques, electromagnetic torques, and gravitational torques (Jault, 2003; Ponsar *et al.*, 2003). Viscous coupling is caused by the drag of the core flow on the core–mantle boundary, with the strength of the coupling depending on the viscosity of the core fluid. Given current estimates of core viscosity, it is generally agreed that viscous torques are too weak to be effective in coupling the core to the mantle (Rochester, 1984).

If the core–mantle boundary is not smooth but exhibits undulations or 'bumps', then the flow of the core fluid can exert a torque on the mantle due to the fluid pressure acting on the boundary topography (Hide, 1969, 1977, 1989, 1993, 1995a; Jault and Le Mouël, 1989, 1990, 1991; Hide *et al.*, 1993; Jault *et al.*, 1996; Buffett, 1998; Kuang and Chao, 2001; Mound and Buffett, 2005; Asari *et al.*, 2006). The strength of this topographic coupling, a mechanism first suggested by Hide (1969), depends on the amplitude of the topography at the core–mantle boundary. Because of uncertainties in the size of this topography and a controversy about how the topographic torque should be computed (Bloxham and Kuang, 1995; Hide, 1995b, 1998; Kuang and Bloxham, 1997; Jault and Le Mouël, 1999), there is as yet no consensus on the importance of topographic coupling as a mechanism for exchanging angular momentum between the core and mantle.

Electromagnetic torques arise from the interaction between the magnetic field within the core and the flow of electric currents in the weakly conducting mantle that are induced by both time variations of the magnetic field and by diffusion of electric currents from the core into the mantle (Bullard *et al.*, 1950; Rochester, 1960, 1962; Roden, 1963; Roberts, 1972; Stix and Roberts, 1984; Jault and Le Mouël, 1991; Love and Bloxham, 1994; Stewart *et al.*, 1995; Holme, 1998a, 1998b, 2000; Wicht and Jault, 1999, 2000; Mound and Buffett, 2005). The strength of this electromagnetic torque, a mechanism first suggested by Bullard *et al.* (1950), depends on both the conductivity of the mantle and on the strength of the magnetic field crossing the core–mantle boundary. If the conductivity of the mantle, or of a narrow layer at the base of the mantle, is sufficiently large, then electromagnetic torques can produce decadal LOD variations as large as those observed. But because of uncertainties in the conductivity at the base of the mantle, the importance of electromagnetic coupling,

like that of topographic coupling, as a mechanism for exchanging angular momentum between the core and mantle remains unclear.

Gravitational attraction between density heterogeneities in the fluid core and mantle can exert a torque on the mantle, leading to changes in the length of the day (Jault and Le Mouël, 1989; Buffett, 1996a). The strength of the gravitational torque depends upon the size of the mass anomalies in the core and mantle, which are poorly known. As a result, there have been few quantitative estimates of the magnitude of the gravitational torque. However, Buffett (1996a, 1996b) has suggested that the inner core may be gravitationally locked to the mantle. If so, then any rotational disturbance of the inner core, possibly caused by electromagnetic torques acting on the inner core, will be transmitted to the mantle, causing LOD changes. While Buffett (1998) and Mound and Buffett (2005) consider this last mechanism to be the most viable mechanism for exchanging angular momentum between the core and mantle, Zatman (2003) finds that it is inconsistent with a model of inner core rotation rate determined from the core flow within the tangent cylinder.

3.09.4.1.3 Tidal variations and solid Earth, oceanic, and atmospheric tides

Tidal forces due to the gravitational attraction of the Sun, Moon, and planets deform the solid and fluid parts of the Earth, causing the Earth's inertia tensor to change and hence the Earth's rotation to change (*see* Chapter 3.06). Jeffreys (1928) was the first to predict that the periodic displacement of the solid and fluid masses of the Earth associated with the tides should cause periodic changes in the Earth's rate of rotation at the tidal frequencies (*see* Chapter 3.08). While Markowitz (1955, 1959) reported observing such periodic variations at the fortnightly and monthly tidal frequencies from observations taken at two photographic zenith tubes, these observations were later thrown into doubt by the error analysis of Fliegel and Hawkins (1967). By combining observations from about 55 instruments, Guinot (1970) was able to detect variations in the Earth's rate of rotation at the fortnightly and monthly tidal frequencies that had amplitudes significantly greater than the level of observation noise. Today, the high accuracy of the space-geodetic measurement systems allow long-period tidal effects on UT1 and LOD to be unambiguously observed (e.g., Hefty and Capitaine, 1990; Nam and Dickman, 1990; McCarthy and Luzum, 1993; Robertson *et al.*, 1994; Schastok *et al.*, 1994; Chao *et al.*, 1995a; Dickman and Nam, 1995; Schuh and Schmitz-Hübsch, 2000; Bellanger *et al.*, 2002).

In a seminal paper, Yoder *et al.* (1981) derived a model for the long-period tidal variations in the rotation of the Earth assuming that the crust and mantle of the Earth is elastic, that the core is decoupled from the mantle, and that the ocean tides are in equilibrium. **Table 5** gives their results for the long-period tidal variations in UT1 and LOD, where the LOD results have been derived here from their UT1 results by using eqn [64]. On intraseasonal timescales, the largest effects are found to be at the fortnightly and monthly tidal periods. The large tidal variations at annual and semiannual periods are obscured in Earth rotation observations by meteorological effects (see Section 3.09.4.1.4), while those having periods of 9.3 and 18.6 years are obscured by the decadal variations in the Earth's rotation (see Section 3.09.4.1.2).

Effects of mantle anelasticity on the tidal variations in the Earth's rate of rotation have been discussed by Merriam (1984, 1985), Wahr and Bergen (1986), and Defraigne and Smits (1999). Dissipation associated with mantle anelasticity causes the deformational and hence rotational response of the Earth to lag behind the forcing tidal potential. As a result, not only does mantle anelasticity modify the in-phase rotational response of the Earth to the tidal potential, but out-of-phase terms are introduced as well. Anelastic effects are found to modify the elastic rotational response of the Earth by a few percent.

Defraigne and Smits (1999) also considered the effects of nonhydrostatic structure within the Earth on the tidal variations in the Earth's rotation. A nonhydrostatic initial state of the Earth was determined by computing the buoyancy-driven flow in the mantle due to the seismically observed mass anomalies there, while accounting for the associated flow-induced boundary deformation, potential readjustment, and mass readjustment in the outer and inner cores. Their results indicate that nonhydrostatic structure within the Earth modifies the rotational response of the Earth to the zonal tide generating potential by less than 0.1%.

Dynamic effects of long-period ocean tides on the Earth's rotation using ocean tide models based upon Laplace's tidal equations have been computed by Brosche *et al.* (1989), Seiler (1990, 1991), Wünsch and Busshoff (1992), Dickman (1993), Gross (1993), and Seiler and Wünsch (1995). But the accuracy of ocean tide models greatly improved when

Table 5 Modeled variations in UTI and LOD caused by elastic solid body and equilibrium ocean tides

Argument					Period	ΔUTI (μs)	Δ(t) (μs)	Argument					Period	ΔUTI (μs)	Δ(t) (μs)
l	l′	F	D	Ω	(days)	sin	cos	l	l′	F	D	Ω	(days)	sin	cos
1	0	2	2	2	5.64	−2.35	2.62	1	0	0	0	−1	27.44	53.39	−12.22
2	0	2	0	1	6.85	−4.04	3.71	1	0	0	0	0	27.56	−826.07	188.37
2	0	2	0	2	6.86	−9.87	9.04	1	0	0	0	1	27.67	54.43	−12.36
0	0	2	2	1	7.09	−5.08	4.50	0	0	0	1	0	29.53	4.70	−1.00
0	0	2	2	2	7.10	−12.31	10.90	1	−1	0	0	0	29.80	−5.55	1.17
1	0	2	0	0	9.11	−3.85	2.66	−1	0	0	2	−1	31.66	11.75	−2.33
1	0	2	0	1	9.12	−41.08	28.30	−1	0	0	2	0	31.81	−182.36	36.02
1	0	2	0	2	9.13	−99.26	68.29	−1	0	0	2	1	31.96	13.16	−2.59
3	0	0	0	0	9.18	−1.79	1.22	1	0	−2	2	−1	32.61	1.79	−0.34
−1	0	2	2	1	9.54	−8.18	5.38	−1	−1	0	2	0	34.85	−8.55	1.54
−1	0	2	2	2	9.56	−19.74	12.98	0	2	2	−2	2	91.31	−5.73	0.39
1	0	0	2	0	9.61	−7.61	4.98	0	1	2	−2	1	119.61	3.29	−0.17
2	0	2	−2	2	12.81	2.16	−1.06	0	1	2	−2	2	121.75	−188.47	9.73
0	1	2	0	2	13.17	2.54	−1.21	0	0	2	−2	0	173.31	25.10	−0.91
0	0	2	0	0	13.61	−29.89	13.80	0	0	2	−2	1	177.84	117.03	−4.13
0	0	2	0	1	13.63	−320.82	147.86	0	0	2	−2	2	182.62	−4824.74	166.00
0	0	2	0	2	13.66	−775.69	356.77	0	2	0	0	0	182.63	−19.36	0.67
2	0	0	0	−1	13.75	2.16	−0.99	2	0	0	−2	−1	199.84	4.89	−0.15
2	0	0	0	0	13.78	−33.84	15.43	2	0	0	−2	0	205.89	−54.71	1.67
2	0	0	0	1	13.81	1.79	−0.81	2	0	0	−2	1	212.32	3.67	−0.11
0	−1	2	0	2	14.19	−2.44	1.08	0	−1	2	−2	1	346.60	−4.51	0.08
0	0	0	2	−1	14.73	4.70	−2.00	0	1	0	0	−1	346.64	9.21	−0.17
0	0	0	2	0	14.77	−73.41	31.24	0	−1	2	−2	2	365.22	82.81	−1.42
0	0	0	2	1	14.80	−5.26	2.24	0	1	0	0	0	365.26	−1535.87	26.42
0	−1	0	2	0	15.39	−5.08	2.07	0	1	0	0	1	386.00	−13.82	0.22
1	0	2	−2	1	23.86	4.98	−1.31	1	0	0	−1	0	411.78	3.48	−0.05
1	0	2	−2	2	23.94	10.06	−2.64	2	0	−2	0	0	−1095.17	−13.72	−0.08
1	1	0	0	0	25.62	3.95	−0.97	−2	0	2	0	1	1305.47	42.11	−0.20
−1	0	2	0	0	26.88	4.70	−1.10	−1	1	0	1	0	3232.85	−4.04	0.01
−1	0	2	0	1	26.98	17.67	−4.11	0	0	0	0	2	−3399.18	789.98	1.46
−1	0	2	0	2	27.09	43.52	−10.09	0	0	0	0	1	−6798.38	−161726.81	−149.47

The tabulated coefficients are derived using a constant value of $k/C = 0.94$ as recommended by Yoder *et al*. (1981). Terms with UTI amplitudes less than 2 μs are not tabulated *l*, *l′*, *F*, *D*, and Ω are the Delaunay arguments, expressions for which are given in Simon *et al*. (1994). The period, given in solar days, is the approximate period of the term as viewed in the terrestrial reference frame.
Source: Yoder CF, Williams JG, and Parke ME (1981) Tidal Variations of Earth rotation. *Journal of Geophysical Research* 86: 881–891.

Table 6 Modeled variations in UTI and LOD caused by long-period dynamic ocean tides

	Argument					Period	ΔUT1 mass (μs)		ΔUT1 motion (μs)		ΔΛ(t) mass (μs)		ΔΛ(t) motion (μs)	
Tide	l	l′	F	D	Ω	(days)	sin	cos	sin	cos	cos	sin	cos	sin
M_f	0	0	2	0	2	13.66	−102.8	33.0	−1.4	15.4	47.28	15.18	0.64	7.08
M_m	1	0	0	0	0	27.56	−119.1	8.8	5.7	10.7	27.15	2.01	−1.30	2.44

The tabulated coefficients are from the assimilated (A) model of Kantha *et al*. (1998). *l*, *l′ F*, *D*, and Ω are the Delaunay arguments, expressions for which are given in Simon *et al*. (1994). The period, given in solar days, is the approximate period of the term as viewed in the terrestrial reference frame.
Source: Kantha LH, Stewart JS, and Desai SD (1998) Long-period lunar fortnightly and monthly ocean tides. *Journal of Geophysical Research* 103(C6): 12639–12647.

TOPEX/POSEIDON (T/P) sea surface height measurements became available. Dynamic effects of long-period ocean tides on the Earth's rotation using tide models based upon T/P sea surface height measurements have been computed by Kantha *et al.* (1998) and Desai and Wahr (1999). **Table 6** gives the results obtained by Kantha *et al.* (1998) from their ocean tide model that assimilates T/P-derived tides. As expected, dynamic tide effects are seen to be larger at the fortnightly tidal frequency than they are at the monthly frequency, with the amplitude of the out-of-phase mass and motion terms (the cosine coefficients for UT1, the sine coefficients for LOD) each being larger for the fortnightly tide than they are for the monthly tide.

Ocean tides in the diurnal and semidiurnal tidal bands also affect the Earth's rate of rotation. While Yoder *et al.* (1981) were the first to predict these effects using theoretical ocean tide models based upon Laplace's tidal equations, they were not actually observed until Dong and Herring (1990) detected them in VLBI measurements. Subdaily variations in UT1 and LOD at the diurnal and semidiurnal tidal frequencies have now been unambiguously observed in measurements taken by VLBI (Brosche *et al.*, 1991; Herring and Dong, 1991, 1994; Wünsch and Busshoff, 1992; Herring, 1993; Sovers *et al.*, 1993; Gipson, 1996; Haas and Wünsch, 2006), SLR (Watkins and Eanes, 1994), and GPS (Lichten *et al.*, 1992; Malla *et al.*, 1993; Freedman *et al.*, 1994b; Grejner-Brzezinska and Goad, 1996; Hefty *et al.*, 2000; Rothacher *et al.*, 2001; Steigenberger *et al.*, 2006).

Following Yoder *et al.* (1981), predictions of subdaily tidal variations in the Earth's rate of rotation using theoretical ocean tide models have been made by Brosche (1982), Baader *et al.* (1983), Brosche *et al.* (1989), Seiler (1990, 1991), Wünsch and Busshoff (1992), Dickman (1993), Gross (1993), and Seiler and Wünsch (1995). But as with long-period ocean tide models, the accuracy of diurnal and semidiurnal tide models greatly improved when T/P sea surface height measurements became available. Dynamic effects of diurnal and semidiurnal ocean tides on the Earth's rotation computed from tide models incorporating T/P sea surface height measurements have been given by Ray *et al.* (1994), Chao *et al.* (1995b, 1996), and Chao and Ray (1997). McCarthy and Petit (2004, chapter 8) give extensive tables of coefficients for the effect of diurnal and semidiurnal ocean tides on UT1 and LOD. Updated models for these effects are available through the IERS Special Bureau for Tides (SBT) website (see **Table 4**).

Comparisons of observations with models show the dominant role that ocean tides play in causing subdaily UT1 and LOD variations (**Figure 5**(**a**)), with as much as 90% of the observed UT1 variance being explained by diurnal and semidiurnal ocean tides (Chao *et al.*, 1996). Apart from errors in observations and models, the small difference that remains (e.g., Schuh and Schmitz-Hübsch, 2000) may be due to nontidal atmospheric and oceanic effects.

The diurnally varying solar heating of the atmosphere excites diurnal and semidiurnal tidal waves in the atmosphere that travel westward with the Sun (Chapman and Lindzen, 1970; Haurwitz and Cowley, 1973; Volland, 1988, 1997; Dai and Wang, 1999). These radiational tides are much larger than the gravitational tides in the atmosphere, with the amplitude of the surface pressure variations due to the radiational tides being about 20 times larger than the amplitude due to the gravitational tides. While gravitational tides in the atmosphere have no discernible effect on the Earth's rotation, the radiational tides do have an effect (Zharov and Gambis, 1996; Brzezinski *et al.*, 2002a; de Viron *et al.*, 2005). Using the National Centers for Environmental Prediction (NCEP)/National Center for Atmospheric Research (NCAR) reanalysis wind

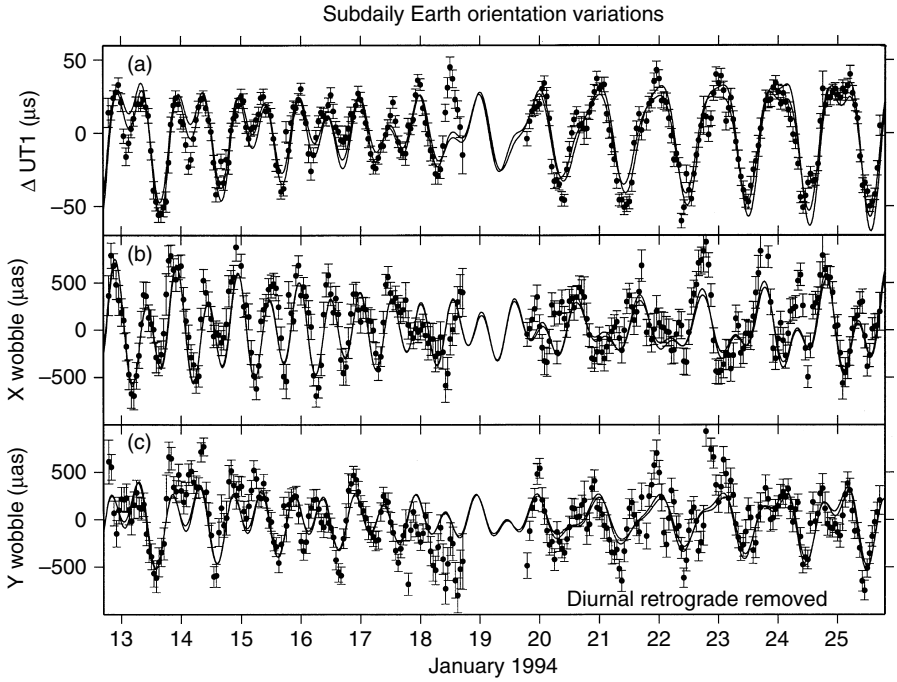

Figure 5 Plots of observed and modeled (a) UTI, (b) x-component of polar motion, and (c) *y*-component of polar motion during the Cont94 measurement campaign of 12–26 January 1994. The dots with 1σ error bars are the hourly VLBI observations. Polar motion variations in the retrograde nearly diurnal frequency band have been removed from the observed series and are not included in the modeled series. The solid lines are the predicted effects from the diurnal and semidiurnal T/P ocean tide models B and C of Chao *et al*. (1996). Each tide model explains about 90% of the observed UTI variance and about 60% of the observed polar motion variance. From Chao BF, Ray RD, Gipson JM, Egbert GD, and Ma C (1996) Diurnal/semidiurnal polar motion excited by oceanic tidal angular momentum. *Journal of Geophysical Research* 101(B9): 20151–20163.

and pressure fields, Brzezinski *et al.* (2002a) predict that the UT1 variations caused by the diurnal S_1 radiational tide should have an amplitude of about 0.5 μs and that the LOD variations should have an amplitude of about 3.3 μs. Since the NCEP/NCAR reanalysis winds and pressure are given every 6 h, the semidiurnal tidal frequency band is incompletely sampled, making it difficult to estimate the effect on UT1 and LOD of the semidiurnal S_2 radiational tide. In addition, since the oceans will respond dynamically to the tidal variations in the atmospheric wind and pressure fields, the oceans will also contribute to the excitation of UT1 and LOD by the radiational tides. In fact, the effect of radiational tides on UT1 and LOD is typically included in tables of the effects of diurnal and semidiurnal ocean tides on the Earth's rate of rotation (see, e.g., McCarthy and Petit, 2004, tables 8.3a and 8.3b).

3.09.4.1.4 Seasonal variations

Seasonal variations in the length of the day were first detected by Stoyko (1937). Numerous studies have since shown that the observed annual and semiannual variations in the LOD are primarily caused by annual and semiannual changes in the angular momentum of the zonal winds (e.g., Munk and MacDonald, 1960; Lambeck, 1980, 1988; Hide and Dickey, 1991; Eubanks, 1993; Rosen, 1993; Höpfner, 1998, 2000; Aoyama and Naito, 2000). In fact, to within the uncertainty of the earlier LOD measurements, seasonal variations in the LOD could be accounted for solely by seasonal variations in the zonal winds (Rosen and Salstein, 1985, 1991; Naito and Kikuchi, 1990, 1991; Dickey *et al*., 1993a; Rosen, 1993). But as measurement accuracies improved, discrepancies between the observed and modeled variations became noticeable.

With the advent of models of the general circulation of the oceans it became possible to evaluate the effect of the oceans on seasonal LOD variations (Brosche and Sündermann, 1985; Brosche *et al*., 1990, 1997; Frische and Sündermann, 1990; Dickey *et al*., 1993b; Segschneider and Sündermann, 1997; Marcus *et al*., 1998; Johnson *et al*., 1999; Ponte and Stammer, 2000; Ponte *et al*., 2001, 2002; Gross, 2004; Gross *et al*., 2004; Kouba and Vondrák, 2005; Yan

et al., 2006). For example, **Table 7** gives the results obtained by Gross *et al.* (2004). They found that during 1992–2000 the amplitude of the observed annual LOD variation was 369.0 ± 6.4 μs with that caused by the effect of zonal winds integrated to a height of 10 hectopascals (hPa) being 414.8 ± 5.0 μs, by atmospheric surface pressure variations being 37.4 ± 0.8 μs, by oceanic currents being 7.6 ± 0.3 μs, and by ocean-bottom pressure variations being 7.9 ± 0.3 μs. The sum of the effects of atmospheric winds up to 10 hPa, surface pressure, oceanic currents, and bottom pressure had an annual amplitude of 363.0 ± 5.2 μs, the same as that observed to within measurement uncertainty, and a phase difference of only 4.5°. But the effects of the winds above 10 hPa have not been taken into account yet.

Although only 1% of the atmospheric mass is located in the region of the atmosphere above 10 hPa, the strength of the zonal winds there is great enough that they have a noticeable effect on seasonal LOD variations (Rosen and Salstein, 1985, 1991; Dickey *et al.*, 1993a; Rosen, 1993; Höpfner, 2001). Gross *et al.* (2004) found that during 1992–2000 the annual LOD variation caused by winds above 10 hPa had an amplitude of 20.5 ± 0.3 μs, larger than the sum of the effects of oceanic currents and bottom pressure. Since the annual stratospheric winds are out of phase with the annual tropospheric winds, including the effect of the winds above 10 hPa brings the amplitude of the modeled annual LOD variations down to 343.5 ± 5.2 μs. Thus, when the effects of stratospheric winds are included, the annual LOD budget is not closed. **Table 7** also gives the results obtained by Gross *et al.* (2004) for the semiannual and terannual (3 cpy) LOD variations. Like the annual LOD budget, the semiannual budget is also not closed. But to within measurement uncertainty, LOD variations at the terannual frequency are completely accounted for by the effects of the atmosphere and oceans.

Apart from errors in observations and models, the residual that remains after modeled atmospheric and oceanic effects have been removed from the observations may be caused by hydrologic processes (Chao and O'Conner, 1988; Chen *et al.*, 2000; Zhong *et al.*, 2003; Chen, 2005). For example, Chen (2005) finds that during 1993.0–2004.3, modeled hydrologic processes cause an annual change in LOD of amplitude 17.2 μs which when added to oceanic effects is reduced to 12.5 μs. However, when the effects of balancing mass within the atmosphere, ocean, and hydrology system are included, this is further reduced to 1.4 μs, which is not large enough to close the annual LOD budget. His results for the semiannual LOD variations are similar. Thus, while models of atmospheric, oceanic, and hydrologic angular momentum have greatly improved, the seasonal LOD budget is still not closed, except perhaps at the terannual frequency.

Since meteorological processes are the predominant cause of seasonal LOD variations, and since these processes can change from year to year, there is no reason to expect that the seasonal LOD variations should be the same from year to year, either in amplitude or in phase. In fact, Feissel and Gavoret (1990) showed that the amplitude of the annual LOD oscillation was about twice as large as normal during the 1982–83 El Niño/Southern Oscillation (ENSO) event, with the amplitude of the semiannual LOD oscillation being about half as large as normal. Gross *et al.* (1996a, 2002) extended this study, showing that during 1962–2000 the amplitudes of the seasonal LOD and wind-driven AAM variations at both annual and semiannual frequencies have not been constant but have fluctuated by as much as 50%. They also showed that the changing amplitudes of the annual and semiannual LOD and AAM variations are significantly correlated with the Southern Oscillation index (SOI), an index defined to be the normalized difference in surface pressure between Darwin and Tahiti. Since the SOI is also correlated with LOD and AAM variations occurring on interannual timescales (see Section 3.09.4.1.5), the significant correlation they observed between changes in the amplitude of the seasonal cycle and the SOI is evidence of a linkage between the seasonal cycle and interannual LOD and AAM variations, a linkage that can only occur through nonlinear interactions.

3.09.4.1.5 Interannual variations and the ENSO

Like seasonal variations in the length of the day, variations on interannual timescales are also predominantly caused by changes in the angular momentum of the zonal winds (e.g., Hide and Dickey, 1991; Eubanks, 1993; Rosen, 1993). The most prominent feature of the climate system on these timescales is the ENSO phenomenon. ENSO is a global-scale oscillation of the coupled atmosphere–ocean system characterized by fluctuations in atmospheric surface pressure and ocean temperatures in the tropical Pacific (e.g., Philander, 1990).

Table 7 Observed and modeled nontidal LOD variations at seasonal frequencies during 1992–2000

	Annual		Semiannual		Terannual	
Excitation process	**Amplitude (μs)**	**Phase (degrees)**	**Amplitude (μs)**	**Phase (degrees)**	**Amplitude (μs)**	**Phase (degrees)**
Observed	369.0 ± 6.4	31.6 ± 1.0	294.3 ± 6.3	−116.5 ± 1.2	52.4 ± 6.4	20.9 ± 7.0
Atmospheric						
Winds (grounds to 10 hPa)	414.8 ± 5.0	34.7 ± 0.7	244.3 ± 5.0	−110.0 ± 1.2	54.1 ± 5.0	30.4 ± 5.3
Winds (10–0.3 hPa)	20.5 ± 0.3	−161.0 ± 0.9	29.4 ± 0.3	−122.7 ± .0.6	3.5 ± 0.3	−165.7 ± 5.1
All winds (ground to 0.3 hPa)	395.1 ± 5.0	35.5 ± 0.7	273.1 ± 5.0	−111.3 ± 1.0	50.7 ± 5.0	31.4 ± 5.6
Surface pressure (IB)	37.4 ± 0.8	−154.6 ± 1.3	9.2 ± 0.8	113.3 ± 5.1	2.6 ± 0.8	−48.8 ± 18.1
All winds and surface pressure	358.3 ± 5.1	36.5 ± 0.8	266.7 ± 5.1	−112.7 ± 1.1	51.2 ± 5.1	28.6 ± 5.7
Oceanic						
Currents	7.6 ± 0.3	−165.5 ± 2.3	0.9 ± 0.3	115.5 ± 18.7	1.6 ± 0.3	35.9 ± 11.1
Bottom pressure	7.9 ± 0.3	−148.4 ± 2.2	3.1 ± .0.3	176.7 ± 5.5	1.0 ± 0.3	−67.3 ± 16.4
Currents and bottom pressure	15.3 ± 0.5	−156.8 ± 2.0	3.6 ± 0.5	163.4 ± 8.6	1.7 ± 0.5	−0.6 ± 18.4
Atmospheric and oceanic						
All winds and currents	388.0 ± 5.0	35.9 ± 0.7	272.5 ± 5.0	−111.5 ± 1.1	52.3 ± 5.0	31.6 ± 5.5
Surface and bottom pressure	45.2 ± 0.9	−153.5 ± 1.2	10.9 ± 0.9	127.9 ± 4.9	3.6 ± 0.9	−54.1 ± 15.1
Total of all atmos. and oceanic						
Without winds above 10 hPa	363.0 ± 5.2	36.1 ± 0.8	238.1 ± 5.2	−112.4 ± 1.3	56.1 ± 5.2	26.9 ± 5.3
With winds above 10 hPa	343.5 ± 5.2	37.1 ± 0.9	267.1 ± 5.2	−113.5 ± 1.1	52.7 ± 5.2	27.7 ± 5.7

IB, inverted barometer. The amplitude A and phase α of the observed and modeled seasonal LOD variations are defined by $\Delta\Lambda(t) = A\cos[\sigma(t - t_o) - \alpha]$ where σ is the annual, semiannual, or terannual frequency and the reference date t_o is January 1.0, 1990.

Source: Gross RS, Fukumori I. Menemenlis D, and Gegout P (2004) Atmospheric and oceanic excitation of length-of-day variations during 1980–2000. *Journal of Geophysical Research* 109:B01406 (doi:10.1029/2003JB002432).

During an ENSO event, in which the SOI decreases, the tropical easterlies collapse causing the AAM to increase. By the conservation of angular momentum, as the AAM increases, the solid Earth's angular momentum decreases and the LOD increases. Numerous studies (e.g., Stefanick, 1982; Chao, 1984, 1988, 1989; Rosen *et al.*, 1984; Eubanks *et al.*, 1986; Salstein and Rosen, 1986; Feissel and Gavoret, 1990; Gambis, 1992; Dickey *et al.*, 1992a, 1993a, 1994b, 1999; Jordi *et al.*, 1994; Abarca del Rio *et al.*, 2000; Zhou *et al.*, 2001; Zheng *et al.*, 2003) have shown that observed LOD variations on interannual timescales, as well as interannual variations in the angular momentum of the zonal winds, are (negatively) correlated with the SOI, reflecting the impact on the LOD of changes in the zonal winds associated with ENSO. For example, Chao (1984) reported finding a correlation between interannual LOD variations and the SOI during 1957–83 with a maximum negative value for the correlation coefficient of –0.56 obtained when the SOI leads the interannual LOD by 1 month; Eubanks *et al.* (1986) reported a maximum negative correlation coefficient during 1962–84 of about –0.5 when the SOI leads the interannual LOD by 3 months; Chao (1988) reported a maximum negative value for the correlation coefficient during 1972–86 of –0.68 for a 2-month lead time; and Dickey *et al.* (1993a) reported a maximum negative correlation coefficient during 1964–89 of –0.67 for a 1-month lead time.

In a detailed study of the 1982–83 ENSO event, Dickey *et al.* (1994b) showed that up to 92% of the observed interannual LOD variance could be explained by atmospheric wind and pressure fluctuations. They suggested that variations in oceanic angular momentum could explain the remaining signal. But studies (Johnson *et al.*, 1999; Ponte *et al.*, 2002; Gross *et al.*, 2004) of the effects of oceanic processes show that they are only marginally effective in causing interannual LOD variations. For example, Gross *et al.* (2004) found that during 1980–2000 atmospheric winds were the dominant mechanism causing the LOD to change on interannual timescales, explaining 85.8% of the observed variance, and having a correlation coefficient of 0.93 with the observations. The effect of atmospheric surface pressure changes explained only 2.6% of the observed variance and was not significantly correlated with the observations. However, including the effect of surface pressure changes with that of the winds increased the observed variance explained from 85.8% to 87.3%. Oceanic currents and bottom pressure changes were found to have only a marginal effect on interannual LOD variations, each explaining less than 1% of the observed variance, and neither being significantly correlated with the observations. However, including their effects with those of atmospheric winds and surface pressure changes increased the observed variance explained from 87.3% to 87.9%, and increased the correlation coefficient with the observations from 0.93 to 0.94.

The interannual LOD signal that remains after atmospheric and oceanic effects are removed may be caused by hydrologic processes (Chen *et al.*, 2000; Chen, 2005). For example, Chen (2005) finds a significant correlation between the sum of the mass-balanced oceanic and hydrologic angular momenta with the observed interannual LOD variations from which atmospheric effects have been removed, although the modeled variations are of smaller amplitude than those observed. Like seasonal variations, better atmospheric, oceanic, and hydrologic models are needed to close the LOD budget on interannual timescales.

There is also a persistent oscillation in LOD over the last century with a period of about 6 years and an amplitude of about 0.12 ms that is not caused by atmospheric fluctuations (Vondrák, 1977; Djurovic and Paquet, 1996; Abarca del Rio *et al.*, 2000). Mound and Buffett (2003) suggest that it is caused by the exchange of angular momentum between the mantle and core arising from gravitational coupling between the mantle and inner core.

3.09.4.1.6 Intraseasonal variations and the Madden–Julian oscillation

Like the seasonal and interannual variations in the length of the day, variations on intraseasonal timescales are also predominantly caused by changes in the angular momentum of the zonal winds (e.g., Hide and Dickey, 1991; Eubanks, 1993; Rosen, 1993). The Madden–Julian oscillation (Madden and Julian, 1971, 1972, 1994) with a period of 30–60 days is the most prominent feature in the atmosphere on these timescales and a number of studies have shown that fluctuations in the zonal winds associated with this oscillation cause the LOD to change (Feissel and Gambis, 1980; Langley *et al.*, 1981b; Anderson and Rosen, 1983; Feissel and Nitschelm, 1985; Madden, 1987; Dickey *et al.*, 1991; Hendon, 1995; Marcus *et al.*, 2001).

Studies of the effects of oceanic processes show that they are only marginally effective in causing intraseasonal LOD variations (Ponte, 1997; Johnson *et al.*, 1999; Ponte and Stammer, 2000; Ponte and Ali, 2002; Gross *et al.*, 2004; Kouba and Vondrák, 2005).

For example, Gross *et al.* (2004) found that during 1992–2000 atmospheric winds were the dominant mechanism causing the LOD to change on intraseasonal timescales, explaining 85.9% of the observed intraseasonal variance and having a correlation coefficient of 0.93 with the observations. Atmospheric surface pressure, oceanic currents, and ocean-bottom pressure were found to have only a minor effect on intraseasonal LOD changes, each explaining only about 3–4% of the observed variance. However, including the effect of surface pressure changes with that of the winds increased the variance explained from 85.9% to 90.2% and increased the correlation coefficient with the observations from 0.93 to 0.95. Additionally, including the effects of changes in oceanic currents and bottom pressure further increased the variance explained from 90.2% to 92.2% and further increased the correlation coefficient from 0.95 to 0.96. Thus, although the impact of the oceans is relatively minor, closer agreement with the observations in the intraseasonal frequency band is obtained when the effects of oceanic processes are added to that of atmospheric.

Hydrologic effects on intraseasonal LOD variations are thought to be relatively insignificant (Chen *et al.*, 2000; Chen, 2005), although the monthly sampling interval of current hydrologic models makes it difficult to study such rapid variations.

3.09.4.2 Polar Motion

Observations of polar motion (**Figure 6**) show that it consists mainly of (1) a forced annual wobble having a nearly constant amplitude of about 100 mas, (2) the free Chandler wobble having a period of about 433 days and a variable amplitude ranging from about 100 to 200 mas, (3) quasiperiodic variations on decadal timescales having amplitudes of about 30 mas known as the Markowitz wobble, (4) a linear trend having a rate of about 3.5 mas yr^{-1} and a direction towards 79° W longitude, and (5) smaller amplitude variations occurring on all measurable timescales. Here, the polar motion variations that are observed and the models that have been developed to explain them are reviewed.

The motion of the pole is usually described by giving the x- and y-components of its location in the terrestrial reference frame. But since polar motion is inherently a two-dimensional quantity, periodic motion of the pole can also be described by giving the amplitude A and phase α of its prograde and retrograde components defined by

$$\begin{aligned}\mathbf{p}(t) &= p_x(t) - i\,p_y(t) \\ &= A_\mathrm{p}\,\mathrm{e}^{\mathrm{i}\alpha_\mathrm{p}}\mathrm{e}^{\mathrm{i}\sigma(t-t_\mathrm{o})} + A_\mathrm{r}\mathrm{e}^{\mathrm{i}\alpha_\mathrm{r}}\mathrm{e}^{-\mathrm{i}\sigma(t-t_\mathrm{o})}\end{aligned} \quad [68]$$

where the subscript p denotes prograde, the subscript r denotes retrograde, σ is the strictly positive frequency of motion, and t_o is the reference date. Prograde motion of the pole is circular motion in a counter-clockwise direction; retrograde motion is circular motion in a clockwise direction. In general, the sum of prograde and retrograde circular motion is elliptical motion, with linear motion resulting when the amplitudes of the prograde and retrograde components are the same.

By eqns [41]–[42] and [57], the observed polar motion variations are excited by changes in the equatorial components $h_x(t)$ and $h_y(t)$ of relative angular momentum and by changes in the equatorial components $\Omega\,\Delta I_{xz}(t)$ and $\Omega\,\Delta I_{yz}(t)$ of angular momentum due to changes in the mass distribution of the Earth. Like modeling the observed LOD changes, modeling the observed polar motion excitation requires computing both types of changes in angular momentum for the different components of the Earth system. From eqn [65], and again assuming for this purpose that the terrestrial reference frame is uniformly rotating at the rate Ω about the z-coordinate axis, the equatorial components of the mass term of the angular momentum can be written as

$$\Omega\,\Delta I_{xz}(t) = -\Omega\int_V \rho(\mathbf{r},\,t)\,r^2 \sin\phi\cos\phi\cos\lambda\,\mathrm{d}V \quad [69]$$

$$\Omega\,\Delta I_{yz}(t) = -\Omega\int_V \rho(\mathbf{r},\,t)\,r^2 \sin\phi\cos\phi\sin\lambda\,\mathrm{d}V \quad [70]$$

where ϕ is north latitude and λ is east longitude. Similarly, the equatorial components of the motion term of the angular momentum can be written as

$$\begin{aligned}h_x(t) = \int_V \rho(\mathbf{r},\,t)\,[&r\sin\lambda\,\nu(\mathbf{r},\,t) \\ &- r\sin\phi\cos\lambda\,u(\mathbf{r},\,t)]\,\mathrm{d}V\end{aligned} \quad [71]$$

$$\begin{aligned}h_y(t) = \int_V \rho(\mathbf{r},\,t)\,[&-r\cos\lambda\,\nu(\mathbf{r},\,t) \\ &- r\sin\phi\sin\lambda\,u(\mathbf{r},\,t)]\,\mathrm{d}V\end{aligned} \quad [72]$$

where $u(\mathbf{r},t)$ is the eastward component of the velocity and $\nu(\mathbf{r},t)$ is the northward component.

3.09.4.2.1 True polar wander and GIA

Determining an unbiased estimate of the linear trend in the observed path of the pole over the past 100 years is complicated by the presence of

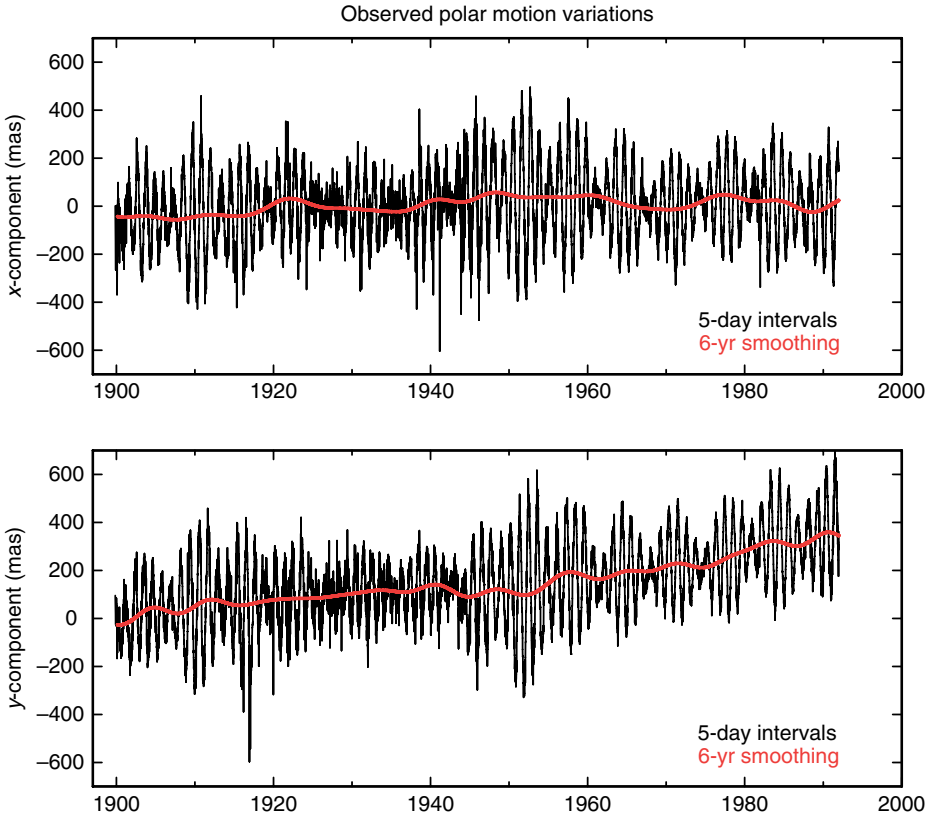

Figure 6 Observed polar motion variations from the HIPPARCOS optical astrometric series. The low-frequency variations shown in red were obtained by applying to the 5-day HIPPARCOS series a low-pass boxcar filter having a 6-year cutoff period. The beating between the 12-month annual wobble and the 14-month Chandler wobble is readily apparent.

the annual, Chandler, and Markowitz wobbles. Various approaches have been taken to estimate the trend in the presence of these large-amplitude periodic and quasiperiodic variations (see **Table 8** for the resulting trend estimates). The annual wobble has been removed by both a least-squares fit (Wilson and Gabay, 1981; McCarthy and Luzum, 1996; Schuh *et al.*, 2000, 2001), and by a seasonal adjustment of the polar motion series (Wilson and Vicente, 1980). The Chandler wobble has been removed by both a least-squares fit for periodic terms (Dickman, 1981; McCarthy and Luzum, 1996; Schuh *et al.*, 2000, 2001), and by deconvolution (Wilson and Vicente, 1980; Wilson and Gabay, 1981; Vicente and Wilson, 2002). Smoothing has also been used to remove the annual and Chandler wobbles (Okamoto and Kikuchi, 1983; Höpfner, 2004). The decadal-scale variations have been removed by modeling them as being strictly periodic at a single frequency of 1/31 cpy and then least-squares fitting a sinusoid at this single frequency (Dickman, 1981; McCarthy and Luzum, 1996).

Rather than modeling the decadal variations as being strictly periodic at a single frequency, Gross and Vondrák (1999) devised a method to account for their quasiperiodic nature when estimating the linear trend. The annual and Chandler wobbles were first removed from the observations by applying to the polar motion series a low-pass boxcar filter having a 6-year cutoff period. A spectrum of the resulting low-pass-filtered polar motion series was then computed and the linear trend estimated by a simultaneous weighted least-squares fit for a mean, trend, and periodic terms at the frequencies of all the peaks evident in the spectrum. The estimates for the linear trend that they obtained by applying this technique to the ILS, HIPPARCOS, and SPACE96 polar motion series are given in **Table 8**. **Figure 7** shows the observed low-pass-filtered polar motion series they used (solid lines), the modeled series they obtained by the simultaneous weighted least-squares fit for a mean, trend, and all periodic terms evident in the spectrum (dashed lines that coincide with the solid lines and are therefore difficult to see),

Table 8 Observed linear trend in the path of the pole

Rate (mas yr^{-1})	Direction (degrees W)	Data span	Source
HIPPARCOS polar motion			
3.39	78.5	1899.7–1992.0	(a)
3.51 ± 0.01	**79.2 ± 0.20**	**1900.0–1992.0**	**(b)**
3.31 ± 0.05	76.1 ± 0.80	1899.7–1992.0	(c)
HIPPARCOS polar motion excitation			
2.84	73.03	1899–1992	(d)
ILS polar motion			
3.4	78	1900–1977	(e)
3.521 ± 0.094	80.1 ± 1.6	1899.8–1979.0	(f)
3.52	79.4	1899.8–1979.0	(g)
3.456	80.56	1899.0–1979.0	(h)
3.81 ± 0.07	75.5 ± 1.0	1899.8–1979.0	(b)
ILS polar motion excitation			
3.4	66	1900–77	(e)
3.3	65	1901–70	(i)
3.49	79.5	1899–1979	(d)
Latitude observations			
3.62	89	1900–78	(j*)
3.51	79	1900–78	(j†)
3.24	84.9	1899.8–1979.0	(k†)
2.97	77.7	1899.8–1979.0	(k‡)
Space-geodetic polar motion			
3.39 ± 0.53	85.4 ± 4.0	1976–94	(l)
4.123 ± 0.002	73.9 ± 0.03	1976.7–97.1	(b)
Combined astrometric and space-geodetic polar motion			
3.29	78.2	1900.0–84.0	(m)
3.33 ± 0.08	75.0 ± 1.1	1899.8–1994.1	(l)
3.901 ± 0.022	65.17 ± 0.22	1891.0–1999.0	(n)
Combined astrometric and space-geodetic excitation			
3.35	76.3	1900–99	(d)
3.54	69.92	1900–99	(d)

The recommended estimate is given in bold.
Sources: (a) Vondrák *et al*. (1998); (b) Gross and Vondrák (1999); (c) Schuh *et al*. (2000, 2001); (d) Vicente and Wilson (2002); (e) Wilson and Vicente (1980); (f) Dickman (1981); (g) Chao (1983); (h) Okamoto and Kikuchi (1983); (i) Wilson and Gabay (1981); (j*) Zhao and Dong (1988) based on measurements taken at nine latitude observing stations; (j†) Zhao and Dong (1988) based on measurements taken at the 5 ILS latitude observing stations located at Mizusawa, Kitab, Carloforte, Gaithersburg, and Ukiah; (k†) Vondrák (1994) based on measurements taken at the 5 ILS latitude observing stations located at Mizusawa, Kitab, Carloforte, Gaithersburg, and Ukiah; (k‡) Vondrák (1994) based on measurements taken at the 4 ILS latitude observing stations located at Mizusawa, Kitab, Carloforte, and Gaithersburg; (l) McCarthy and Luzum (1996); (m) Vondrák (1985); (n) Höpfner (2004).

and the resulting linear trend estimates (dotted lines). As can be seen, their model is an excellent fit to the observations and hence their estimates for the linear trend should be unbiased by the presence of the quasiperiodic decadal-scale polar motion variations. For this reason, and because the HIPPARCOS series spans a greater length of time than the other series that they studied, the recommended estimate for the linear trend in the pole path is the estimate that they obtained for the HIPPARCOS series, namely, a trend of rate 3.51 ± 0.01 mas yr^{-1} toward $79.2 \pm 0.20°$ W longitude.

The estimates given in **Table 8** for the observed linear trend in the path of the pole are with respect to a terrestrial reference frame that has been attached to the mean lithosphere in such a manner that within it the tectonic plates exhibit no net rotation. Argus and Gross (2004) argue that ideally the motion of the pole should be given with respect to a reference frame that is attached to the mean solid Earth. They argue that it would therefore be better to use a reference frame that is attached to hotspots rather than the mean lithosphere because hotspots move slower than the

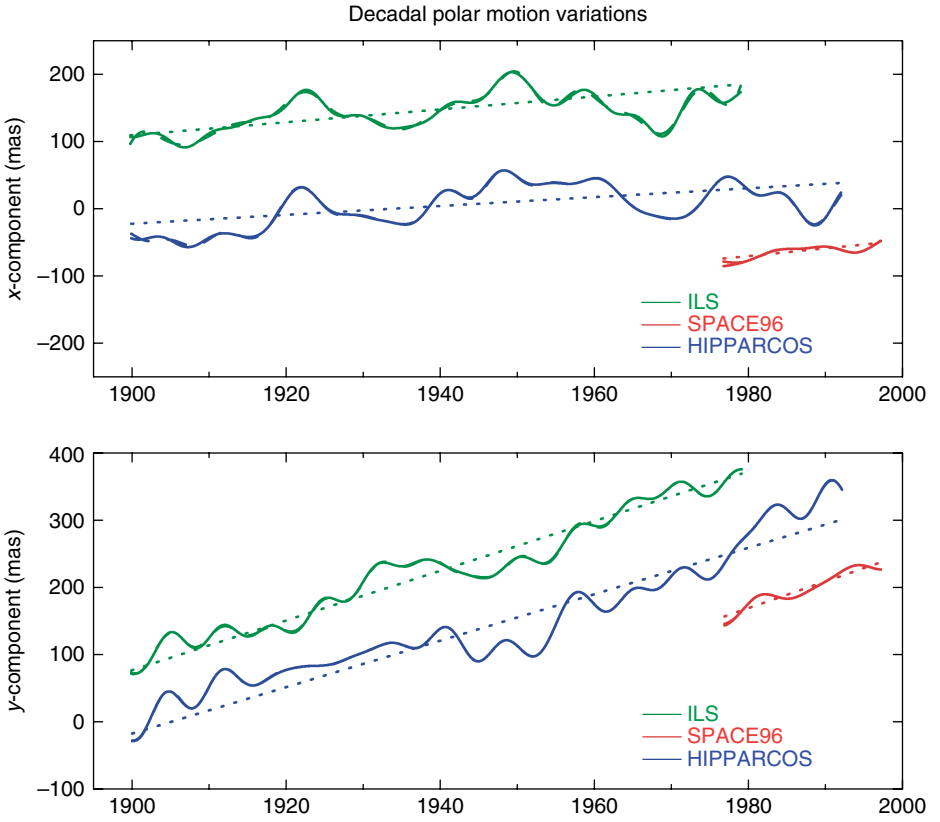

Figure 7 Observed decadal-scale polar motion variations from the ILS optical astrometric series (solid green curve), the HIPPARCOS optical astrometric series (solid blue curve), and the SPACE96 combined space-geodetic series (solid red curve). The decadal-scale variations were obtained by applying to the original series a low-pass boxcar filter having a 6-year cutoff period. The dotted lines show the linear trends in the pole path that were estimated from these series by Gross and Vondrák (1999). The dashed lines that coincide with the solid lines and that are therefore hidden from view show the model of the decadal variations that they used when estimating the trend. For clarity of display the curves have been offset from each other by an arbitrary amount. From Gross RS and Vondrák J (1999) Astrometric and space-geodetic observations of polar wander. *Geophysical Research Letters* 26(14): 2085–2088.

mean lithosphere with respect to the mean solid Earth and hence better represent the mean solid Earth. Transforming the HIPPARCOS trend results of Gross and Vondrák (1999) to a hotspot reference frame, they find that during the past century the linear trend in the path of the pole relative to hotspots was 4.03 mas yr^{-1} towards 68.4° W longitude, or about 15% faster and in a more eastward direction than the trend relative to the mean lithosphere.

One of the most important mechanisms acting to cause a linear trend in the path of the pole on timescales of a few thousand years is GIA. The isostatic adjustment of the solid Earth as it responds to the decreasing load on it following the last deglaciation causes the figure of the Earth to change, and hence the pole to drift. Models of GIA show that its effect on the pole path is sensitive to the assumed value of lower-mantle viscosity, to the assumed thickness and rheology of the lithosphere, to the treatment of the density discontinuity at 670 km depth, and to the assumed compressibility of the Earth model (e.g., Wu and Peltier, 1984; Peltier and Jiang, 1996; Vermeersen and Sabadini, 1996, 1999; Vermeersen *et al.*, 1996, 1997; Mitrovica and Milne, 1998; Johnston and Lambeck, 1999; Nakada, 2000, 2002; Sabadini and Vermeersen, 2002; Tamisea *et al.*, 2002; Sabadini and Vermeersen, 2004; Mitrovica *et al.*, 2005).

However, GIA is not the only mechanism that will cause a trend in the pole path. The present-day change in glacier and ice sheet mass and the accompanying change in nonsteric sea level will also cause a linear trend in polar motion (e.g., Gasperini *et al.*, 1986; Peltier, 1988; Trupin *et al.*, 1992; Trupin, 1993;

James and Ivins, 1995, 1997; Nakada and Okuno, 2003). But the effect of this mechanism is very sensitive to the still-unknown present-day mass change of glaciers and ice sheets, particularly of the Antarctic ice sheet. By adopting various scenarios for the mass change of Antarctica, models predict that its mass change alone should cause a linear trend in the pole path ranging anywhere in rate from 0.31 to 4.46 mas yr^{-1} and in direction from 101° to 281° W longitude (James and Ivins, 1997). Other mechanisms that may cause a linear trend in the path of the pole include tectonic processes taking place under non-isostatic conditions (Vermeersen and Vlaar, 1993; Vermeersen *et al.*, 1994; Sabadini and Vermeersen, 2004), plate subduction (Ricard *et al.*, 1992, 1993; Spada *et al.*, 1992; Richards *et al.*, 1997; Alfonsi and Spada, 1998), mantle convection (Steinberger and O'Connell, 1997; Richards *et al.*, 1999), upwelling mantle plumes (Steinberger and O'Connell, 2002; Greff-Lefftz, 2004), and earthquakes (Chao and Gross, 1987).

3.09.4.2.2 Decadal variations, the Markowitz wobble, and core–mantle interactions

By analyzing ILS latitude measurements taken during 1900–59, Markowitz (1960, 1961) found that at long periods the motion of the pole with respect to the Earth's crust and mantle includes a periodic component superimposed on a linear drift. He found that the periodic component, now known as the Markowitz wobble in his honor, had a period of 24 years and an amplitude of 22 mas and that the linear drift had a rate of 3.2 mas yr^{-1} and a direction towards 60° W longitude, remarkably close to the recent determination of 3.51 mas yr^{-1} toward 79.2° W longitude (Gross and Vondrák, 1999) that is recommended here.

In more recent re-reductions of the ILS and other optical astrometric measurements, which extend more than three decades past those analyzed by Markowitz (1960, 1961), rather than appearing as a strictly periodic phenomenon of well-defined frequency, the Markowitz wobble now appears as a quasiperiodic variation on decadal timescales having an amplitude of about 30 mas (see **Figure 7**). However, since optical astrometric measurements are known to be corrupted by systematic errors, there has always been some doubt about the reality of the decadal variations seen in the ILS and HIPPARCOS series. Since the highly accurate space-geodetic measurements are less susceptible to systematic error than are optical astrometric measurements, any decadal variations seen in the space-geodetic measurements can be considered to be reliable. **Figure 7** compares the decadal variations seen in the SPACE96 combined space-geodetic series with those seen in the ILS and HIPPARCOS optical astrometric series. While decadal variations are seen to be present in the SPACE96 series, and hence can be considered to be real, they have a smaller amplitude and a different phase than those seen in either the ILS or HIPPARCOS series. Thus, space-geodetic measurements both confirm the reality of decadal polar motion variations and demonstrate that the decadal variations seen in the ILS and HIPPARCOS series are unreliable and should be used only to place an upper bound on the size of the decadal variations.

The cause of the decadal-scale polar motion variations is currently unknown. Gross *et al.* (2005) found that redistribution of mass within the atmosphere and oceans cannot be the main excitation source of decadal polar motion variations during 1949–2002 since it amounts to only 20% (x-component) and 38% (y-component) of that observed, and with the modeled excitation being 180° out of phase with that observed. However, the ocean model used in their study was not forced by mass changes associated with precipitation, evaporation, or runoff from rivers including that from glaciers and ice sheets, and so had a constant total mass. Thus, their study did not address the question of the excitation of decadal polar motion by processes that change the total mass of the oceans, such as a nonsteric sea level height change associated with glacier and ice sheet mass change. Wilson (1993) noted that an oscillation in global sea level on decadal timescales would excite decadal polar motion variations with a polarization similar to that observed, implying that mass change of the oceans is responsible for exciting the observed decadal polar motions. In fact, using a climate model, Celaya *et al.* (1999) showed that changes in Antarctic snow pack are capable of inducing decadal polar motion variations of nearly the same amplitude as that observed. But realistic estimates of mass change in glaciers and the Antarctic and other ice sheets, along with estimates of the accompanying nonsteric change in sea level, are required to further evaluate this possible source of decadal polar motion excitation.

Since core–mantle processes are known to cause decadal variations in the length of the day, they may also excite decadal variations in polar motion. But electromagnetic coupling between the core and mantle appears to be 2–3 orders of magnitude too weak

(Greff-Lefftz and Legros, 1995), and topographic coupling appears to be too weak by a factor of 3–10 (Greff-Lefftz and Legros, 1995; Hide *et al.*, 1996; Hulot *et al.*, 1996; Asari *et al.*, 2006). In addition, the modeled decadal polar motion variations resulting from these studies show little agreement in phase with the observed variations.

Following the study of Jochmann (1989), Greiner-Mai *et al.* (2000, 2003) and Greiner-Mai and Barthelmes (2001) have suggested that irregular motion of a tilted oblate inner core may excite decadal polar motion variations, although they did not account for the dynamic effects of the fluid core in their model. Dumberry and Bloxham (2002), who did account for the dynamic effects of the fluid core, suggested that a tilt of the inner core with respect to the mantle of only 0.07°, perhaps caused by an electromagnetic torque acting on the inner core, would generate gravitational and pressure torques on the mantle strong enough to excite decadal polar motion variations having amplitudes as large as those observed and, like the observed variations, having a preferred direction of motion. But when Mound (2005) examined this mechanism, he concluded that while torsional oscillations may excite both decadal LOD and polar motion variations, when the oscillations are constrained to match the observed LOD amplitude, the resulting electromagnetic torque on the inner core is too weak to excite decadal polar motions to their observed level. Despite these conflicting conclusions, invoking the inner core when modeling core–mantle processes may ultimately provide the long-sought explanation for the cause of the Markowitz wobble.

3.09.4.2.3 Tidal wobbles and oceanic and atmospheric tides

Tidally induced deformations of the solid Earth caused by the second-degree zonal tide raising potential cause long-period changes in the Earth's rate of rotation (see Section 3.09.4.1.3). But since this potential is symmetric about the polar axis, tidal deformations of the axisymmetric solid Earth cannot excite polar motion. However, due to the nonaxisymmetric shape of the coastlines, the second-degree zonal tide raising potential acting on the oceans can generate polar motion via the exchange of nonaxial oceanic tidal angular momentum with the solid Earth. Yoder *et al.* (1981) discussed the possible existence of long-period tidal variations in polar motion and tables of such variations predicted from theoretical ocean tide models have been given by Seiler (1990, 1991), Dickman (1993), Gross (1993), Brosche and Wünsch (1994), and Seiler and Wünsch (1995) (*see* Chapter 10.04).

Long-period tidal variations in polar motion were first observed by Chao (1994) and have been discussed by Gross *et al.* (1996b, 1997). **Table 9** gives the results of Gross *et al.* (1997) for the observed variations. As discussed by them, the observations at the two fortnightly tidal frequencies M_f and $M_{f'}$, and perhaps at the other tidal frequencies as well, are suspect, because at such close frequencies the oceans, and hence the rotational response of the Earth, should have the same relative response to the tidal potential. This implies that the results at the M_f and $M_{f'}$ tidal frequencies should have the same phase and an amplitude ratio, 2.4, the same as that of the tidal potential at these frequencies. But they do not. Better observations of the effect of long-period ocean tides on polar motion are clearly needed, as are better models for these effects because, as also discussed by Gross *et al.* (1997), predictions from the available theoretical ocean tide models do not agree with each other or with the observations. And predictions from the T/P tide model of Desai and Wahr (1995) as quoted by Gross *et al.* (1997) have not converged even though data through T/P cycle 130 were used.

Ocean tides in the diurnal and semidiurnal tidal bands also cause polar motion variations. While Yoder *et al.* (1981) discussed the possible existence of such polar motion variations, they were not actually observed until Dong and Herring (1990) detected them in VLBI measurements. Subdaily variations in polar motion at the diurnal and semidiurnal tidal frequencies have now been observed in measurements taken by VLBI (Herring and Dong, 1994; Herring, 1993; Sovers *et al.*, 1993; Gipson, 1996; Haas and Wünsch, 2006), SLR (Watkins and Eanes, 1994), and GPS (Hefty *et al.*, 2000; Rothacher *et al.*, 2001; Steigenberger *et al.*, 2006). Predictions of subdaily tidal variations in polar motion using theoretical ocean tide models have been given by Seiler (1990, 1991), Dickman (1993), Gross (1993), Brosche and Wünsch (1994), and Seiler and Wünsch (1995). Predictions of subdaily tidal variations in polar motion using tide models based upon T/P sea surface height measurements have been given by Chao *et al.* (1996) and Chao and Ray (1997). McCarthy and Petit (2004, chapter 8) give extensive tables of coefficients for the effect of diurnal and semidiurnal ocean tides on polar motion. Updated models for these effects are available through the IERS Special Bureau for Tides website (see **Table 4**).

Table 9 Observed variations in polar motion and polar motion excitation caused by long-period ocean tides

	Argument						Polar motion				Polar motion excitation			
							Prograde		Retrograde		Prograde		Retrograde	
Tide	l	l′	F	D	Ω	Period (days)	amp (μas)	phase (degrees)	amp (μas)	phase (degrees)	amp (μas)	phase (degrees)	amp (μas)	phase (degrees)
M_t'	1	0	2	0	1	9.12	14.65	174.3	12.47	140.8	680.82	−5.8	604.66	140.7
M_t	1	0	2	0	2	9.13	4.73	−161.1	6.84	−36.4	219.41	18.7	330.95	−36.6
M_f'	0	0	2	0	1	13.63	44.42	−149.4	41.65	69.2	1366.47	30.4	1364.30	69.0
M_f	0	0	2	0	2	13.66	55.16	−64.1	79.01	31.5	1693.09	115.8	2583.21	31.3
M_m	1	0	0	0	0	27.56	43.97	−85.0	58.62	−55.2	646.96	94.8	979.84	−55.3

l, l', F, D, and Ω are the Delaunay arguments, expressions for which are given in Simon *et al*. (1994). The period, given in solar days, is the approximate period of the term as viewed in the terrestrial reference frame. The amplitude (amp) and phase of the prograde and retrograde components of polar motion are defined by eqn [68]. The amplitutde and phase of the prograde and retrograde components of polar motion excitation are similarly defined but with $\chi(t) = \chi_x(t) + i\,\chi_y(t)$.

Source: Gross RS, Chao BF, and Desai S (1997) Effect of long-period ocean tides on the Earth's polar motion. *Progress in Oceanography* 40: 385–397.

Comparisons of observations with models show the major role that ocean tides play in causing subdaily polar motion variations (**Figures 5(b)** and **5(c)**), with as much as 60% of the observed polar motion variance being explained by diurnal and semidiurnal ocean tides (Chao *et al.*, 1996). Apart from errors in observations and models, the difference that remains (e.g., Schuh and Schmitz-Hübsch, 2000) may be due to nontidal atmospheric and oceanic effects.

The effects on polar motion of the radiational tides in the atmosphere have been studied by Zharov and Gambis (1996), Brzezinski *et al.* (2002a), and de Viron *et al.* (2005). However, since the oceans will respond dynamically to subdaily tidal variations in the atmospheric wind and pressure fields, the oceans will also contribute to the excitation of polar motion by the radiational tides. Brzezinski *et al.* (2004) have predicted the effects on polar motion of the subdaily radiational tides in the atmosphere and oceans using a barotropic ocean model forced by the 6-h NCEP/NCAR reanalysis wind and pressure fields (also see Gross, 2005a). **Table 10** gives their results at prograde nearly diurnal frequencies. They find the largest effect to be at the prograde S_1 tidal frequency with an amplitude of 9 μas that is primarily excited by ocean-bottom pressure variations. Their predictions at retrograde, nearly diurnal frequencies affect the nutations and are therefore not reproduced here. Since the NCEP/NCAR reanalysis winds and pressure are given every 6 h, the semidiurnal tidal frequency band is incompletely sampled, making it difficult to estimate atmospheric and oceanic effects on polar motion at these frequencies. More complete models for the effects of the radiational tides at nearly semidiurnal frequencies must await the availability of atmospheric fields sampled more often than every 6 h.

3.09.4.2.4 Chandler wobble and its excitation

Any irregularly shaped solid body rotating about some axis that is not aligned with its figure axis will freely wobble as it rotates (Euler, 1765). The Eulerian free wobble of the Earth is known as the Chandler wobble in honor of Seth Carlo Chandler, Jr., who first observed it (Chandler, 1891). Unlike the forced wobbles of the Earth, such as the annual wobble, whose periods are the same as the periods of the forcing mechanisms, the period of the free Chandler wobble is a function of the internal structure and rheology of the Earth (see Section 3.09.2.1), and its decay time constant, or quality factor Q, is a function of the dissipation mechanisms acting to dampen it. The observed values for the period and Q of the Chandler wobble can therefore be used to better understand the internal structure of the Earth and the dissipation mechanisms, such as mantle anelasticity, that dampen the Chandler wobble causing its amplitude to decay in the absence of excitation.

Determining an unbiased estimate for the period and Q of the Chandler wobble is complicated by the relatively short duration of the observational record and by incomplete and inaccurate models of the mechanisms acting to excite it. In the absence of any knowledge of its excitation, statistical models of the excitation can be adopted (e.g., Jeffreys, 1972; Wilson and Haubrich, 1976; Ooe, 1978; Wilson and Vicente, 1980, 1990). Since atmospheric, oceanic, and hydrologic processes are thought to be major sources of Chandler excitation, its period and Q have also been estimated by using AAM data (Furuya and Chao, 1996; Kuehne *et al.*, 1996), atmospheric and oceanic angular momentum data (Gross, 2005b), and atmospheric, oceanic, and hydrologic angular momentum data

Table 10 Modeled variations in polar motion caused by the diurnal radiational tide in the atmosphere and oceans

	Fundamental argument						Period	$p_x(t)$, μas		$p_y(t)$, μas	
Tide	γ	l	l′	F	D	Ω	(solar days)	sin	cos	sin	cos
P_1	1	0	0	−2	2	−2	1.00275	0.1 ± 0.4	0.0 ± 0.4	−0.0 ± 0.4	0.1 ± 0.4
S_1	1	0	−1	0	0	0	1.00000	8.3 ± 0.4	−3.4 ± 0.4	3.4 ± 0.4	8.3 ± 0.4
K_1	1	0	0	0	0	0	0.99727	−0.1 ± 0.5	0.5 ± 0.5	−0.5 ± 0.5	−0.1 ± 0.5

γ is GMST reckoned from the lower culmination of the vernal equinox (GMST + π). l, l', F, D, and Ω are the Delaunay arguments, expressions for which are given in Simon *et al*. (1994). The period, given in solar days, is the approximate period of the term as viewed in the terrestrial reference frame. Since the diumal radiational tide is seasonally modulated, it also affects polar motion at the P_1 and K_1 tidal frequencies.

Source: Brzezinski A, Ponte RM, and Ali AH (2004) Nontidal oceanic excitation of nutation and diurnal/semidiurnal polar motion revisited. *Journal of Geophysical Research* 109: B11407 (doi:10.1029/2004JB003054).

Table 11 Estimated period and *Q* of Chandler wobble

Period (solar days)	Q	Data span (years)	Source
Statistical excitation			
433.2 ± 2.2	63 (36, 192)	67.6	(a)
434.0 ± 2.6	100 (50, 400)	70	(b)
434.8 ± 2.0	96 (50, 300)	76	(c)
433.3 ± 3.1	170 (47, 1000)	78	(d)
433.0 ± 1.1	**179 (74, 789)**	**86**	**(e)**
433.1 ± 1.7		93	(f)
Atmospheric excitation			
439.5 ± 2.1	72 (30, 500)	8.6	(g)
433.7 ± 1.8	49 (35, 100)	10.8	(h)
430.8	41	10	(i)
Atmospheric and oceanic excitation			
429.4	107	10	(i)
431.9	83	51	(i)

The recommended estimate is given in bold. The 1σ confidence interval for the *Q* estimates is given in parentheses.
Sources: (a) Jeffreys (1972); (b) Wilson and Haubrich (1976); (c) Ooe (1978); (d) Wilson and Vicente (1980); (e) Wilson and Vicente (1990); (f) Vicente and Wilson (1997); (g) Kuehne *et al*. (1996); (h) Furuya and Chao (1996); (i) Gross (2005b).

(Wilson and Chen, 2005). **Table 11** gives the resulting estimates for the period and Q of the Chandler wobble.

Gross (2005b) discusses the sensitivity of the estimated period and Q of the Chandler wobble to the length of the data sets that he analyzed, concluding that data sets spanning at least 31 years are needed to obtain stable estimates. He also notes the need for Monte Carlo simulations to determine corrections to the bias of the estimated Q values. Since Gross (2005b) did not do this, but since it was done by Wilson and Vicente (1990) who also used data spanning 86 years to estimate the period and Q of the Chandler wobble, the recommended estimate is that determined by them, namely, a period of 433.0 ± 1.1 (1σ) solar days and a Q of 179 with a 1σ range of 74–789.

With these recommended values for the period T and quality factor Q of the Chandler wobble, in the absence of excitation it would freely decay to the minimum rotational energy state of rotation about the figure axis with an *e*-folding amplitude decay time constant $\tau = 2QT/2\pi$ of about 68 years. But a damping time of 68 years is short on a geological timescale, and since the amplitude of the Chandler wobble has at times been observed to actually increase, some mechanism or mechanisms must be acting to excite it. Since its discovery, many possible excitation mechanisms have been studied, including core–mantle interactions (Gire and Le Mouël, 1986; Hinderer *et al*., 1987; Jault and Le Mouël, 1993), earthquakes (Souriau and Cazenave, 1985; Gross, 1986), continental water storage (Chao *et al*., 1987; Hinnov and Wilson, 1987; Kuehne and Wilson, 1991), atmospheric wind and surface pressure variations (Wilson and Haubrich, 1976; Wahr, 1983; Furuya *et al*., 1996, 1997; Aoyama and Naito, 2001; Aoyama *et al*., 2003; Aoyama, 2005; Stuck *et al*., 2005), and oceanic current and bottom pressure variations (Ponte and Stammer, 1999; Gross, 2000b; Brzezinski and Nastula, 2002; Brzezinski *et al*., 2002b; Gross *et al*., 2003; Liao *et al*., 2003; Seitz *et al*., 2004, 2005; Liao, 2005; Ponte, 2005; Seitz and Schmidt, 2005; Thomas *et al*., 2005).

While there is growing agreement that the Chandler wobble is excited by a combination of atmospheric, oceanic, and hydrologic processes, the relative contribution of each process to its excitation is still being debated. For example, Gross *et al*. (2003) studied the excitation of the Chandler wobble during 1980–2000, finding that atmospheric winds and surface pressure and oceanic currents and bottom pressure combined are significantly coherent with and have enough power to excite the Chandler wobble. They found that during this time interval the observed power in the Chandler band is 1.90 mas^2, with the sum of all atmospheric and oceanic excitation processes having more than enough power, at 2.22 mas^2, to excite the Chandler wobble. Ocean-bottom pressure variations were found to be the single most effective process exciting the Chandler wobble, with atmospheric surface pressure variations having about two-thirds as much power as

ocean-bottom pressure variations, and with the power of winds and currents combined being less than one-third the power of the combined effects of surface and bottom pressure. The conclusion that oceanic processes are more effective than atmospheric in exciting the Chandler wobble has also been reached by Gross (2000b), Brzezinski and Nastula (2002), Brzezinski *et al.* (2002b), and Liao *et al.* (2003). Studies of the excitation of the Chandler wobble using coupled atmosphere–ocean climate models also confirm that atmospheric and oceanic processes have enough power to maintain the Chandler wobble and indicate that the relative contribution of individual atmospheric and oceanic processes changes with time (Celaya *et al.*, 1999; Leuliette and Wahr, 2002; Ponte *et al.*, 2002). However, other studies have concluded that atmospheric processes alone have enough power to excite the Chandler wobble (Furuya *et al.*, 1996, 1997; Aoyama and Naito, 2001; Aoyama *et al.*, 2003; Aoyama, 2005). Resolution of the debate about the relative importance of atmospheric, oceanic, and hydrologic processes to exciting the Chandler wobble awaits the availability of more accurate models of these processes and, because the power needed to maintain the Chandler wobble depends upon its damping (Gross, 2000b), of more accurate estimates of its period and Q.

3.09.4.2.5 Seasonal wobbles

While continuing to analyze variation of latitude measurements, Chandler (1892) soon discovered that the wobbling motion of the Earth includes an annual component as well as a 14-month component. The annual wobble is a forced wobble of the Earth that is caused largely by the annual appearance of a high atmospheric pressure system over Siberia every winter (e.g., Munk and MacDonald, 1960; Lambeck, 1980, 1988; Eubanks, 1993).

Chao and Au (1991) have shown that during 1980–88 the amplitude of the prograde annual polar motion excitation can be accounted for by atmospheric wind and pressure fluctuations, with equatorial winds contributing about 25% and pressure fluctuations contributing about 75% to the total atmospheric excitation. But even though the amplitude of the observed prograde annual polar motion excitation is consistent with atmospheric wind and pressure fluctuations, there is a rather large phase discrepancy of about 30°. Furthermore, no agreement was found by Chao and Au (1991) between the observed retrograde annual polar motion excitation and that due to atmospheric processes, with atmospheric excitation being about twice as large as the observed excitation. Discrepancies as large as a factor of 2 in amplitude were also found by Chao and Au (1991) between observed semiannual polar motion excitation and that due to atmospheric processes (also see Wilson and Haubrich, 1976; Merriam, 1982; Barnes *et al.*, 1983; Wahr, 1983; King and Agnew, 1991; Chao, 1993; Aoyama and Naito, 2000; Nastula and Kolaczek, 2002; Kolaczek *et al.*, 2003; Stuck *et al.*, 2005).

Since the agreement with atmospheric excitation is poor except for the prograde annual amplitude, other processes must be contributing to the excitation of seasonal wobbles. Recently, near-global general circulation models of the oceans have been used to investigate the contribution that nontidal oceanic processes make to exciting the seasonal wobbles of the Earth (Furuya and Hamano, 1998; Ponte *et al.*, 1998, 2001; Johnson *et al.*, 1999; Ponte and Stammer, 1999; Nastula *et al.*, 2000, 2003; Wünsch, 2000; Gross *et al.*, 2003; Chen *et al.*, 2004; Gross, 2004; Seitz *et al.*, 2004; Johnson, 2005; Seitz and Schmidt, 2005; Zhou *et al.*, 2005; Zhong *et al.*, 2006). These studies have shown that adding nontidal oceanic excitation to atmospheric improves the agreement with the observed excitation. For example, **Table 12** gives the results obtained by Gross *et al.* (2003) for the atmospheric and oceanic excitation of polar motion at the the annual and semiannual frequencies. They found that atmospheric processes were more effective than oceanic in exciting the annual and semiannual wobbles. Atmospheric surface pressure variations were found to be the single most important mechanism exciting the annual and semiannual wobbles, with the sum of surface and ocean-bottom pressure variations being about 2–3 times as effective as the sum of winds and currents.

A rather large residual remains after the effects of the atmosphere and oceans are removed from the observed seasonal polar motion excitation. This residual is probably at least partly due to errors in the atmospheric and oceanic models, but could also be due to the neglect of other excitation processes such as hydrologic processes (Hinnov and Wilson, 1987; Chao and O'Conner, 1988; Kuehne and Wilson, 1991; Chen *et al.*, 2000; Wünsch, 2002; Chen and Wilson, 2005; Nastula and Kolaczek, 2005). Wünsch (2002) has summarized the contribution of soil moisture and snow load to exciting the annual and semiannual wobbles. Although the available soil moisture models exhibit large differences, Wünsch (2002) concludes that soil moisture and snow load effects are important

Table 12 Observed and modeled nontidal polar motion excitation at annual and semiannual frequencies

	Annual				Semiannual			
	Prograde		Retrograde		Prograde		Retrograde	
Excitation process	**Amplitude (mas)**	**Phase (degrees)**	**Amplitude (mas)**	**Phase (degrees)**	**Amplitude (mas)**	**Phase (degrees)**	**Amplitude (mas)**	**Phase (degrees)**
Observed excitation	14.52 ± 0.33	−62.77 ± 1.30	7.53 ± 0.33	−120.09 ± 2.50	5.67 ± 0.33	107.56 ± 3.32	5.80 ± 0.33	123.66 ± 3.24
Atmospheric								
Winds	2.97 ± 0.12	−34.92 ± 2.30	2.04 ± 0.12	12.06 ± 3.36	0.36 ± 0.12	71.76 ± 19.0	0.55 ± 0.12	−134.43 ± 12.4
Surface pressure (IB)	15.12 ± 0.17	−101.92 ± 0.66	15.05 ± 0.17	−105.30 ± 0.66	2.60 ± 0.17	47.45 ± 3.81	4.75 ± 0.17	103.77 ± 2.08
Winds & surface pressure	16.51 ± 0.23	−92.38 ± 0.81	14.23 ± 0.23	−98.00 ± 0.94	2.93 ± 0.23	50.36 ± 4.58	4.49 ± 0.23	109.77 ± 2.99
Oceanic								
Currents	2.31 ± 0.09	39.72 ± 2.13	2.11 ± 0.09	50.70 ± 2.33	1.32 ± 0.09	176.16 ± 3.71	1.41 ± 0.09	−143.46 ± 3.49
Bottom pressure	3.45 ± 0.11	63.18 ± 1.87	3.42 ± 0.11	110.24 ± 1.89	0.77 ± 0.11	133.89 ± 8.41	1.48 ± 0.11	−136.46 ± 4.35
Currents & bottom pressure	5.64 ± 0.16	53.81 ± 1.61	4.84 ± 0.16	88.22 ± 1.87	1.96 ± 0.16	160.89 ± 4.62	2.89 ± 0.16	−139.87 ± 3.14
Atmospheric & oceanic								
Winds & currents	4.22 ± 0.15	−3.09 ± 2.08	3.91 ± 0.15	31.71 ± 2.24	1.28 ± 0.15	160.38 ± 6.83	1.96 ± 0.15	−140.92 ± 4.48
Surface & bottom pressure	11.82 ± 0.20	−97.61 ± 0.99	12.43 ± 0.20	−114.51 ± 0.94	2.75 ± 0.20	63.61 ± 4.26	4.22 ± 0.20	121.55 ± 2.78
Total of all modeled excitation	12.23 ± 0.28	−77.50 ± 1.32	9.43 ± 0.28	−101.18 ± 1.71	2.90 ± 0.28	89.70 ± 5.57	4.41 ± 0.28	147.63 ± 3.66

IB, inverted barometer. The amplitude and phase of the prograde and retrograde components of polar motion excitation are defined by eqn [68] but with $\chi(t) = \chi_x(t) + i\,\chi_y(t)$. The reference date t_o for the phase is January 1.0 1990.

Source: Gross RS, Fukumori I, and Menemenlis D (2003) Atmospheric and oceanic excitation of the Earth's wobbles during 1980–2000. *Journal of Geophysical Research* 108(B8): 2370 (doi: 10.1029/2002JB002143).

contributors to exciting the annual and semiannual wobbles. Climate models have also been used to study atmospheric, oceanic, and hydrologic excitation of seasonal polar motion (Celaya *et al.*, 1999; Ponte *et al.*, 2002; Zhong *et al.*, 2003).

3.09.4.2.6 Nonseasonal wobbles

Like the seasonal wobbles, the wobbling motion of the Earth on interannual timescales is a forced response of the Earth to its excitation mechanisms. Abarca del Rio and Cazenave (1994) compared the observed excitation of the Earth's wobbles to atmospheric excitation during 1980–91, finding similar fluctuations in both components on timescales between 1 and 3 years, and in the y-component on timescales between 1.2 and 8 years, but only when the atmospheric excitation is computed assuming that the oceans fully transmit the imposed atmospheric pressure variations to the floor of the oceans (rigid ocean approximation). Chao and Zhou (1999) studied the correlation of the observed polar motion excitation functions on interannual timescales during 1964–94 with the SOI and the North Atlantic Oscillation index (NAOI). Although little agreement was found with the SOI, significant agreement was found with the NAOI, especially for the x-component of the observed excitation function, indicating a possible meteorological origin of the interannual wobbles (also see Zhou *et al.*, 1998). Johnson *et al.* (1999) compared the observed polar motion excitation functions on interannual timescales during 1988–98 with atmospheric and oceanic excitation functions, finding only weak agreement between the observed and modeled excitation functions. For periods between 1 and 6 years excluding the annual cycle, oceanic processes were found by Gross *et al.* (2003) to be much more important than atmospheric in exciting interannual polar motions, explaining 33% of the observed variance compared to 6% for atmospheric processes, and having a correlation coefficient of 0.59 with the observations compared to 0.28 for atmospheric processes. Ocean-bottom pressure variations were found to be the single most important excitation mechanism, explaining 30% of the observed variance and having a correlation coefficient of 0.59 with the observations. Although the other processes were not nearly as effective as ocean-bottom pressure variations in exciting interannual polar motions, when all the processes were combined they were found to explain 40% of the observed variance and to have a correlation coefficient of 0.64 with the observations (also see Johnson, 2005; Chen and Wilson, 2005).

Like the seasonal and interannual wobbles, the wobbling motion of the Earth on intraseasonal timescales is a forced response of the Earth to its excitation mechanisms. Eubanks *et al.* (1988) were the first to study the Earth's wobbles on timescales between 2 weeks and several months, concluding that these rapid polar motions during 1983.75–86.75 are at least partially driven by atmospheric surface pressure changes and suggesting that the remaining excitation may be caused by dynamic ocean-bottom pressure variations. Subsequent studies confirmed the importance of atmospheric processes in exciting rapid polar motions (Salstein and Rosen, 1989; Nastula *et al.*, 1990; Gross and Lindqwister, 1992; Nastula, 1992, 1995, 1997; Kuehne *et al.*, 1993; Salstein, 1993; Kosek *et al.*, 1995; Nastula and Salstein, 1999; Stieglitz and Dickman, 1999; Kolaczek *et al.*, 2000a, 2000b; Schuh and Schmitz-Hübsch, 2000; di Leonardo and Dickman, 2004), although the existence of significant discrepancies indicates that nonatmospheric processes must also play an important role.

The contribution of oceanic processes to exciting rapid polar motions has been studied using both barotropic (Ponte, 1997; Nastula and Ponte, 1999) and baroclinic (Ponte *et al.*, 1998, 2001; Johnson *et al.*, 1999; Nastula *et al.*, 2000; Gross *et al.*, 2003; Chen *et al.*, 2004; Nastula and Kolaczek, 2005; Zhou *et al.*, 2005; Lambert *et al.*, 2006) models of the oceans. Such studies have shown that while better agreement with the observations is obtained when oceanic excitation is added to that of the atmosphere, significant discrepancies still remain. For example, Gross *et al.* (2003) found that on intraseasonal timescales, with periods between 5 days and 1 year excluding the seasonal cycles, atmospheric processes were found to be more effective than oceanic in exciting polar motion, explaining 45% of the observed variance compared to 19% for oceanic processes, and having a correlation coefficient of 0.67 with the observations compared to 0.44 for oceanic processes. Of these processes, atmospheric surface pressure variations were found to be the single most effective process exciting intraseasonal polar motions, with winds being the next most important process; ocean-bottom pressure was about half as effective as atmospheric surface pressure, and currents were about half as effective as winds. Atmospheric winds and surface pressure and oceanic currents and bottom pressure combined explained 65% of the observed variance and had a correlation coefficient of 0.81 with the observations.

On the shortest intraseasonal timescales, Ponte and Ali (2002) used the NCEP/NCAR reanalysis atmospheric model and a barotropic ocean model forced by the NCEP/NCAR reanalysis surface pressure and wind stress fields to study atmospheric and oceanic excitation of polar motion during July 1996 through June 2000 on timescales of 2–20 days. They confirmed the importance of oceanic processes in exciting rapid polar motions, finding that about 60% of the observed polar motion excitation variance between periods of 6–20 days is explained by atmospheric excitation, increasing to about 80% when oceanic excitation is added to that of the atmosphere (also see Kouba, 2005).

Spectra of subdaily atmospheric and oceanic excitation functions (Brzezinski *et al.*, 2002a; Gross, 2005a) reveal the presence of atmospheric normal modes: (1) a peak at about −0.83 cycles per day (cpd) due to the ${\psi_1}^1$ atmospheric normal mode; (2) a peak of smaller amplitude at about +1.8 cpd due to the ${\xi_2}^1$ atmospheric normal mode; and (3) slight enhancement in power at about −0.12 cpd due to the ${\psi_3}^1$ atmospheric normal mode. Because of their small amplitudes, the effects of these normal modes on polar motion are difficult to detect, although the effect of the ${\psi_3}^1$ mode was detected by Eubanks *et al.* (1988).

Acknowledgments

The work described in this paper was performed at the Jet Propulsion Laboratory, California Institute of Technology, under contract with the National Aeronautics and Space Administration. Support for this work was provided by the Solid Earth and Natural Hazards program of NASA's Science Mission Directorate.

References

Abarca del Rio R and Cazenave A (1994) Interannual variations in the Earth's polar motion for 1963–1991: Comparison with atmospheric angular momentum over 1980–1991. *Geophysical Research Letters* 21(22): 2361–2364.

Abarca del Rio R, Gambis D, and Salstein DA (2000) Interannual signals in length of day and atmospheric angular momentum. *Annales Geophysicae* 18: 347–364.

Alfonsi L and Spada G (1998) Effect of subductions and trends in seismically induced Earth rotational variations. *Journal of Geophysical Research* 103(B4): 7351–7362.

Amit H and Olson P (2006) Time-average and time-dependent parts of core flow. *Physics of the Earth and Planetary Interiors* 155: 120–139.

Anderson JD and Rosen RD (1983) The latitude-height structure of 40–50 day variations in atmospheric angular momentum. *Journal of Atmospheric Science* 40: 1584–1591.

Aoyama Y (2005) Quasi-14 month wind fluctuation and excitation of the Chandler wobble. In: Plag H-P, Chao BF, Gross RS, and van Dam T (eds.) *Forcing of Polar Motion in the Chandler Frequency Band: A Contribution to Understanding Interannual Climate Change*, Cahiers du Centre Européen de Géodynamique et de Séismologie, vol. 24, pp. 135–141. Luxembourg: Cahiers du centre Européen de Géodynamique et de Séismologie.

Aoyama Y and Naito I (2000) Wind contributions to the Earth's angular momentum budgets in seasonal variation. *Journal of Geophysical Research* 105(D10): 12417–12431.

Aoyama Y and Naito I (2001) Atmospheric excitation of the Chandler wobble, 1983–1998. *Journal of Geophysical Research* 106(B5): 8941–8954.

Aoyama Y, Naito I, Iwabuchi T, and Yamazaki N (2003) Atmospheric quasi-14 month fluctuation and excitation of the Chandler wobble. *Earth Planets Space* 55: e25–e28.

Argus DF and Gross RS (2004) An estimate of motion between the spin axis and the hotspots over the past century. *Geophysical Research Letters* 31: L06614 (doi:10.1029/ 2004GL019657).

Asari S, Shimizu H, and Utada H (2006) Variability of the topographic core–mantle torque calculated from core surface flow models. *Physics of Earth and Planetary Interiors* 154: 85–111.

Baader H-R, Brosche P, and Hovel W (1983) Ocean tides and periodic variations of the Earth's rotation. *Journal of Geophysics* 52: 140–142.

Barnes RTH, Hide R, White AA, and Wilson CA (1983) Atmospheric angular momentum fluctuations, length-of-day changes and polar motion. *Proceedings of the Royal Society of London A* 387: 31–73.

Bellanger E, Blanter EM, Le Mouël J-L, and Shnirman MG (2002) Estimation of the 13.63-day lunar tide effect on length of day. *Journal of Geophysical Research* 107(B5): 2102 (doi:10.1029/ 2000JB000076).

Beutler G, Hein GW, Melbourne WG, and Seeber G (eds.) (1996) GPS Trends in Precise Terrestrial, Airborne, and Spaceborne Applications. *Proceedings of the IAG Symposium no. 115*, 351p. New York: Springer.

Beutler G, Rothacher M, Schaer S, Springer TA, Kouba J, and Neilan RE (1999) The International GPS Service (IGS): An interdisciplinary service in support of the Earth sciences. *Advances in Space Research* 23(4): 631–653.

Blewitt G (1993) Advances in Global Positioning System technology for geodynamics investigations: 1978–1992. In: Smith DE and Turcotte DL (eds.) *Contributions of Space Geodesy to Geodynamics: Technology*, American Geophysical Union Geodynamics Series, vol. 25, pp. 195–213. Washington, DC: American Geophysical Union.

Bloxham J (1990) On the consequences of strong stable stratification at the top of the Earth's outer core. *Geophysical Research Letters* 17(12): 2081–2084.

Bloxham J and Jackson A (1991) Fluid flow near the surface of the Earth's core. *Reviews of Geophysics* 29(1): 97–120.

Bloxham J and Kuang W (1995) Comment on ''The topographic torque on a bounding surface of a rotating gravitating fluid and the excitation by core motions of decadal fluctuations in the Earth's rotation''. *Geophysical Research Letters* 22(24): 3561–3562.

Bock Y and Leppard N (eds.) (1990) Global Positioning System: An Overview. *Proceedings of the IAG Symposium no. 102,* 459p. New York: Springer.

Braginsky SI (1970) Torsional magnetohydrodynamic vibrations in the Earth's core and variations in day length. *Geomagnetizm I Aeronomiya* (English translation) 10: 1–8.

Brosche P (1982) Oceanic tides and the rotation of the Earth. In: Fricke W and Teleki G (eds.) *Sun and Planetary System*, pp. 179–184. Dordrecht, Holland: Reidel.

Brosche P and Sündermann J (1985) The Antarctic circumpolar current and its influence on the Earth's rotation. *Deutsche Hydrographische Zeitschrift* 38: 1–6.

Brosche P and Wünsch J (1994) On the ''rotational angular momentum'' of the oceans and the corresponding polar motion. *Astronomische Nachrichten* 315: 181–188.

Brosche P, Seiler U, Sündermann J, and Wünsch J (1989) Periodic changes in Earth's rotation due to oceanic tides. *Astronomy and Astrophysics* 220: 318–320.

Brosche P, Wünsch J, Frische A, Sündermann J, Maier-Reimer E, and Mikolajewicz U (1990) The seasonal variation of the angular momentum of the oceans. *Naturwissenschaften* 77: 185–186.

Brosche P, Wünsch J, Campbell J, and Schuh H (1991) Ocean tide effects in Universal Time detected by VLBI. *Astronomy and Astrophysics* 245: 676–682.

Brosche P, Wünsch J, Maier-Reimer E, Segschneider J, and Sündermann J (1997) The axial angular momentum of the general circulation of the oceans. *Astronomische Nachrichten* 318: 193–199.

Brzezinski A (1992) Polar motion excitation by variations of the effective angular momentum function: Considerations concerning deconvolution problem. *Manuscripta Geodaetica* 17: 3–20.

Brzezinski A and Capitaine N (1993) The use of the precise observations of the celestial ephemeris pole in the analysis of geophysical excitation of Earth rotation. *Journal of Geophysical Research* 98(B4): 6667–6675.

Brzezinski A and Nastula J (2002) Oceanic excitation of the Chandler wobble. *Advances in Space Research* 30: 195–200.

Brzezinski A, Bizouard Ch, and Petrov S (2002a) Influence of the atmosphere on Earth rotation: What new can be learned from the recent atmospheric angular momentum estimates? *Surveys in Geophysics* 23: 33–69.

Brzezinski A, Nastula J, and Ponte RM (2002b) Oceanic excitation of the Chandler wobble using a 50-year time series of ocean angular momentum. In: Adám J and Schwarz K-P (eds.) *Vistas for Geodesy in the New Millennium*, IAG Symposia, vol. 125, pp. 434–439. New York: Springer.

Brzezinski A, Ponte RM, and Ali AH (2004) Nontidal oceanic excitation of nutation and diurnal/semidiurnal polar motion revisited. *Journal of Geophysical Research* 109: B11407 (doi:10.1029/2004JB003054).

Buffett BA (1996a) Gravitational oscillations in the length of day. *Geophysical Research Letters* 23(17): 2279–2282.

Buffett BA (1996b) A mechanism for decade fluctuations in the length of day. *Geophysical Research Letters* 23(25): 3803–3806.

Buffett BA (1998) Free oscillations in the length of day: Inferences on physical properties near the core–mantle boundary. In: Gurnis M, Wysession ME, Knittle E, and Buffett BA (eds.) *The Core–Mantle Boundary Region*, American Geophysical Union Geodynamics Series, vol. 28, pp. 153–165. Washington, DC: American Geophysical Union.

Buffett BA and Mound JE (2005) A Green's function for the excitation of torsional oscillations in the Earth's core. *Journal of Geophysical Research* 110: B08104 (doi:10.1029/ 2004JB003495).

Bullard EC, Freeman C, Gellman H, and Nixon J (1950) The westward drift of the Earth's magnetic field. *Philosophical Transactions of the Royal Society London A* 243: 61–92.

Capitaine N (2000) Definition of the celestial ephemeris pole and the celestial ephemeris origin. In: Johnston KJ, McCarthy DD, Luzum BJ, and Kaplan GH (eds.) *Towards Models and Constants for Sub-Microarcsecond Astrometry*, Proc. IAU Colloquium 180, US Naval Obs, pp. 153–163. Washington, DC: US Naval Observatory.

Celaya MA, Wahr JM, and Bryan FO (1999) Climate-driven polar motion. *Journal of Geophysical Research* 104(B6): 12813–12829.

Chandler SC (1891) On the variation of latitude, II. *The Astronomical Journal* 11: 65–70.

Chandler SC (1892) On the variation of latitude, VII. *The Astronomical Journal* 12: 97–101.

Chao BF (1983) Autoregressive harmonic analysis of the Earth's polar motion using homogeneous International Latitude Service data. *Journal of Geophysical Research* 88(B12): 10299–10307.

Chao BF (1984) Interannual length-of-day variations with relation to the Southern Oscillation/El Niño. *Geophysical Research Letters* 11(5): 541–544.

Chao BF (1988) Correlation of interannual length-of-day variation with El Niño/Southern Oscillation, 1972–1986. *Journal of Geophysical Research* 93(B7): 7709–7715.

Chao BF (1989) Length-of-day variations caused by El Niño/ Southern Oscillation and Quasi-Biennial Oscillation. *Science* 243: 923–925.

Chao BF (1993) Excitation of Earth's polar motion by atmospheric angular momentum variations, 1980–1990. *Geophysical Research Letters* 20(2): 253–256.

Chao BF (1994) Zonal tidal signals in the Earth's polar motion. *Eos Transactions of the American Geophysical Union* 75(44): 158.

Chao BF and Au AY (1991) Atmospheric excitation of the Earth's annual wobble: 1980–1988. *Journal of Geophysical Research* 96(B4): 6577–6582.

Chao BF and Gross RS (1987) Changes in the Earth's rotation and low-degree gravitational field introduced by earthquakes. *Geophysical Journal of the Royal Astronomical Society* 91: 569–596.

Chao BF and O'Connor WP (1988) Global surface-water-induced seasonal variations in the Earth's rotation and gravitational field. *Geophysical Journal of the Royal Astronomical Society* 94: 263–270.

Chao BF and Ray RD (1997) Oceanic tidal angular momentum and Earth's rotation variations. *Progress in Oceanography* 40: 399–421.

Chao BF and Zhou Y-H (1999) Meteorological excitation of interannual polar motion by the North Atlantic Oscillation. *Journal of Geodynamics* 27: 61–73.

Chao BF, O'Connor WP, Chang ATC, Hall DK, and Foster JL (1987) Snow load effect on the Earth's rotation and gravitational field, 1979–1985. *Journal of Geophysical Research* 92(B9): 9415–9422.

Chao BF, Merriam JB, and Tamura Y (1995a) Geophysical analysis of zonal tidal signals in length of day. *Geophysical Journal International* 122: 765–775.

Chao BF, Ray RD, and Egbert GD (1995b) Diurnal/semidiurnal oceanic tidal angular momentum: Topex/Poseidon models in comparison with Earth's rotation rate. *Geophysical Research Letters* 22(15): 1993–1996.

Chao BF, Ray RD, Gipson JM, Egbert GD, and Ma C (1996) Diurnal/semidiurnal polar motion excited by oceanic tidal angular momentum. *Journal of Geophysical Research* 101(B9): 20151–20163.

Chapman S and Lindzen RS (1970) *Atmospheric Tides*. Dordrecht, The Netherlands: D. Reidel.

Chapront J, Chapront-Touzé M, and Francou G (2002) A new determination of lunar orbital parameters, precession constant and tidal acceleration from LLR measurements. *Astronomy and Astrophysics* 387: 700–709.

Chen J (2005) Global mass balance and the length-of-day variations. *Journal of Geophysical Research* 110: B08404 (doi:10.1029/ 2004JB003474).

Chen JL and Wilson CR (2005) Hydrological excitations of polar motion, 1993–2002. *Geophysical Journal International* 160: 833–839.

Chen JL, Wilson CR, Chao BF, Shum CK, and Tapley BD (2000) Hydrological and oceanic excitations to polar motion and length-of-day variation. *Geophysical Journal International* 141: 149–156.

Chen JL, Wilson CR, Hu X-G, Zhou Y-H, and Tapley BD (2004) Oceanic effects on polar motion determined from an ocean model and satellite altimetry: 1993–2001. *Journal of Geophysical Research* 109: B02411 (doi:10.1029/2003JB002664).

Cheng MK, Eanes RJ, and Tapley BD (1992) Tidal deceleration of the Moon's mean motion. *Geophysical Journal International* 108: 401–409.

Cheng MK, Shum CK, Eanes RJ, Schutz BE, and Tapley BD (1990) Long-period perturbations in Starlette orbit and tide solution. *Journal of Geophysical Research* 95(B6): 8723–8736.

Christodoulidis DC, Smith DE, Williamson RG, and Klosko SM (1988) Observed tidal braking in the Earth/Moon/Sun system. *Journal of Geophysical Research* 93(B6): 6216–6236.

Dahlen FA (1976) The passive influence of the oceans upon the rotation of the Earth. *Geophysical Journal of the Royal Astronomical Society* 46: 363–406.

Dai A and Wang J (1999) Diurnal and semidiurnal tides in global surface pressure fields. *Journal of Atmospheric Science* 56: 3874–3891.

Davis RG and Whaler KA (1996) Determination of a steady velocity in a rotating frame of reference at the surface of the Earth's core. *Geophysical Journal International* 126: 92–100.

Defraigne P and Smits I (1999) Length of day variations due to zonal tides for an inelastic Earth in non-hydrostatic equilibrium. *Geophysical Journal International* 139: 563–572.

Desai SD and Wahr JM (1995) Empirical ocean tide models estimated from Topex/Poseidon altimetry. *Journal of Geophysical Research* 100(C12): 25205–25228.

Desai SD and Wahr JM (1999) Monthly and fortnightly tidal variations of the Earth's rotation rate predicted by a Topex/Poseidon empirical ocean tide model. *Geophysical Research Letters* 26(8): 1035–1038.

de Viron O, Salstein D, Bizouard Ch, and Fernandez L (2004) Low-frequency excitation of length of day and polar motion by the atmosphere. *Journal of Geophysical Research* 109: B03408 (doi:10.1029/2003JB002817).

de Viron O, Schwarzbaum G, Lott F, and Dehant V (2005) Diurnal and subdiurnal effects of the atmosphere on the Earth rotation and geocenter motion. *Journal of Geophysical Research* 110: B11404 (doi:10.1029/2005JB003761).

Dickey JO, Bender PL, Faller JE, *et al.* (1994a) Lunar laser ranging: A continuing legacy of the Apollo program. *Science* 265: 482–490.

Dickey JO, Gegout P, and Marcus SL (1999) Earth-atmosphere angular momentum exchange and ENSOs: The rotational signature of the 1997–98 event. *Geophysical Research Letters* 26(16): 2477–2480.

Dickey JO, Ghil M, and Marcus SL (1991) Extratropical aspects of the 40–50 day oscillation in length-of-day and atmospheric angular momentum. *Journal of Geophysical Research* 96(D12): 22643–22658.

Dickey JO, Marcus SL, Eubanks TM, and Hide R (1993a) Climate studies via space geodesy: Relationships between ENSO and interannual length-of-day variations. In: McBean GA and Hantel M (eds.) *Interactions Between Global Climate Subsystems: The Legacy of Hann*, American Geophysical Union Geophysical Monograph Series, vol. 75, pp. 141–155. Washington, DC: American Geophysical Union.

Dickey JO, Marcus SL, and Hide R (1992) Global propagation of interannual fluctuations in atmospheric angular momentum. *Nature* 357: 482–488.

Dickey JO, Marcus SL, Hide R, Eubanks TM, and Boggs DH (1994b) Angular momentum exchange among the solid Earth, atmosphere and oceans: A case study of the 1982–83 El Niño event. *Journal of Geophysical Research* 99(B12): 23921–23937.

Dickey JO, Marcus SL, Johns CM, Hide R, and Thompson SR (1993b) The oceanic contribution to the Earth's seasonal angular momentum budget. *Geophysical Research Letters* 20: 2953–2956.

Dickey JO, Newhall XX, and Williams JG (1985) Earth orientation from lunar laser ranging and an error analysis of polar motion services. *Journal of Geophysical Research* 90: 9353–9362.

Dickman SR (1981) Investigation of controversial polar motion features using homogeneous International Latitude Service data. *Journal of Geophysical Research* 86(B6): 4904–4912.

Dickman SR (1993) Dynamic ocean-tide effects on Earth's rotation. *Geophysical Journal International* 112: 448–470.

Dickman SR (1994) Ocean tidal effects on Earth's rotation and on the lunar orbit. In: Schutz BE, Anderson A, Froidevaux C, and Parke M (eds.) *Gravimetry and Space Techniques Applied to Geodynamics and Ocean Dynamics*, American Geophysical Union Geophysical Monograph Series, vol. 82, pp. 87–94. Washington, DC: American Geophysical Union.

Dickman SR (2003) Evaluation of ''effective angular momentum function'' formulations with respect to core–mantle coupling. *Journal of Geophysical Research* 108(B3): 2150 (doi:10.1029/2001JB001603).

Dickman SR (2005) Rotationally consistent Love numbers. *Geophysical Journal International* 161: 31–40.

Dickman SR and Nam YS (1995) Revised predictions of long-period ocean tidal effects on Earth's rotation rate. *Journal of Geophysical Research* 100(B5): 8233–8243.

di Leonardo SM and Dickman SR (2004) Isolation of atmospheric effects on rapid polar motion through Wiener filtering. *Geophysical Journal International* 159: 863–873.

Djurovic D and Pâquet P (1996) The common oscillations of solar activity, the geomagnetic field, and the Earth's rotation. *Solar Physics* 167: 427–439.

Dong D and Herring T (1990) Observed variations of UT1 and polar motion in the diurnal and semidiurnal bands. *EOS Transactions of the American Geophysical Union* 71: 482.

Dumberry M and Bloxham J (2002) Inner core tilt and polar motion. *Geophysical Journal International* 151: 377–392.

Dumberry M and Bloxham J (2004) Variations in the Earth's gravity field caused by torsional oscillations in the core. *Geophysical Journal International* 159: 417–434.

Dumberry M and Bloxham J (2006) Azimuthal flows in the Earth's core and changes in length of day at millennial timescales. *Geophysical Journal International* 165: 32–46.

Dziewonski AM and Anderson DL (1981) Preliminary reference Earth model. *Physics of Earth and Planetary Interiors* 25: 297–356.

Eubanks TM (1993) Variations in the orientation of the Earth. In: Smith DE and Turcotte DL (eds.) *Contributions of Space Geodesy to Geodynamics: Earth Dynamics*, American Geophysical Union Geodynamics Series, vol. 24, pp. 1–54. Washington, DC: American Geophysical Union.

Eubanks TM, Steppe JA, and Dickey JO (1986) The El Niño, the Southern Oscillation and the Earth's rotation. In: Cazenave A (ed.) *Earth Rotation: Solved and Unsolved Problems*, pp. 163–186. Hingham, MA: D. Reidel.

Eubanks TM, Steppe JA, Dickey JO, Rosen RD, and Salstein DA (1988) Causes of rapid motions of the Earth's pole. *Nature* 334: 115–119.

Euler L (1765) *Theoria Motus Corporum Solidorum*. Rostock, Germany: Litteris et impensis A.F. Röse.

Fang M, Hager BH, and Herring TA (1996) Surface deformation caused by pressure changes in the fluid core. *Geophysical Research Letters* 23(12): 1493–1496.

Feissel M and Gambis D (1980) La mise en evidence de variations rapides de la durée du jour. *Comptes Rendus De L Academie Des Sciences Paris, Series B* 291: 271–273.

Feissel M and Gambis D (1993) The International Earth Rotation Service: Current results for research on Earth rotation and reference frames. *Advances in Space Research* 13(11): 143–150.

Feissel M and Gavoret J (1990) ENSO-related signals in Earth rotation, 1962–87. In: McCarthy DD and Carter WE (eds.) *Variations in Earth Rotation*, AGU Geophysical Monograph Series, vol. 59, pp. 133–137. Washington, DC: American Geophysical Union.

Feissel M and Nitschelm C (1985) Time dependent aspects of the atmospheric driven fluctuations in the duration of the day. *Annales Geophysicae* 3: 180–186.

Fliegel HF and Hawkins TP (1967) Analysis of variations in the rotation of the Earth. *Astronomical Journal* 72(4): 544–550.

Freedman AP, Ibañez-Meier R, Herring TA, Lichten SM, and Dickey JO (1994b) Subdaily Earth rotation during the Epoch '92 campaign. *Geophysical Research Letters* 21(9): 769–772.

Freedman AP, Steppe JA, Dickey JO, Eubanks TM, and Sung L-Y (1994a) The short-term prediction of universal time and length of day using atmospheric angular momentum. *Journal of Geophysical Research* 99(B4): 6981–6996.

Frische A and Sündermann J (1990) The seasonal angular momentum of the thermohaline ocean circulation. In: Brosche P and Sündermann J (eds.) *Earth's Rotation From Eons to Days*, pp. 108–126. New York: Springer.

Furuya M and Chao BF (1996) Estimation of period and *Q* of the Chandler wobble. *Geophysical Journal International* 127: 693–702.

Furuya M and Hamano Y (1998) Effect of the Pacific Ocean on the Earth's seasonal wobble inferred from National Center for Environmental Prediction ocean analysis data. *Journal of Geophysical Research* 103(B5): 10131–10140.

Furuya M, Hamano Y, and Naito I (1996) Quasi-periodic wind signal as a possible excitation of Chandler wobble. *Journal of Geophysical Research* 101(B11): 25537–25546.

Furuya M, Hamano Y, and Naito I (1997) Importance of wind for the excitation of Chandler wobble as inferred from wobble domain analysis. *Journal of Physics of the Earth* 45: 177–188.

Gambis D (1992) Wavelet transform analysis of the length of the day and the El-Niño/Southern Oscillation variations at intra-seasonal and interannual time scales. *Annales Geophysicae* 10: 429–437.

Gambis D (2004) Monitoring Earth orientation using space-geodetic techniques: State-of-the-art and prospective. *Journal of Geodesy* 78: 295–303.

Gasperini P, Sabadini R, and Yuen DA (1986) Excitation of the Earth's rotational axis by recent glacial discharges. *Geophysical Research Letters* 13(6): 533–536.

Gilbert F and Dziewonski AM (1975) An application of normal mode theory to the retrieval of structural parameters and source mechanisms from seismic spectra. *Philosophical Transactions of the Royal Society London* A 278: 187–269.

Gipson JM (1996) Very long baseline interferometry determination of neglected tidal terms in high-frequency Earth orientation variation. *Journal of Geophysical Research* 101(B12): 28051–28064.

Gire C and Le Mouël J-L (1986) Flow in the fluid core and Earth's rotation. In: Cazenave A (ed.) *Earth Rotation: Solved and Unsolved Problems*, pp. 241–258. Dordrecht, Holland: D. Reidel.

Goldstein H (1950) *Classical Mechanics*. Reading, MA: Addison-Wesley.

Greff-Lefftz M (2004) Upwelling mantle plumes, superswells, and true polar wander. *Geophysical Journal International* 159: 1125–1137.

Greff-Lefftz M and Legros H (1995) Core–mantle coupling and polar motion. *Physics of Earth and Planetary Interiors* 91: 273–283.

Greff-Lefftz M, Pais MA, and Le Mouël J-L (2004) Surface gravitational field and topography changes induced by the Earth's fluid core motions. *Journal of Geodesy* 78: 386–392.

Greiner-Mai H and Barthelmes F (2001) Relative wobble of the Earth's inner core derived from polar motion and associated gravity variations. *Geophysical Journal International* 144: 27–36.

Greiner-Mai H, Jochmann H, and Barthelmes F (2000) Influence of possible inner-core motions on the polar motion and the gravity field. *Physics of Earth and Planetary Interiors* 117: 81–93.

Greiner-Mai H, Jochmann H, Barthelmes F, and Ballani L (2003) Possible influences of core processes on the Earth's rotation and the gravity field. *Journal of Geodynamics* 36: 343–358.

Grejner-Brzezinska DA and Goad CC (1996) Subdaily Earth rotation determined from GPS. *Geophysical Research Letters* 23(19): 2701–2704.

Gross RS (1986) The influence of earthquakes on the Chandler wobble during 1977–1983. *Geophysical Journal of the Royal Astronomical Society* 85: 161–177.

Gross RS (1992) Correspondence between theory and observations of polar motion. *Geophysical Journal International* 109: 162–170.

Gross RS (1993) The effect of ocean tides on the Earth's rotation as predicted by the results of an ocean tide model. *Geophysical Research Letters* 20(4): 293–296.

Gross RS (2000a) Combinations of Earth orientation measurements: SPACE97, COMB97, and POLE97. *Journal of Geodesy* 73: 627–637.

Gross RS (2000b) The excitation of the Chandler wobble. *Geophysical Research Letters* 27(15): 2329–2332.

Gross RS (2001) A combined length-of-day series spanning 1832–1997: LUNAR97. *Physics of Earth and Planetary Interiors* 123: 65–76.

Gross RS (2004) Angular momentum in the Earth system. In: Sanso F (ed.) *V Hotine-Marussi Symposium on Mathematical Geodesy*, IAG Symposia, vol. 127, pp. 274–284. New York: Springer.

Gross RS (2005a) Oceanic excitation of polar motion: A review. In: Plag H-P, Chao BF, Gross RS, and van Dam T (eds.) *Forcing of Polar Motion in the Chandler Frequency Band: A Contribution to Understanding Interannual Climate Change,* Cahiers du Centre Européen de Géodynamique et de Séismologie, vol. 24, pp. 89–102. Luxembourg: Cahiers du Centre Européen de Géodynamique et de Séismologie.

Gross RS (2005b) The observed period and Q of the Chandler wobble. In: Plag H-P, Chao BF, Gross RS, and van Dam T (eds.) *Forcing of Polar Motion in the Chandler Frequency Band: A Contribution to Understanding Interannual Climate Change,* Cahiers du Centre Européen de Géodynamique et de Séismologie, vol. 24, pp. 31–37. Luxembourg: Cahiers du Centre Européen de Géodynamique et de Séismologie.

Gross RS and Lindqwister UJ (1992) Atmospheric excitation of polar motion during the GIG '91 measurement campaign. *Geophysical Research Letters* 19(9): 849–852.

Gross RS and Vondrák J (1999) Astrometric and space-geodetic observations of polar wander. *Geophysical Research Letters* 26(14): 2085–2088.

Gross RS, Marcus SL, Eubanks TM, Dickey JO, and Keppenne CL (1996a) Detection of an ENSO signal in

seasonal length-of-day variations. *Geophysical Research Letters* 23(23): 3373–3376.

Gross RS, Chao BF, and Desai S (1997) Effect of long-period ocean tides on the Earth's polar motion. *Progress in Oceanography* 40: 385–397.

Gross RS, Eubanks TM, Steppe JA, Freedman AP, Dickey JO, and Runge TF (1998) A Kalman-filter-based approach to combining independent Earth-orientation series. *Journal of Geodesy* 72: 215–235.

Gross RS, Fukumori I, and Menemenlis D (2003) Atmospheric and oceanic excitation of the Earth's wobbles during 1980–2000. *Journal of Geophysical Research* 108(B8): 2370 (doi:10.1029/2002JB002143).

Gross RS, Fukumori I, Menemenlis D, and Gegout P (2004) Atmospheric and oceanic excitation of length-of-day variations during 1980–2000. *Journal of Geophysical Research* 109: B01406 (doi:10.1029/2003JB002432).

Gross RS, Fukumori I, and Menemenlis D (2005) Atmospheric and oceanic excitation of decadal-scale Earth orientation variations. *Journal of Geophysical Research* 110: B09405 (doi:10.1029/2004JB003565).

Gross RS, Hamdan KH, and Boggs DH (1996b) Evidence for excitation of polar motion by fortnightly ocean tides. *Geophysical Research Letters* 23(14): 1809–1812.

Gross RS, Marcus SL, and Dickey JO (2002) Modulation of the seasonal cycle in length-of-day and atmospheric angular momentum. In: Adám J and Schwarz K-P (eds.) *Vistas for Geodesy in the New Millennium*, IAG Symposia, vol. 125, pp. 457–462. New York: Springer.

Groten E (2004) Fundamental parameters and current (2004) best estimates of the parameters of common relevance to astronomy, geodesy, and geodynamics. *Journal of Geodesy* 77: 724–731.

Gubbins D (1982) Finding core motions from magnetic observations. *Philosophical Transactions of the Royal Society London* A 306: 247–254.

Guinot B (1970) Short-period terms in Universal Time. *Astronomy and Astrophysics* 8: 26–28.

Haas R and Wünsch J (2006) Sub-diurnal earth rotation variations from the VLBI CONT02 campaign. *Journal of Geodynamics* 41: 94–99.

Halley E (1695) Some account of the ancient state of the city of Palmyra; with short remarks on the inscriptions found there. *Philosophical Transactions of the Royal Society London* 19: 160–175.

Haurwitz B and Cowley AD (1973) The diurnal and semidiurnal barometric oscillations, global distribution and annual variation. *Pure and Applied Geophysics* 102: 193–222.

Hefty J and Capitaine N (1990) The fortnightly and monthly zonal tides in the Earth's rotation from 1962 to 1988. *Geophysical Journal International* 103: 219–231.

Hefty J, Rothacher M, Springer T, Weber R, and Beutler G (2000) Analysis of the first year of Earth rotation parameters with a sub-daily resolution gained at the CODE processing center of the IGS. *Journal of Geodesy* 74: 479–487.

Hendon HH (1995) Length of day changes associated with the Madden–Julian oscillation. *Journal of Atmospheric Science* 52(13): 2373–2383.

Herring TA (1993) Diurnal and semidiurnal variations in Earth rotation. *Advances in Space Research* 13(11): 281–290.

Herring TA and Dong D (1991) Current and future accuracy of Earth rotation measurements. In: Carter WE (ed.) *Proceedings of the AGU Chapman Conference on Geodetic VLBI: Monitoring Global Change*, NOAA Technical Report NOS 137 NGS 49, pp. 306–324. Washington, DC: NOAA.

Herring TA and Dong D (1994) Measurement of diurnal and semidiurnal rotational variations and tidal parameters of Earth. *Journal of Geophysical Research* 99(B9): 18051–18071.

Hide R (1969) Interaction between the Earth's liquid core and solid mantle. *Nature* 222: 1055–1056.

Hide R (1977) Towards a theory of irregular variations in the length of the day and core–mantle coupling. *Philosophical Transactions of the Royal Society London A* 284: 547–554.

Hide R (1989) Fluctuations in the Earth's rotation and the topography of the core–mantle interface. *Philosophical Transactions of the Royal Society London A* 328: 351–363.

Hide R (1993) Angular momentum transfer between the Earth's core and mantle. In: Le Moüel J-L, Smylie DE, and Herring T (eds.) *Dynamics of the Earth's Deep Interior and Earth Rotation,* American Geophysical Union Geophysical Monograph Series, vol. 72, pp. 109–112. Washington, DC: American Geophysical Union.

Hide R (1995a) The topographic torque on a bounding surface of a rotating gravitating fluid and the excitation by core motions of decadal fluctuations in the Earth's rotation. *Geophysical Research Letters* 22(8): 961–964.

Hide R (1995b) Reply to the comment by Bloxham J. and Kuang W. on a paper entitled "The topographic torque on a bounding surface of a rotating gravitating fluid and the excitation by core motions of decadal fluctuations in the Earth's rotation". *Geophysical Research Letters* 22(24): 3563–3565.

Hide R (1998) A note on topographic core–mantle coupling. *Physics of Earth and Planetary Interiors* 109: 91–92.

Hide R and Dickey JO (1991) Earth's variable rotation. *Science* 253: 629–637.

Hide R, Birch NT, Morrison LV, Shea DJ, and White AA (1980) Atmospheric angular momentum fluctuations and changes in the length of the day. *Nature* 286: 114–117.

Hide R, Clayton RW, Hager BH, Spieth MA, and Voorhies CV (1993) Topographic core–mantle coupling and fluctuations in the Earth's rotation. In: Aki K and Dmowska R (eds.) *Relating Geophysical Structures and Processes: The Jeffreys Volume*, American Geophysical Union Geophysical Monograph Series, vol. 76, pp. 107–120. Washington, DC: American Geophysical Union.

Hide R, Boggs DH, Dickey JO, Dong D, Gross RS, and Jackson A (1996) Topographic core–mantle coupling and polar motion on decadal time scales. *Geophysical Journal International* 125: 599–607.

Hide R, Boggs DH, and Dickey JO (2000) Angular momentum fluctuations within the Earth's liquid core and torsional oscillations of the core–mantle system. *Geophysical Journal International* 143: 777–786.

Hinderer J, Legros H, Gire C, and Le Mouël J-L (1987) Geomagnetic secular variation, core motions and implications for the Earth's wobbles. *Physics of Earth and Planetary Interiors* 49: 121–132.

Hinnov LA and Wilson CR (1987) An estimate of the water storage contribution to the excitation of polar motion. *Geophysical Journal of the Royal Astronomical Society* 88: 437–459.

Hofmann-Wellenhof B, Lichtenegger H, and Collins J (1997) *Global Positioning System: Theory and Practice*. New York: Springer.

Holme R (1998a) Electromagnetic core–mantle coupling—I. Explaining decadal changes in the length of day. *Geophysical Journal International* 132: 167–180.

Holme R (1998b) Electromagnetic core–mantle coupling II: Probing deep mantle conductance. In: Gurnis M, Wysession ME, Knittle E, and Buffett BA (eds.) *The Core-Mantle Boundary Region*, American Geophysical Union Geodynamics Series, vol. 28, pp. 139–151. Washington, DC: American Geophysical Union.

Holme R (2000) Electromagnetic core–mantle coupling III. Laterally varying mantle conductance. *Physics of Earth and Planetary Interiors* 117: 329–344.

Holme R and Whaler KA (2001) Steady core flow in an azimuthally drifting reference frame. *Geophysical Journal International* 145: 560–569.

Höpfner J (1998) Seasonal variations in length of day and atmospheric angular momentum. *Geophysical Journal International* 135: 407–437.

Höpfner J (2000) Seasonal length-of-day changes and atmospheric angular momentum oscillations in their temporal variability. *Journal of Geodesy* 74: 335–358.

Höpfner J (2001) Atmospheric, oceanic, and hydrological contributions to seasonal variations in length of day. *Journal of Geodesy* 75: 137–150.

Höpfner J (2004) Low-frequency variations, Chandler and annual wobbles of polar motion as observed over one century. *Surveys in Geophysics* 25: 1–54.

Hough SS (1895) The oscillations of a rotating ellipsoidal shell containing fluid. *Philosophical Transactions of the Royal Society London A* 186: 469–506.

Hulot G, Le Huy M, and Le Mouël J-L (1996) Influence of core flows on the decade variations of the polar motion. *Geophysical and Astrophysical Fluid Dynamics* 82: 35–67.

Jackson A (1997) Time-dependency of tangentially geostrophic core surface motions. *Physics of Earth and Planetary Interiors* 103: 293–311.

Jackson A, Bloxham J, and Gubbins D (1993) Time-dependent flow at the core surface and conservation of angular momentum in the coupled core–mantle system. In: Le Moüel J-L, Smylie DE, and Herring T (eds.) *Dynamics of the Earth's Deep Interior and Earth Rotation*, American Geophysical Union Geophysical Monograph Series, vol. 72, pp. 97–107. Washington, DC: American Geophysical Union.

James TS and Ivins ER (1995) Present-day Antarctic ice mass changes and crustal motion. *Geophysical Research Letters* 22(8): 973–976.

James TS and Ivins ER (1997) Global geodetic signatures of the Antarctic ice sheet. *Journal of Geophysical Research* 102(B1): 605–633.

Jault D (2003) Electromagnetic and topographic coupling and LOD variations. In: Jones CA, Soward AM, and Zhang K (eds.) *Earth's core and lower mantle*, pp. 56–76. London: Taylor & Francis.

Jault D and Le Mouël J-L (1989) The topographic torque associated with tangentially geostrophic motion at the core surface and inferences on the flow inside the core. *Geophysical and Astrophysical Fluid Dynamics* 48: 273–296.

Jault D and Le Mouël J-L (1990) core–mantle boundary shape: Constraints inferred from the pressure torque acting between the core and the mantle. *Geophysical Journal International* 101: 233–241.

Jault D and Le Mouël J-L (1991) Exchange of angular momentum between the core and the mantle. *Journal of Geomagnetism and Geoelectricity* 43: 111–129.

Jault D and Le Mouël J-L (1993) Circulation in the liquid core and coupling with the mantle. *Advances in Space Research* 13(11): 221–233.

Jault D and Le Mouël J-L (1999) Comment on ''On the dynamics of topographical core-mantle coupling'' by Weijia Kuang and Jeremy Bloxham. *Physics of Earth and Planetary Interiors* 114: 211–215.

Jault D, Gire C, and Le Mouël J-L (1988) Westward drift, core motions and exchanges of angular momentum between core and mantle. *Nature* 333: 353–356.

Jault D, Hulot G, and Le Mouël J-L (1996) Mechanical core–mantle coupling and dynamo modelling. *Physics of Earth and Planetary Interiors* 98: 187–191.

Jeffreys H (1928) Possible tidal effects on accurate time keeping. *Monthly Notices of the Royal Astronomical Society Geophysical Supplement* 2: 56–58.

Jeffreys H (1972) The variation of latitude. In: Melchior P and Yumi S (eds.) *Rotation of the Earth*, Int. Astron. Union Symp. No. 48, pp. 39–42. Dordrecht, Holland: D. Reidel.

Jochmann H (1989) Motion of the Earth's inner core and related variations of polar motion and the rotational velocity. *Astronomische Nachrichten* 310: 435–442.

Johnson TJ (2005) The interannual spectrum of the atmosphere and oceans. In: Plag H-P, Chao BF, Gross RS, and van Dam T (eds.) *Forcing of Polar Motion in the Chandler Frequency Band: A Contribution to Understanding Interannual Climate Change,* Cahiers du Centre Européen de Géodynamique et de Séismologie, vol. 24, pp. 69–75. Luxembourg: Cahiers du Centre Européen de Géodynamique et de Séismologie.

Johnson TJ, Wilson CR, and Chao BF (1999) Oceanic angular momentum variability estimated from the Parallel Ocean Climate Model, 1988–1998. *Journal of Geophysical Research* 104(B11): 25183–25195.

Johnson TJ, Luzum BJ, and Ray JR (2005) Improved near-term Earth rotation predictions using atmospheric angular momentum analysis and forecasts. *Journal of Geodynamics* 39: 209–221.

Johnston P and Lambeck K (1999) Postglacial rebound and sea level contributions to changes in the geoid and the Earth's rotation axis. *Geophysical Journal International* 136: 537–558.

Jordi C, Morrison LV, Rosen RD, Salstein DA, and Rosselló G (1994) Fluctuations in the Earth's rotation since 1830 from high-resolution astronomical data. *Geophysical Journal International* 117: 811–818.

Kantha LH, Stewart JS, and Desai SD (1998) Long-period lunar fortnightly and monthly ocean tides. *Journal of Geophysical Research* 103(C6): 12639–12647.

King NE and Agnew DC (1991) How large is the retrograde annual wobble? *Geophysical Research Letters* 18(9): 1735–1738.

Kinoshita H, Nakajima K, Kubo Y, Nakagawa I, Sasao T, and Yokoyama K (1979) Note on nutation in ephemerides. *Publications of the International Latitude Observatory of Mizusawa* 12(2): 71–108.

Kolaczek B, Kosek W, and Schuh H (2000a) Short-period oscillations of Earth rotation. In: Dick S, McCarthy D, and Luzum B (eds.) *Polar Motion: Historical and Scientific Problems, IAU Colloq. 178*, Astron. Soc. Pacific Conf. Ser, vol. 208, pp. 533–544. San Francisco: Astronomical Society of Pacific.

Kolaczek B, Nuzhdina M, Nastula J, and Kosek W (2000b) El Niño impact on atmospheric polar motion excitation. *Journal of Geophysical Research* 105(B2): 3081–3087.

Kolaczek B, Nastula J, and Salstein D (2003) El Nino-related variations in atmosphere-polar motion interactions. *Journal of Geodynamics* 36: 397–406.

Kosek W, Nastula J, and Kolaczek B (1995) Variability of polar motion oscillations with periods from 20 to 150 days in 1979–1991. *Bulletin Géodesique* 69: 308–319.

Kouba J (2005) Comparison of polar motion with oceanic and atmospheric angular momentum time series for 2-day to Chandler periods. *Journal of Geodesy* 79: 33–42.

Kouba J and Vondrák J (2005) Comparison of length of day with oceanic and atmospheric angular momentum series. *Journal of Geodesy* 79: 256–268.

Kuang W and Bloxham J (1997) On the dynamics of topographical core–mantle coupling. *Physics of Earth and Planetary Interiors* 99: 289–294.

Kuang W and Chao B (2001) Topographic core–mantle coupling in geodynamo modeling. *Geophysical Research Letters* 28(9): 1871–1874.

Kuehne J and Wilson CR (1991) Terrestrial water storage and polar motion. *Journal of Geophysical Research* 96(B3): 4337–4345.

Kuehne J, Johnson S, and Wilson CR (1993) Atmospheric excitation of nonseasonal polar motion. *Journal of Geophysical Research* 98(B11): 19973–19978.

Kuehne J, Wilson CR, and Johnson S (1996) Estimates of the Chandler wobble frequency and *Q. Journal of Geophysical Research* 101(B6): 13573–13579.

Lambeck K (1980) *The Earth's Variable Rotation: Geophysical Causes and Consequences*. New York: Cambridge University Press.

Lambeck K (1988) *Geophysical Geodesy: The Slow Deformations of the Earth*. New York: Oxford University Press.

Lambert SB, Bizouard C, and Dehant V (2006) Rapid variations in polar motion during the 2005–2006 winter season. *Geophysical Research Letters* 33: L13303 (doi:10.1029/2006GL026422).

Langley RB, King RW, and Shapiro II (1981a) Earth rotation from lunar laser ranging. *Journal of Geophysical Research* 86: 11913–11918.

Langley RB, King RW, Shapiro II, Rosen RD, and Salstein DA (1981b) Atmospheric angular momentum and the length of the day: A common fluctuation with a period near 50 days. *Nature* 294: 730–733.

Leick A (2003) *GPS Satellite Surveying*. New York: Wiley.

Lerch FJ, Nerem RS, Putney BH, *et al.* (1994) A geopotential model from satellite tracking, altimeter, and surface gravity data: GEM-T3. *Journal of Geophysical Research* 99(B2): 2815–2839.

Leuliette EW and Wahr JM (2002) Climate excitation of polar motion. In: Adám J and Schwarz K-P (eds.) *Vistas for Geodesy in the New Millennium*, IAG Symposia, vol. 125, pp. 428–433. New York: Springer.

Li Z (1985) Earth rotation from optical astrometry, 1962.0–1982.0. In: *Bureau International de l'Heure Annual Report for 1984*, pp. D31–D63. Paris: Observation de Paris.

Li Z and Feissel M (1986) Determination of the Earth rotation parameters from optical astrometry observations, 1962.0–1982.0. *Bulletin Géodesique* 60: 15–28.

Liao D-C (2005) A brief review of atmospheric and oceanic excitation of the Chandler wobble. In: Plag H-P, Chao BF, Gross RS, and van Dam T (eds.) *Forcing of Polar Motion in the Chandler Frequency Band: A Contribution to Understanding Interannual Climate Change,* Cahiers du Centre Européen de Géodynamique et de Séismologie, vol. 24, pp. 155–162. Luxembourg: Cahiers du Centre Européen de Géodynamique et de Séismologie.

Liao DC and Greiner-Mai H (1999) A new ΔLOD series in monthly intervals (1892.0–1997.0) and its comparison with other geophysical results. *Journal of Geodesy* 73: 466–477.

Liao D, Liao X, and Zhou Y (2003) Oceanic and atmospheric excitation of the Chandler wobble. *Geophysical Journal International* 152: 215–227.

Lichten SM, Marcus SL, and Dickey JO (1992) Sub-daily resolution of Earth rotation variations with global positioning system measurements. *Geophysical Research Letters* 19(6): 537–540.

Love JJ and Bloxham J (1994) Electromagnetic coupling and the toroidal magnetic field at the core–mantle boundary. *Geophysical Journal International* 117: 235–256.

Luzum BJ, Ray JR, Carter MS, and Josties FJ (2001) Recent improvements to IERS Bulletin A combination and prediction. *GPS Solutions* 4(3): 34–40.

Malla RP, Wu SC, and Lichten SM (1993) Geocenter location and variations in Earth orientation using global positioning system measurements. *Journal of Geophysical Research* 98(B3): 4611–4617.

Madden RA (1987) Relationships between changes in the length of day and the 40- to 50-day oscillations in the tropics. *Journal of Geophysical Research* 92: 8391–8399.

Madden RA and Julian PR (1971) Detection of a 40–50 day oscillation in the zonal wind in the tropical Pacific. *Journal of Atmospheric Science* 28: 702–708.

Madden RA and Julian PR (1972) Description of global-scale circulation cells in the tropics with a 40–50 day period. *Journal of Atmospheric Science* 29: 1109–1123.

Madden RA and Julian PR (1994) Observations of the 40–50-day tropical oscillation — A review. *Monthly Weather Review* 122: 814–837.

Marcus SL, Chao Y, Dickey JO, and Gegout P (1998) Detection and modeling of nontidal oceanic effects on Earth's rotation rate. *Science* 281: 1656–1659.

Marcus SL, Dickey JO, and de Viron O (2001) Links between intraseasonal (extended MJO) and ENSO timescales: Insights via geodetic and atmospheric analysis. *Geophysical Research Letters* 28(18): 3465–3468.

Markowitz W (1955) The annual variation in the rotation of the Earth, 1951–54. *Astronomical Journal* 60: 171.

Markowitz W (1959) Variations in rotation of the Earth, results obtained with the dual-rate Moon camera and photographic zenith tubes. *Astronomical Journal* 64: 106–113.

Markowitz W (1960) Latitude and longitude, and the secular motion of the pole. In: Runcorn SK (ed.) *Methods and Techniques in Geophysics*, pp. 325–361. New York: Interscience Publishers.

Markowitz W (1961) International determination of the total motion of the pole. *Bulletin Géodesique* 59: 29–41.

Marsh JG, Lerch FJ, Putney BH, *et al.* (1990) The GEM-T2 gravitational model. *Journal of Geophysical Research* 95(B13): 22043–22071.

Marsh JG, Lerch FJ, Putney BH, *et al.* (1991) Correction to ''The GEM-T2 gravitational model''. *Journal of Geophysical Research* 96(B10): 16651.

Martin CF (1969) *A Study of the Rate of Rotation of the Earth from Occultations of Stars by the Moon 1627–1860.* PhD Thesis, 144p. Yale University, New Haven.

Mathews PM and Bretagnon P (2003) Polar motions equivalent to high frequency nutations for a nonrigid Earth with anelastic mantle. *Astronomy and Astrophysics* 400: 1113–1128.

Mathews PM, Buffett BA, Herring TA, and Shapiro II (1991) Forced nutations of the Earth: Influence of inner core dynamics 2. Numerical results and comparisons. *Journal of Geophysical Research* 96: 8243–8257.

McCarthy DD (1976) The determination of Universal Time at the U.S. Naval Observatory. *U.S. Naval Obs. Circ.*, No. 154.

McCarthy DD and Babcock AK (1986) The length of day since 1656. *Physics of Earth and Planetary Interiors* 44: 281–292.

McCarthy DD and Luzum BJ (1993) An analysis of tidal variations in the length of day. *Geophysical Journal International* 114: 341–346.

McCarthy DD and Luzum BJ (1996) Path of the mean rotational pole from 1899 to 1994. *Geophysical Journal International* 125: 623–629.

McCarthy DD and Petit G (eds.) (2004) *IERS Conventions* (2003). IERS Tech. Note no. 32, 127p. Frankfurt, Germany: Bundesamts für Kartographie und Geodäsie.

Melchior P and Dejaiffe R (1969) Calcul des déclinaisons et mouvements propres des étoiles du Service International des Latitudes à partir des catalgues méridiens. *Annales Observatoire Royal de Belgique 3e Serie* 10: 63–339.

Merriam JB (1980) Zonal tides and changes in the length of day. *Geophysical Journal of the Royal Astronomical Society* 62: 551–561.

Merriam JB (1982) Meteorological excitation of the annual polar motion. *Geophysical Journal of the Royal Astronomical Society* 70: 41–56.

Merriam JB (1984) Tidal terms in Universal Time: Effects of zonal winds and mantle Q. *Journal of Geophysical Research* 89(B12): 10109–10114.

Merriam JB (1985) LAGEOS and UT measurements of long-period Earth tides and mantle Q. *Journal of Geophysical Research* 90(B11): 9423–9430.

Mitrovica JX and Forte AM (1997) Radial profile of mantle viscosity: Results from the joint inversion of convection and postglacial rebound observables. *Journal of Geophysical Research* 102(B2): 2751–2769.

Mitrovica JX and Milne GA (1998) Glaciation-induced perturbations in the Earth's rotation: A new appraisal. *Journal of Geophysical Research* 103(B1): 985–1005.

Mitrovica JX and Peltier WR (1993) Present-day secular variations in the zonal harmonics of Earth's geopotential. *Journal of Geophysical Research* 98(B3): 4509–4526.

Mitrovica JX, Wahr J, Matsuyama I, and Paulson A (2005) The rotational stability of an ice-age Earth. *Geophysical Journal International* 161: 491–506.

Moritz H and Mueller II (1988) *Earth Rotation: Theory and Observation*. New York: Ungar.

Morrison LV (1978) Catalogue of observations of occultations of stars by the Moon for the years 1943 to 1971. *Royal Greenwich Observatory Bulletin* No.183.

Morrison LV (1979) Re-determination of the decade fluctuations in the rotation of the Earth in the period 1861–1978. *Geophysical Journal of the Royal Astronomical Society* 58: 349–360.

Morrison LV and Stephenson FR (2001) Historical eclipses and the variability of the Earth's rotation. *Journal of Geodynamics* 32: 247–265.

Morrison LV and Ward CG (1975) An analysis of the transits of Mercury: 1677–1973. *Monthly Notices of the Royal Astronomical Society* 173: 183–206.

Morrison LV, Lukac MR, and Stephenson FR (1981) Catalogue of observations of occultations of stars by the Moon for the years 1623–1942 and solar eclipses for the years 1621–1806. *Royal Greenwich Observatory Bulletin* No.186.

Mound J (2005) Electromagnetic torques in the core and resonant excitation of decadal polar motion. *Geophysical Journal International* 160: 721–728.

Mound JE and Buffett BA (2003) Interannual oscillations in length of day: Implications for the structure of the mantle and core. *Journal of Geophysical Research* 108(B7): 2334 (doi:10.1029/2002JB002054).

Mound JE and Buffett BA (2005) Mechanisms of core–mantle angular momentum exchange and the observed spectral properties of torsional oscillations. *Journal of Geophysical Research* 110: B08103 (doi:10.1029/2004JB003555).

Mulholland JD (1980) Scientific advances from ten years of lunar laser ranging. *Reviews of Geophysics and Space Physics* 18: 549–564.

Munk WH and MacDonald GJF (1960) *The Rotation of the Earth: A Geophysical Discussion*. New York: Cambridge University Press.

Naito I and Kikuchi N (1990) A seasonal budget of the Earth's axial angular momentum. *Geophysical Research Letters* 17: 631–634.

Naito I and Kikuchi N (1991) Reply to Rosen and Salstein's comment. *Geophysical Research Letters* 18: 1927–1928.

Nakada M (2000) Effect of the viscoelastic lithosphere on polar wander speed caused by the Late Pleistocene glacial cycles. *Geophysical Journal International* 143: 230–238.

Nakada M (2002) Polar wander caused by the Quaternary glacial cycles and fluid Love number. *Earth and Planetary Science Letters* 200: 159–166.

Nakada M and Okuno J (2003) Perturbations of the Earth's rotation and their implications for the present-day mass balance of both polar ice caps. *Geophysical Journal International* 152: 124–138.

Nam YS and Dickman SR (1990) Effects of dynamic long-period ocean tides on changes in Earth's rotation rate. *Journal of Geophysical Research* 95(B5): 6751–6757.

Nastula J (1992) Short periodic variations in the Earth's rotation in the period 1984–1990. *Annales Geophysicae* 10: 441–448.

Nastula J (1995) Short periodic variations of polar motion and hemispheric atmospheric angular momentum excitation functions in the period 1984–1992. *Annales Geophysicae* 13: 217–225.

Nastula J (1997) The regional atmospheric contributions to the polar motion and EAAM excitation functions. In: Segawa J, Fujimoto H, and Okubo S (eds.) *Gravity*, *Geoid*, *and Marine Geodesy*, IAG Symposia, vol. 117, pp. 281–288. New York: Springer.

Nastula J and Kolaczek B (2002) Seasonal oscillations in regional and global atmospheric excitation of polar motion. *Advances in Space Research* 30(2): 381–386.

Nastula J and Kolaczek B (2005) Analysis of hydrological excitation of polar motion. In: Plag H-P, Chao BF, Gross RS, and van Dam T (eds.) *Forcing of Polar Motion in the Chandler Frequency Band: A Contribution to Understanding Interannual Climate Change,* Cahiers du Centre Européen de Géodynamique et de Séismologie, vol. 24, pp. 149–154. Luxembourg: Cahiers du Centre Européen de Géodynamique et de Séismologie.

Nastula J and Ponte RM (1999) Further evidence for oceanic excitation of polar motion. *Geophysical Journal International* 139: 123–130.

Nastula J and Salstein D (1999) Regional atmospheric angular momentum contributions to polar motion excitation. *Journal of Geophysical Research* 104: 7347–7358.

Nastula J, Gambis D, and Feissel M (1990) Correlated high-frequency variations in polar motion and length of the day in early 1988. *Annales Geophysical* 8: 565–570.

Nastula J, Ponte RM, and Salstein DA (2000) Regional signals in atmospheric and oceanic excitation of polar motion. In: Dick S, McCarthy D, and Luzum B (eds.) *Polar Motion: Historical and Scientific Problems, IAU Colloq. 178*, Astron. Soc. Pacific Conf. Ser, vol. 208, pp. 463–472. San Francisco: Astronomical Society of Pacific.

Nastula J, Salstein DA, and Ponte RM (2003) Empirical patterns of variability in atmospheric and oceanic excitation of polar motion. *Journal of Geodynamics* 36: 383–396.

Newhall XX, Williams JG, and Dickey JO (1988) Earth rotation from lunar laser ranging. In: Babcock AK and Wilkins GA (eds.) *The Earth's Rotation and Reference Frames for Geodesy and Geodynamics*, pp. 159–164. Dordrecht, Holland: D. Reidel.

Okamoto I and Kikuchi N (1983) Low frequency variations of homogeneous ILS polar motion data. *Publications of the International Latitude Observatory of Mizusawa* 16: 35–40.

Ooe M (1978) An optimal complex ARMA model of the Chandler wobble. *Geophysical Journal of the Royal Astronomical Society* 53: 445–457.

Pais A and Hulot G (2000) Length of day decade variations, torsional oscillations, and inner core superrotation: Evidence from recovered core surface zonal flows. *Physics of Earth and Planetary Interiors* 118: 291–316.

Pais MA, Oliveira O, and Nogueira F (2004) Nonuniqueness of inverted core-mantle boundary flows and deviations from tangential geostrophy. *Journal of Geophysical Research* 109: B8105 (doi:10.1029/2004JB003012).

Pearlman MR, Degnan JJ, and Bosworth JM (2002) The International Laser Ranging Service. *Advances in Space Research* 30(2): 135–143.

Pearlman M, Noll C, Dunn P, *et al.* (2005) The International Laser Ranging Service and its support for IGGOS. *Journal of Geodynamics* 40: 470–478.

Peltier WR (1988) Global sea level and Earth rotation. *Science* 240: 895–901.

Peltier WR and Jiang X (1996) Glacial isostatic adjustment and Earth rotation: Refined constraints on the viscosity of the deepest mantle. *Journal of Geophysical Research* 101(B2): 3269–3290.

Philander SG (1990) *El Niño, La Niña, and the Southern Oscillation*. San Diego, CA: Academic Press.

Ponsar S, Dehant V, Holme R, Jault D, Pais A, and Van Hoolst T (2003) The core and fluctuations in the Earth's rotation. In: Dehant V, Creager KC, Karato S, and Zatman S (eds.) *Earth's Core: Dynamics, Structure, Rotation*, American Geophysical Union Geodynamics Series, vol. 31, pp. 251–261. Washington, DC: American Geophysical Union.

Ponte RM (1997) Oceanic excitation of daily to seasonal signals in Earth rotation: Results from a constant-density numerical model. *Geophysical Journal International* 130: 469–474.

Ponte RM (2005) What do we know about low frequency signals in ocean angular momentum? In: Plag H-P, Chao BF, Gross RS, and van Dam T (eds.) *Forcing of Polar Motion in the Chandler Frequency Band: A Contribution to Understanding Interannual Climate Change, Cahiers du Center Européen de Géodynamique et de Séismologie*, vol. 24, pp. 77–82. Luxembourg: Cahiers du Center Européen de Géodynamique et de Séismologie.

Ponte RM and Ali AH (2002) Rapid ocean signals in polar motion and length of day. *Geophysical Research Letters* 29(15): 1711 (10.1029/2002GL015312).

Ponte RM and Stammer D (1999) Role of ocean currents and bottom pressure variability on seasonal polar motion. *Journal of Geophysical Research* 104: 23393–23409.

Ponte RM and Stammer D (2000) Global and regional axial ocean angular momentum signals and length-of-day variations (1985–1996). *Journal of Geophysical Research* 105: 17161–17171.

Ponte RM, Stammer D, and Marshall J (1998) Oceanic signals in observed motions of the Earth's pole of rotation. *Nature* 391: 476–479.

Ponte RM, Stammer D, and Wunsch C (2001) Improving ocean angular momentum estimates using a model constrained by data. *Geophysical Research Letters* 28: 1775–1778.

Ponte RM, Rajamony J, and Gregory JM (2002) Ocean angular momentum signals in a climate model and implications for Earth rotation. *Climate Dynamics* 19: 181–190.

Ray RD (1994) Tidal energy dissipation: Observations from astronomy, geodesy, and oceanography. In: Majumdar SK, Miller EW, Forbes GS, Schmalz RF, and Panah AA (eds.) *The Oceans: Physical-Chemical Dynamics and Human Impact*, pp. 171–185. Pittsburgh: Pennsylvania Academic of Science.

Ray RD, Steinberg DJ, Chao BF, and Cartwright DE (1994) Diurnal and semidiurnal variations in the Earth's rotation rate induced by oceanic tides. *Science* 264: 830–832.

Ricard Y, Sabadini R, and Spada G (1992) Isostatic deformations and polar wander induced by redistribution of mass within the Earth. *Journal of Geophysical Research* 97(B10): 14223–14236.

Ricard Y, Spada G, and Sabadini R (1993) Polar wandering of a dynamic Earth. *Geophysical Journal International* 113: 284–298.

Richards MA, Ricard Y, Lithgow-Bertelloni C, Spada G, and Sabadini R (1997) An explanantion for Earth's long-term rotational stability. *Science* 275: 372–375.

Richards MA, Bunge H-P, Ricard Y, and Baumgardner JR (1999) Polar wandering in mantle convection models. *Geophysical Research Letters* 26(12): 1777–1780.

Roberts PH (1972) Electromagnetic core–mantle coupling. *Journal of Geomagnetism and Geoelectricity* 24: 231–259.

Robertson DS (1991) Geophysical applications of very-long-baseline interferometry. *Reviews of Modern Physics* 63(4): 899–918.

Robertson DS, Ray JR, and Carter WE (1994) Tidal variations in UT1 observed with very long baseline interferometry. *Journal of Geophysical Research* 99(B1): 621–636.

Rochester MG (1960) Geomagnetic westward drift and irregularities in the Earth's rotation. *Philosophical Transactions of the Royal Society of London A* 252: 531–555.

Rochester MG (1962) Geomagnetic core–mantle coupling. *Journal of Geophysical Research* 67: 4833–4836.

Rochester MG (1984) Causes of fluctuations in the rotation of the Earth. *Philosophical Transactions of the Royal Society of London A* 313: 95–105.

Roden RB (1963) Electromagnetic core–mantle coupling. *Geophysical Journal of the Royal Astronomical Society* 7: 361–374.

Rosen RD (1993) The axial momentum balance of Earth and its fluid envelope. *Surveys in Geophysics* 14: 1–29.

Rosen RD and Salstein DA (1985) Contribution of stratospheric winds to annual and semi-annual fluctuations in atmospheric angular momentum and the length of day. *Journal of Geophysical Research* 90: 8033–8041.

Rosen RD and Salstein DA (1991) Comment on ''A seasonal budget of the Earth's axial angular momentum'' by Naito and Kikucho. *Geophysical Research Letters* 18: 1925–1926.

Rosen RD, Salstein DA, Eubanks TM, Dickey JO, and Steppe JA (1984) An El Niño signal in atmospheric angular momentum and Earth rotation. *Science* 225: 411–414.

Rothacher M, Beutler G, Weber R, and Hefty J (2001) High-frequency variations in Earth rotation from global positioning system data. *Journal of Geophysical Research* 106(B7): 13711–13738.

Rubincam DP (2003) Gravitational core-mantle coupling and the acceleration of the Earth. *Journal of Geophysical Research* 108(B7): 2338 (doi:10.1029/2002JB002132).

Sabadini R and Vermeersen BLA (2002) Long-term rotation instabilities of the Earth: A Reanalysis. In: Mitrovica JX and Vermeersen BLA (eds.) *Ice Sheets, Sea Level and the Dynamic Earth*, American Geophysical Union Geodynamics Series, vol. 29, pp. 51–67. Washington, DC: American Geophysical Union.

Sabadini R and Vermeersen B (2004) *Global Dynamics of the Earth: Applications of Normal Mode Relaxation Theory to Solid-Earth Geophysics*. Dordrecht, The Netherlands: Kluwer.

Salstein DA (1993) Monitoring atmospheric winds and pressures for Earth orientation studies. *Advances in Space Research* 13(11): 175–184.

Salstein DA and Rosen RD (1986) Earth rotation as a proxy for interannual variability in atmospheric circulation, 1860-present. *Journal of Climate and Applied Meteorology* 25: 1870–1877.

Salstein DA and Rosen RD (1989) Regional contributions to the atmospheric excitation of rapid polar motions. *Journal of Geophysical Research* 94: 9971–9978.

Schastok J, Soffel M, and Ruder H (1994) A contribution to the study of fortnightly and monthly zonal tides in UT1. *Astronomy and Astrophysics* 283: 650–654.

Schreiber KU, Velikoseltsev A, Rothacher M, Klügel T, Stedman GE, and Wiltshire DL (2004) Direct measurment of diurnal polar motion by ring laser gyroscopes. *Journal of Geophysical Research* 109: B06405 (doi:10.1029/2003JB002803).

Schlüter W, Himwich E, Nothnagel A, Vandenberg N, and Whitney A (2002) IVS and its important role in the maintenance of the global reference systems. *Advances in Space Research* 30(2): 145–150.

Schuh H and Schmitz-Hübsch H (2000) Short period variations in Earth rotation as seen by VLBI. *Surveys in Geophysics* 21: 499–520.

Schuh H, Richter B, and Nagel S (2000) Analaysis of long time series of polar motion. In: Dick S, McCarthy D, and Luzum B (eds.) *Polar Motion: Historical and Scientific Problems, IAU Colloq. 178*, Astron. Soc. Pacific Conf. Ser, vol. 208, pp. 321–331. San Francisco: Astronomical Society of Pacific.

Schuh H, Nagel S, and Seitz T (2001) Linear drift and periodic variations observed in long time series of polar motion. *Journal of Geodesy* 74: 701–710.

Segschneider J and Sündermann J (1997) Response of a global circulation model to real-time forcing and implications to Earth's rotation. *Journal of Physical Oceanography* 27: 2370–2380.

Seidelmann PK (1982) 1980 IAU theory of nutation: The final report of the IAU working group on nutations. *Celestial Mechanics* 27: 79–106.

Seidelmann PK, Guinot B, and Doggett LE (1992) Time. In: Seidelmann PK (ed.) *Explanatory Supplement to the Astronomical Almanac*, pp. 39–93. Mill Valley, CA: University Science Books.

Seiler U (1990) Variations of the angular momentum budget for tides of the present ocean. In: Brosche P and Sündermann J (eds.) *Earth's Rotation from Eons to Days*, pp. 81–94. New York: Springer.

Seiler U (1991) Periodic changes of the angular momentum budget due to the tides of the world ocean. *Journal of Geophysical Research* 96(B6): 10287–10300.

Seiler U and Wünsch J (1995) A refined model for the influence of ocean tides on UT1 and polar motion. *Astronomische Nachrichten* 316: 419–423.

Seitz F and Schmidt M (2005) Atmospheric and oceanic contributions to Chandler wobble excitation determined by wavelet filtering. *Journal of Geophysical Research* 110: B11406 (doi:10.1029/2005JB003826).

Seitz F, Stuck J, and Thomas M (2004) Consistent atmospheric and oceanic excitation of the Earth's free polar motion. *Geophysical Journal International* 157: 25–35.

Seitz F, Stuck J, and Thomas M (2005) White noise Chandler wobble excitation. In: Plag H-P, Chao BF, Gross RS, and van Dam T (eds.) *Forcing of Polar Motion in the Chandler Frequency Band: A Contribution to Understanding Interannual Climate Change,* Cahiers du Centre Européen de Géodynamique et de Séismologie, vol. 24, pp. 15–21. Luxembourg: Cahiers du Centre Européen de Géodynamique et de Séismologie.

Shelus PJ (2001) Lunar laser ranging: Glorious past and a bright future. *Surveys in Geophysics* 22: 517–535.

Simon JL, Bretagnon P, Chapront J, Chapront-Touzé M, Francou G, and Laskar J (1994) Numerical expressions for precession formulae and mean elements for the Moon and the planets. *Astronomy and Astrophysics* 282: 663–683.

Smith DE, Christodoulidis DC, Kolenkiewicz R, *et al.* (1985) A global geodetic reference frame from LAGEOS ranging (SL5.1AP). *Journal of Geophysical Research* 90: 9221–9233.

Smith DE, Kolenkiewicz R, Dunn PJ, *et al.* (1990) Tectonic motion and deformation from satellite laser ranging to LAGEOS. *Journal of Geophysical Research* 95: 22013–22041.

Smith DE, Kolenkiewicz R, Nerem RS, *et al.* (1994) Contemporary global horizontal crustal motion. *Geophysical Journal International* 119: 511–520.

Smith ML and Dahlen FA (1981) The period and Q of the Chandler wobble. *Geophysical Journal of the Royal Astronomical Society* 64: 223–281.

Souriau A and Cazenave A (1985) Re-evaluation of the seismic excitation of the Chandler wobble from recent data. *Earth and Planetary Science Letters* 75: 410–416.

Sovers OJ, Jacobs CS, and Gross RS (1993) Measuring rapid ocean tidal Earth orientation variations with very long baseline interferometry. *Journal of Geophysical Research* 98(B11): 19959–19971.

Sovers OJ, Fanselow JL, and Jacobs CS (1998) Astrometry and geodesy with radio interferometry: Experiments, models, results. *Reviews of Modern Physics* 70(4): 1393–1454.

Spada G, Ricard Y, and Sabadini R (1992) Excitation of true polar wander by subduction. *Nature* 360: 452–454.

Spencer Jones H (1939) The rotation of the Earth and the secular acceleration of the Sun, Moon, and planets. *Monthly Notices of the Royal Astronomical Society* 99: 541–558.

Stedman GE (1997) Ring-laser tests of fundamental physics and geophysics. *Reports on Progress in Physics* 60: 615–688.

Stefanick M (1982) Interannual atmospheric angular momentum variability 1963–1973 and the southern oscillation. *Journal of Geophysical Research* 87: 428–432.

Steigenberger P, Rothacher M, Dietrich R, Fritsche M, Rülke A, and Vey S (2006) Reprocessing of a global GPS network. *Journal of Geophysical Research* 111: B05402 (doi:10.1029/2005JB003747).

Steinberger BM and O'Connell RJ (1997) Changes of the Earth's rotation axis inferred from advection of mantle density heterogeneities. *Nature* 387: 169–173.

Steinberger B and O'Connell RJ (2002) The convective mantle flow signal in rates of true polar wander. In: Mitrovica JX and Vermeersen BLA (eds.) *Ice Sheets, Sea Level and the Dynamic Earth*, American Geophysical Union Geodynamics Series, vol. 29, pp. 233–256. Washington, DC: American Geophysical Union.

Stephenson FR (1997) *Historical Eclipses and Earth's Rotation*. New York: Cambridge University Press.

Stephenson FR and Morrison LV (1984) Long-term changes in the rotation of the Earth: 700 B.C. to A.D. 1980. *Philosophical Transactions of the Royal Society London* A 313: 47–70.

Stephenson FR and Morrison LV (1995) Long-term fluctuations in the Earth's rotation: 700 BC to AD 1990. *Philosophical Transactions of the Royal Society London* A 351: 165–202.

Stewart DN, Busse FH, Whaler KA, and Gubbins D (1995) Geomagnetism, Earth rotation and the electrical conductivity of the lower mantle. *Physics of Earth and Planetary Interiors* 92: 199–214.

Stieglitz TC and Dickman SR (1999) Refined correlations between atmospheric and rapid polar motion excitation. *Geophysical Journal International* 139: 115–122.

Stix M and Roberts PH (1984) Time-dependent electromagnetic core-mantle coupling. *Physics of Earth and Planetary Interiors* 36: 49–60.

Stolz A, Bender PL, Faller JE, *et al.* (1976) Earth rotation measured by lunar laser ranging. *Science* 193: 997–999.

Stoyko N (1937) Sur la périodicité dans l'irrégularité de la rotation de la terre. *Comptes Rendus De L Academie Des Sciences* 205: 79–81.

Stuck J, Seitz F, and Thomas M (2005) Atmospheric forcing mechanisms of polar motion. In: Plag H-P, Chao BF, Gross RS, and van Dam T (eds.) *Forcing of Polar Motion in the Chandler Frequency Band: A Contribution to Understanding Interannual Climate Change,* Cahiers du Centre Européen de Géodynamique et de Séismologie, vol. 24, pp. 127–133. Luxembourg: Cahiers du Centre Européen de Géodynamique et de Séismologie.

Tamisea ME, Mitrovica JX, Tromp J, and Milne GA (2002) Present-day secular variations in the low-degree harmonics of the geopotential: Sensitivity analysis on spherically symmetric Earth models. *Journal of Geophysical Research* 107(B12): 2378 (doi:10.1029/2001JB000696).

Tapley BD, Schutz BE, and Eanes RJ (1985) Station coordinates, baselines, and Earth rotation from LAGEOS laser

ranging: 1976-1984. *Journal of Geophysical Research* 90: 9235–9248.

Tapley BD, Schutz BE, Eanes RJ, Ries JC, and Watkins MM (1993) Lageos laser ranging contributions to geodynamics, geodesy, and orbital dynamics. In: Smith DE and Turcotte DL (eds.) *Contributions of Space Geodesy to Geodynamics: Earth Dynamics*, American Geophysical Union Geodynamics Series, vol. 24, pp. 147–173. Washington, DC: American Geophysical Union.

Tapley BD, Schutz BE, and Born GH (2004) *Statistical Orbit Determination*. Burlington, MA: Elsevier.

Tavernier G, Fagard H, Feissel-Vernier M, *et al.* (2005) The International DORIS Service (IDS). *Advances in Space Research* 36(3): 333–341.

Thomas M, Dobslaw H, Stuck J, and Seitz F (2005) The ocean's contribution to polar motion excitation – As many solutions as numerical models? In: Plag H-P, Chao BF, Gross RS, and van Dam T (eds.) *Forcing of Polar Motion in the Chandler Frequency Band: A Contribution to Understanding Interannual Climate Change*, Cahiers du Centre Européen de Géodynamique et de Séismologie, vol. 24, pp. 143–148 Luxembourg: Cahiers du Centre Européen de Géodynamique et de Séismologie.

Tisserand F (1891) *Traité de Mécanique Céleste*, vol. II. Paris: Gauthier-Villars.

Trenberth KE and Guillemot CJ (1994) The total mass of the atmosphere. *Journal of Geophysical Research* 99(D11): 23079–23088.

Tosi N, Sabadini R, Marotta AM, and Vermeersen LLA (2005) Simultaneous inversion for the Earth's mantle viscosity and ice mass imbalance in Antarctica and Greenland. *Journal of Geophysical Research* 110: B07402 (doi:10.1029/2004JB003236).

Trupin AS (1993) Effects of polar ice on the Earth's rotation and gravitational potential. *Geophysical Journal International* 113: 273–283.

Trupin AS, Meier MF, and Wahr JM (1992) Effect of melting glaciers on the Earth's rotation and gravitational field: 1965–1984. *Geophysical Journal International* 108: 1–15.

Van Hoolst T and Dehant V (2002) Influence of triaxiality and second-order terms in flattenings on the rotation of terrestrial planets I. Formalism and rotational normal modes. *Physics of Earth and Planetary Interiors* 134: 17–33.

Vermeersen LLA and Sabadini R (1996) Significance of the fundamental mantle rotational relaxation mode in polar wander simulations. *Geophysical Journal International* 127: F5–F9.

Vermeersen LLA and Sabadini R (1999) Polar wander, sea-level variations and ice age cycles. *Surveys in Geophysics* 20: 415–440.

Vermeersen LLA and Vlaar NJ (1993) Changes in the Earth's rotation by tectonic movements. *Geophysical Research Letters* 20(2): 81–84.

Vermeersen LLA, Sabadini R, Spada G, and Vlaar NJ (1994) Mountain building and Earth rotation. *Geophysical Journal International* 117: 610–624.

Vermeersen LLA, Sabadini R, and Spada G (1996) Compressible rotational deformation. *Geophysical Journal International* 126: 735–761.

Vermeersen LLA, Fournier A, and Sabadini R (1997) Changes in rotation induced by Pleistocene ice masses with stratified analytical Earth models. *Journal of Geophysical Research* 102(B12): 27689–27702.

Vicente RO and Wilson CR (1997) On the variability of the Chandler frequency. *Journal of Geophysical Research* 102(B9): 20439–20445.

Vicente RO and Wilson CR (2002) On long-period polar motion. *Journal of Geodesy* 76: 199–208.

Volland H (1988) *Atmospheric Tidal and Planetary Waves*. Dordrecht, The Netherlands: Kluwer.

Volland H (1997) Atmospheric tides. In: Wilhelm H, Zürn W, and Wenzel H-G (eds.) *Tidal Phenomena*, Springer-Verlag Lecture Notes in Earth Sciences, vol. 66, pp. 221–246. Berlin: Springer.

Vondrák J (1977) The rotation of the Earth between 1955.5 and 1976.5. *Studia Geophysica Et Geodaetica* 21: 107–117.

Vondrák J (1985) Long-period behaviour of polar motion between 1900.0 and 1984.0. *Annales Geophysicae* 3: 351–356.

Vondrák J (1991) Calculation of the new series of the Earth orientation parameters in the HIPPARCOS reference frame. *Bulletin of the Astronomical Institutes of Czechoslovakia* 42: 283–294.

Vondrák J (1994) Secular polar motion, crustal movements, and International Latitude Service observations. *Studia Geophysica Et Geodaetica* 38: 256–265.

Vondrák J (1999) Earth rotation parameters 1899.7–1992.0 after reanalysis within the Hipparcos frame. *Surveys in Geophysics* 20(2): 169–195.

Vondrák J and Richter B (2004) International Earth Rotation and Reference Systems Service (IERS). *Journal of Geodesy* 77: 585–586.

Vondrák J, Feissel M, and Essaïfi N (1992) Expected accuracy of the 1900–1990 Earth orientation parameters in the Hipparcos reference frame. *Astronomy and Astrophysics* 262: 329–340.

Vondrák J, Ron C, Pesek I, and Cepek A (1995) New global solution of Earth orientation parameters from optical astrometry in 1900–1990. *Astronomy and Astrophysics* 297: 899–906.

Vondrák J, Ron C, and Pesek I (1997) Earth rotation in the Hipparcos reference frame. *Celestial Mechanics & Dynamical Astronomy* 66: 115–122.

Vondrák J, Pesek I, Ron C, and Cepek A (1998) *Earth Orientation Parameters 1899.7–1992.0 in the ICRS Based on the HIPPARCOS reference frame*, Publication No. 87. Ondrejov, Czech Republic: Astronomical Institute of the Academy of Sciences of the Czech Republic.

Voorhies CV and Backus GE (1985) Steady flows at the top of the core from geomagnetic field models: The steady motions theorem. *Geophysical and Astrophysical Fluid Dynamics* 32: 163–173.

Wahr JM (1981) The forced nutations of an elliptical, rotating, elastic and oceanless earth. *Geophysical Journal of the Royal Astronomical Society* 64: 705–727.

Wahr JM (1982) The effects of the atmosphere and oceans on the Earth's wobble — I. Theory. *Geophysical Journal of the Royal Astronomical Society* 70: 349–372.

Wahr JM (1983) The effects of the atmosphere and oceans on the Earth's wobble and on the seasonal variations in the length of day — II. Results. *Geophysical Journal of the Royal Astronomical Society* 74: 451–487.

Wahr J (2005) Polar motion models: Angular momentum approach. In: Plag H- P, Chao BF, Gross RS, and Van Dam T (eds.) *Forcing of Polar Motion in the Chandler Frequency Band: A Contribution to Understanding Interannual Climate Change*, Cahiers du Centre Européen de Géodynamique et de Séismologie, vol. 24, pp. 89–102. Luxembourg: Cahiers du Centre Européen de Géodynamique et de Séismologie.

Wahr J and Bergen Z (1986) The effects of mantle anelasticity on nutations, Earth tides, and tidal variations in rotation rate. *Geophysical Journal of the Royal Astronomical Society* 87: 633–668.

Wahr JM, Sasao T, and Smith ML (1981) Effect of the fluid core on changes in the length of day due to long period tides. *Geophysical Journal of the Royal Astronomical Society* 64: 635–650.

Watkins MM and Eanes RJ (1994) Diurnal and semidiurnal variations in Earth orientation determined from LAGEOS laser ranging. *Journal of Geophysical Research* 99(B9): 18073–18079.

Whaler KA (1980) Does the whole of the Earth's core convect? *Nature* 287: 528–530.

Whaler KA and Davis RG (1997) Probing the Earth's core with geomagnetism. In: Crossley DJ (ed.) *Earth's Deep Interior*, pp. 114–166. Amsterdam: Gordon and Breach.

Wicht J and Jault D (1999) Constraining electromagnetic core-mantle coupling. *Physics of Earth and Planetary Interiors* 111: 161–177.

Wicht J and Jault D (2000) Electromagnetic core-mantle coupling for laterally varying mantle conductivity. *Journal of Geophysical Research* 105(B10): 23569–23578.

Williams JG, Newhall XX, and Dickey JO (1993) Lunar laser ranging: Geophysical results and reference frames. In: Smith DE and Turcotte DL (eds.) *Contributions of Space Geodesy to Geodynamics: Earth Dynamics*, American Geophysical Union Geodynamics Series, vol. 24, pp. 83–88. Washington, DC: American Geophysical Union.

Williams JG, Boggs DH, Yoder CF, Ratcliff JT, and Dickey JO (2001) Lunar rotational dissipation in solid body and molten core. *Journal of Geophysical Research* 106(E11): 27933–27968.

Willis P, Jayles C, and Bar-Sever Y (2006) DORIS: From orbit determination for altimeter missions to geodesy. *Comptes Rendus Geoscience* 338: 968–979 (doi:10.1016/j.crte.2005.11.013).

Wilson CR (1993) Contributions of water mass redistribution to polar motion excitation. In: Smith DE and Turcotte DL (eds.) *Contributions of Space Geodesy to Geodynamics: Earth Dynamics*, American Geophysical Union Geodynamics Series, vol. 24, pp. 77–82. Washington, DC: American Geophysical Union.

Wilson CR and Chen J (2005) Estimating the period and Q of the Chandler wobble. In: Plag H-P, Chao BF, Gross RS, and van Dam T (eds.) *Forcing of Polar Motion in the Chandler Frequency Band: A Contribution to Understanding Interannual Climate Change*, Cahiers du Centre Européen de Géodynamique et de Séismologie, vol. 24, pp. 23–29. Luxembourg: Cahiers du Centre Européen de Géodynamique et de Séismologie.

Wilson CR and Gabay S (1981) Excitation of the Earth's polar motion: A reassessment with new data. *Geophysical Research Letters* 8: 745–748.

Wilson CR and Haubrich RA (1976) Meteorological excitation of the Earth's wobble. *Geophysical Journal of the Royal Astronomical Society* 46: 707–743.

Wilson CR and Vicente RO (1980) An analysis of the homogeneous ILS polar motion series. *Geophysical Journal of the Royal Astronomical Society* 62: 605–616.

Wilson CR and Vicente RO (1990) Maximum likelihood estimates of polar motion parameters. In: McCarthy DD and Carter WE (eds.) *Variations in Earth Rotation*, American Geophysical Union Geophysical Monograph Series, vol. 59, pp. 151–155. Washington, DC: American Geophysical Union.

Wu P and Peltier WR (1984) Pleistocene deglaciation and the Earth's rotation: a new analysis. *Geophysical Journal of the Royal Astronomical Society* 76: 753–791.

Wünsch J (2000) Oceanic influence on the annual polar motion. *Journal of Geodynamics* 30: 389–399.

Wünsch J (2002) Oceanic and soil moisture contributions to seasonal polar motion. *Journal of Geodynamics* 33: 269–280.

Wünsch J and Busshoff J (1992) Improved observations of periodic UT1 variations caused by ocean tides. *Astronomy and Astrophysics* 266: 588–591.

Yan H, Zhong M, Zhu Y, Liu L, and Cao X (2006) Nontidal oceanic contribution to length-of-day changes estimated from two ocean models during 1992–2001. *Journal of Geophysical Research* 111: B02410 (doi:10.1029/2004JB003538).

Yoder CF (1995) Astrometric and geodetic properties of Earth and the solar system. In: Ahrens TJ (ed.) *Global Earth Physics: A Handbook of Physical Constants*, American Geophysical Union Reference Shelf 1, pp. 1–31. Washington, DC: American Geophysical Union.

Yoder CF and Standish EM (1997) Martian precession and rotation from Viking lander range data. *Journal of Geophysical Research* 102(E2): 4065–4080.

Yoder CF, Williams JG, and Parke ME (1981) Tidal variations of Earth rotation. *Journal of Geophysical Research* 86: 881–891.

Yumi S and Yokoyama K (1980) *Results of the International Latitude Service in a Homogeneous System, 1899.9-1979.0*. Mizusawa, Japan: Publication of the Central Bureau of the International Polar Motion Service and the International Latitude Observatory of Mizusawa.

Zatman S (2003) Decadal oscillations of the Earth's core, angular momentum exchange, and inner core rotation. In: Dehant V, Creager KC, Karato S, and Zatman S (eds.) *Earth's Core: Dynamics, Structure, Rotation*, American Geophysical Union Geodynamics Series, vol. 31, pp. 233–240. Washington, DC: American Geophysical Union.

Zatman S and Bloxham J (1997) Torsional oscillations and the magnetic field within the Earth's core. *Nature* 388: 760–763.

Zatman S and Bloxham J (1998) A one-dimensional map of B_s from torsional oscillations of the Earth's core. In: Gurnis M, Wysession ME, Knittle E, and Buffett BA (eds.) *The Core-Mantle Boundary Region*, American Geophysical Union Geodynamics Series, vol. 28, pp. 183–196. Washington, DC: American Geophysical Union.

Zatman S and Bloxham J (1999) On the dynamical implications of models of B_s in the Earth's core. *Geophysical Journal International* 138: 679–686.

Zhao M and Dong D (1988) A new research for the secular polar motion in this century. In: Babcock AK and Wilkins GA (eds.) *The Earth's Rotation and Reference Frames for Geodesy and Geodynamics*, Int. Astron. Union Symp. No. 128, pp. 385–392. Dordrecht, Holland: D. Reidel.

Zharov VE and Gambis D (1996) Atmospheric tides and rotation of the Earth. *Journal of Geodesy* 70: 321–326.

Zheng D, Ding X, Zhou Y, and Chen Y (2003) Earth rotation and ENSO events: combined excitation of interannual LOD variations by multiscale atmospheric oscillations. *Global and Planetary Change* 36: 89–97.

Zhong M, Naito I, and Kitoh A (2003) Atmospheric, hydrological, and ocean current contributions to Earth's annual wobble and length-of-day signals based on output from a climate model. *Journal of Geophysical Research* 108(B1): 2057 (doi:10.1029/2001JB000457).

Zhong M, Yan H, Wu X, Duan J, and Zhu Y (2006) Non-tidal oceanic contribution to polar wobble estimated from two oceanic assimilation data sets. *Journal of Geodynamics* 41: 147–154.

Zhou YH, Chen JL, Liao XH, and Wilson CR (2005) Oceanic excitations on polar motion: A cross comparison among models. *Geophysical Journal International* 162: 390–398.

Zhou Y, Zheng D, Zhao M, and Chao BF (1998) Interannual polar motion with relation to the North Atlantic Oscillation. *Global and Planetary Change* 18: 79–84.

Zhou YH, Zheng DW, and Liao XH (2001) Wavelet analysis of interannual LOD, AAM, and ENSO: 1997-98 El Niño and 1998-99 La Niña signals. *Journal of Geodesy* 75: 164–168.